Review

The Role of Catalytic Ozonation Processes on the Elimination of DBPs and Their Precursors in Drinking Water Treatment

Fernando J. Beltrán *[iD], Ana Rey [iD] and Olga Gimeno

Departamento de Ingeniería Química y Química Física, Instituto Universitario de Investigación del Agua, Cambio Climático y Sostenibilidad, Universidad de Extremadura, 06006 Badajoz, Spain; anarey@unex.es (A.R.); ogimeno@unex.es (O.G.)
* Correspondence: fbeltran@unex.es

Abstract: Formation of disinfection byproducts (DBPs) in drinking water treatment (DWT) as a result of pathogen removal has always been an issue of special attention in the preparation of safe water. DBPs are formed by the action of oxidant-disinfectant chemicals, mainly chlorine derivatives (chlorine, hypochlorous acid, chloramines, etc.), that react with natural organic matter (NOM), mainly humic substances. DBPs are usually refractory to oxidation, mainly due to the presence of halogen compounds so that advanced oxidation processes (AOPs) are a recommended option to deal with their removal. In this work, the application of catalytic ozonation processes (with and without the simultaneous presence of radiation), moderately recent AOPs, for the removal of humic substances (NOM), also called DBPs precursors, and DBPs themselves is reviewed. First, a short history about the use of disinfectants in DWT, DBPs formation discovery and alternative oxidants used is presented. Then, sections are dedicated to conventional AOPs applied to remove DBPs and their precursors to finalize with the description of principal research achievements found in the literature about application of catalytic ozonation processes. In this sense, aspects such as operating conditions, reactors used, radiation sources applied in their case, kinetics and mechanisms are reviewed.

Keywords: ozone; catalytic ozonation; photocatalytic ozonation; disinfection by-products; natural organic matter; humic acids; drinking water; chlorination

1. Introduction

Safety of drinking water has always been a concern for humankind from at least 500 BC when natural materials were used to purify water [1]. However, it was not until the end of the Middle Age when significant steps in the treatment of water were noticed. In fact, the discovery of the microscope at the end of the 16th century was, years later in 1850, the milestone to know the reason of pandemic problems associated to the use of water. With the aid of microscopes the presence of pathogens in drinking water was discovered and the use of disinfectants would become soon later. Specifically, in 1854 chlorine was first used in London to remove bad odors coming from sewers. Although at that time the disinfectant power of chlorine was not yet well known, the role of contaminated water to spread pandemic illnesses had already been confirmed with the cholera epidemic of London [2]. In 1879 chlorine was first used as a disinfectant also for sewage and in 1903 in drinking water treatment plants [3]. Since then, chlorine has been widely used for some other operations in drinking water treatment such as taste and odor removal, keeping safe water distribution systems, biofouling control, and color removal, to cite a few. For more than 70 years, chlorine was used with great success as a water disinfectant. However, water chlorination began to be questioned after the US National Organics Reconnaissance Survey [4] that revealed the presence of halogenated compounds in 80 USA drinking water plants in 1975. This survey was based on previous studies of Rook [5] and Bellar et al. [6] in 1974 sponsored by the United States Environmental Protection Agency (USEPA) that initiated a work on the analysis of contaminants in rivers such as the Mississippi River at New Orleans [7]. In these

works, six main halogenated compounds were identified: Four trihalomethanes ($CHCl_3$, $CHCl_2Br$, $CHClBr_2$, and $CHBr_3$), CCl_4 and 1,2-dichloroethane [8]. Soon after, many more halogenated compounds, both of volatile and non-volatile nature, were detected in chlorine disinfected water and municipal wastewater secondary effluents. These compounds were not previously present in the untreated waters. For instance, Glaze and Henderson, in 1975, [9] detected in a municipal secondary effluent 39 halogenated compounds of aromatic and aliphatic type with one to at least four chlorine atoms in their molecules to give a total 3 to 4 mg L^{-1} of Cl. These halogenated compounds took the name of disinfection byproducts (DBPs) and the concern about their possible toxic character prompt the development of four questions and subsequent research lines: Which were the organic precursors of DBPs? what kind of alternative disinfectants could be applied? which different groups of DBPs were formed? and what toxicity these compounds have? A brief description about the findings of these research lines is presented below.

2. Nature of Chlorinated DBPs Precursors

There are multiple and variable natural substances present in surface waters that mainly come from plant degradation and animal wastes. Most of them are constituted by macromolecules containing numerous aromatic and aliphatic structures to which other simpler compounds, both of natural or anthropogenic origin, can be linked such as sugars, amino acids, metals, or pesticides [10,11].

These macromolecules are called humic substances that are mainly formed by three fractions: Humic and fulvic acids and humin [12,13]. Humin is not soluble in water and the acid fractions can be separated after precipitation of humic acid at pH = 1. They are mostly colored from yellow to black and of high molecular weight. Up to 90% of total dissolved organic carbon (DOC) in surface waters is due to humic substances with fulvic acid as the major contributing fraction with about 80%. In surface waters, DOC can reach up to 60 mg L^{-1} but the usual concentration ranges from 1 to 6 mg L^{-1} [14]. Figure 1 shows an example of this type of macromolecules where it can be seen the presence of polyphenol structures.
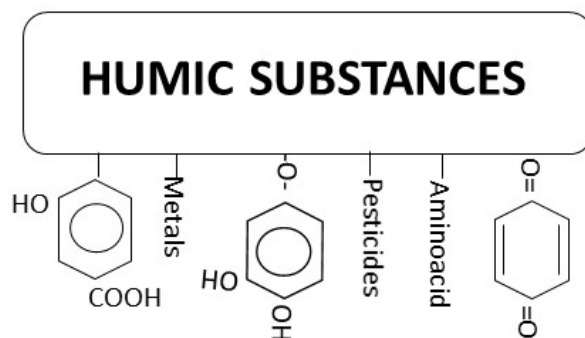
Figure 1. General structure of humic acids.

These polyphenol structures contain nucleophilic points where electrophilic substances such as chlorine can react. These reactions are responsible of halogenated compounds formation [15]. For instance, the molecule of resorcinol that can be found forming part of some humic macromolecule reacts with chlorine as shown in Scheme 1:
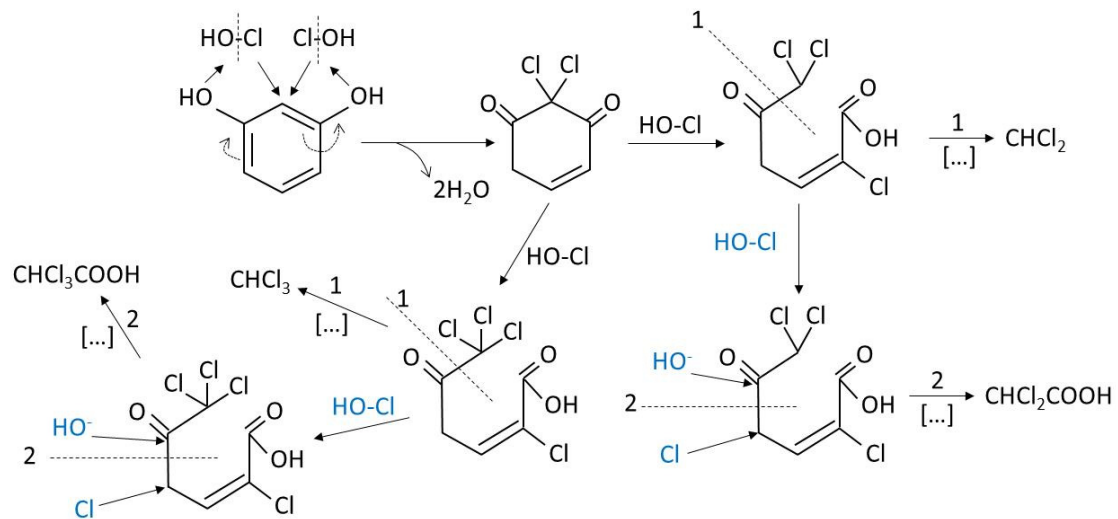
Scheme 1. Mechanism of halogenated compounds formation from the reaction of hypochlorous acid with resorcinol in water: (Way 1): Volatile Chloroform and dichloroethane and (way 2): Non-volatile dichloro and trichloroacetic acids.

As it is seen from Scheme 1 the electrophilic agent (chlorine or hypochlorous acid) attacks the ortho position in the benzene molecule with respect to both hydroxyl groups. This position is strongly activated by the hydroxyl groups becoming a nucleophilic point. Also, chlorine reacts with simpler molecules such as ketones through the well-known haloform reaction [16] shown in Scheme 2.
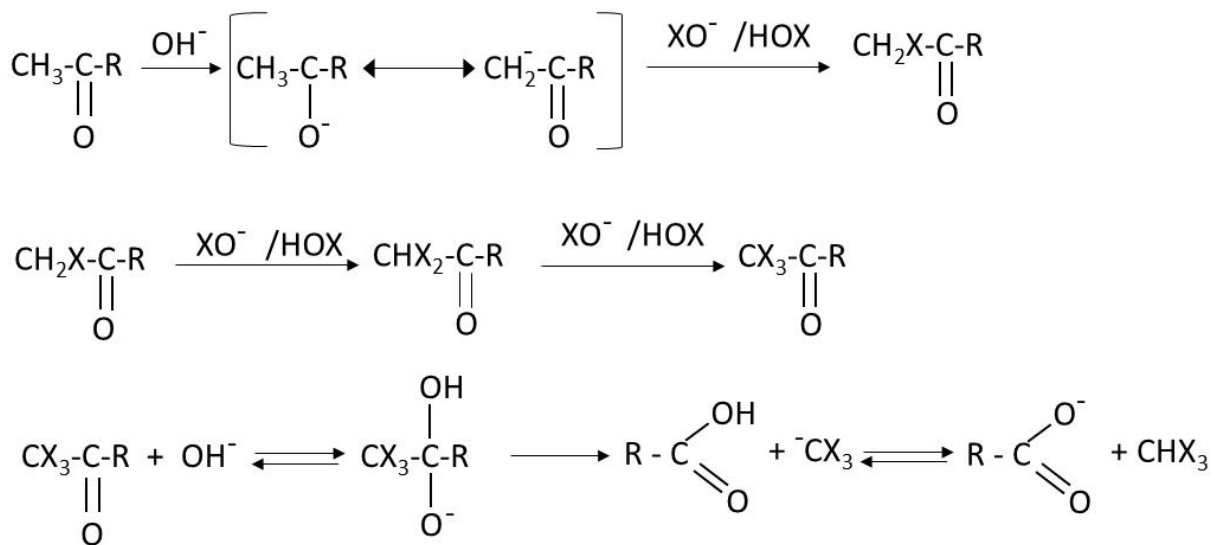
Scheme 2. Reaction of haloform formation (from [16]).

It should be noted that there are other compounds formed during the treatment of water when oxidants or disinfectants (chlorine, ozone, advanced oxidation processes, etc.) are applied. Precursors of these compounds are other pollutants, most of them of anthropogenic origin, such as pesticides, polynuclear aromatics, pharmaceutical compounds, and products of personal care [17–19]. These reaction products are also called DBPs because the reactive agent is a disinfectant. In this work, however, only DBPs coming from disinfection of drinking waters originated in reactions of disinfectants with humic and fulvic acids or generally called natural organic matter (NOM) are considered [20].

3. Alternative Disinfectants to Chlorine

The first possible disinfectant agents to be applied in water treatment alternatives to chlorine were ozone ([21]) and UV radiation. Table 1 shows the oxidation potential of main oxidants that can be used in drinking water treatment and their relative value with respect to that of ozone.

Table 1. Oxidation power of some oxidizing-disinfectants of drinking water [1].

Oxidant-Disinfectant	Oxidation Potential, V	Relative Oxidation Power [2]
Ozone	2.07	1.00
Hydrogen peroxide	1.77	0.86
Potassium permanganate	1.49	0.72
Hypochlorous acid	1.49	0.72
Chlorine	1.36	0.66
Hypobromous acid	1.33	0.64
Chlorine dioxide	1.28	0.62
Monochloramine	1.16	0.56

[1] At 25 °C, relative to hydrogen electrode. [2] Based on ozone.

It can be seen that ozone has the highest oxidizing power among these disinfectants and its oxidation potential is 1.39, 1.52, 1.62, and 1.78 times more oxidant than hypochlorous acid, chlorine, chlorine dioxide, and monochloramine, respectively [22]. These values are in accordance with the CT parameter that gives a measure of the disinfectant power. CT is the product of the disinfectant concentration and the detention time [23]. This reaction time is that needed for the 10% of the water flow through the disinfection contactor be in contact with the indicated disinfectant concentration. CT varies with the nature of pathogen, disinfectant, and disinfection level to be reached. Accordingly, the lower the concentration or the detention time the higher the disinfection power. Table 2 shows, as an example, CT values for the four drinking water chemical oxidants to remove from water two logs or 99% of some microorganisms. It can be seen that in all cases ozone presents the lowest CT values with monochloramine as the weakest disinfectant [23]. Below some comments about chlorine alternative oxidant-disinfectants are given with special emphasis on ozonation.

Table 2. CT values of drinking water disinfectants to inactivate 99% of some pathogens [1].

Pathogen	Chlorine	Chlorine Dioxide	Chloramine	Ozone
E. Coli	0.034–0.05	0.4–0.75	95–180	0.02
Rotavirus	0.01–0.05	0.2–2.1	3810–6480	0.006–0.05
G. Lambia Cyst	47–150	-	-	0.5–0.6
G. Muris	30–630	7.2–18.5	1400	1.8–2.0

[1] pH between 6 and 7 except for chloramines with pH between 8 and 9 [23]. CT values in mg L^{-1}min.

3.1. Ozone

Ozone, similar to chlorine, was first used as bactericide at the end of the 19th century. The first drinking water treatment plant (DWTP) using ozone as disinfectant was in the small city of Oudshorrn in Holland in 1893. After that, ozone was applied, always for disinfection purposes in other cities, such as Wiesbaden, Germany, in 1901, but the first important city using ozone was Nice, France, in 1906. This plant, called Bon Voyage, has been using this oxidant-disinfectant since then [21]. Application of ozone in DWTP, however, experienced a great boost after trihalomethanes (THMs) discovery in chlorinated drinking water and, also, years later, from 1987, when Glaze et al. defined the advanced oxidation processes (AOPs) after studying the combination of ozone, hydrogen peroxide and UVC radiation to yield hydroxyl free radicals [24]. During the second part of the 20th century most of the fundamentals of ozone chemistry in water had already been uncovered [25];

and consequently, its possible application for water treatment [23]. Ozone can react with DOM through two possible routes: Direct reactions on nucleophilic points or addition reactions on unsaturated moieties (double and triple carbon bonds) that form H_2O_2:

$$O_3 + \text{Nucleophilic points}/-C=C- \xrightarrow{\text{Direct reactions}} H_2O_2 + \text{Intermediates} \qquad (1)$$
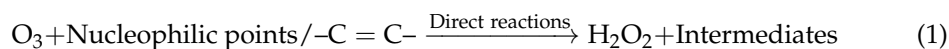
At high pH it predominates the indirect reaction or reaction with hydroxyl radicals formed in ozone decomposition [26].

$$O_3 + OH^- \rightarrow \text{free radicals} \rightarrow HO^\bullet \Rightarrow HO^\bullet + \text{Organics} \xrightarrow{\text{Indirect reactions}} \text{Intermediates} \quad (2)$$
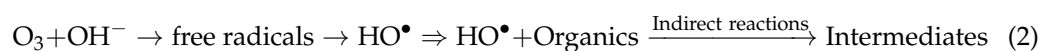
Many ozone reactions with humic substances are of the electrophilic substitution type. These reactions are faster than those with chlorine because the highest oxidizing power and oxidation kinetics of/with ozone [27–29]. In Schemes 3 and 4, the Criegge mechanism, the reaction of ozone with a double carbon bond, and an electrophilic aromatic substitution reaction of ozone with the carbon hydrogen bond in ortho position with respect to the hydroxyl group of a phenol molecule are, respectively, shown [30].
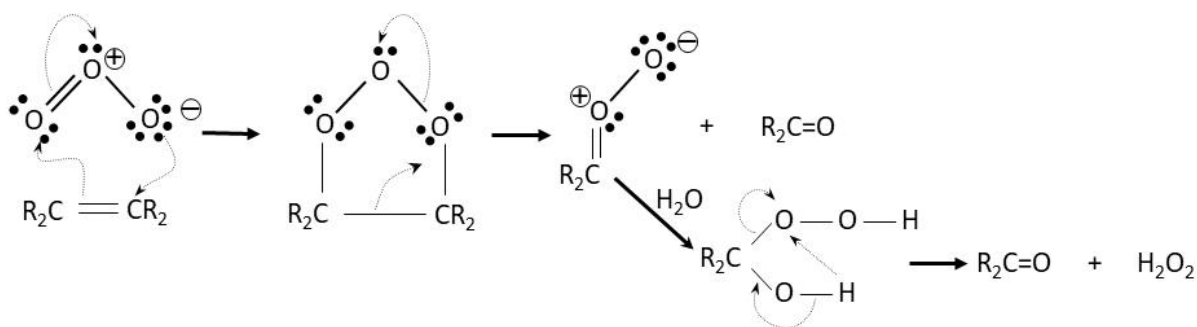
Scheme 3. Cycloaddition of ozone to a carbon double bond.
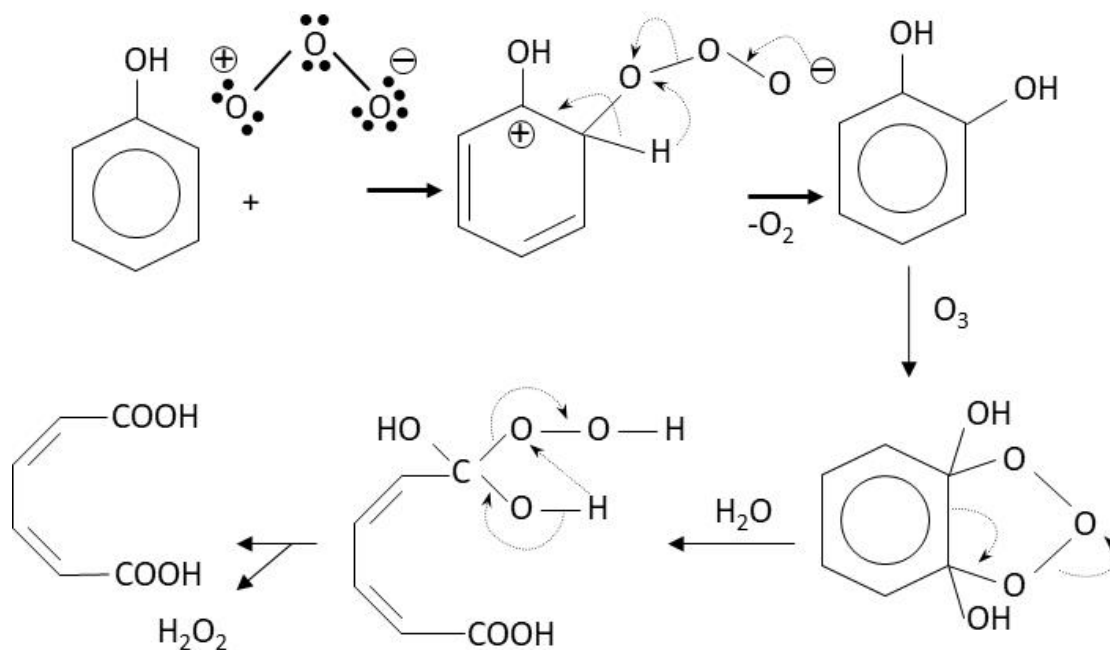
Scheme 4. Electrophilic aromatic substitution reaction of O_3 with phenol.

These are selective fast reactions of ozone with unsaturated compounds and nucleophilic points of organics. Furthermore, in these reactions hydrogen peroxide is formed.

The reaction of the ionic form of this oxidant with ozone constitutes the main initiation step of hydroxyl radical formation mechanism in ozone involving advanced oxidation processes [27]. Regarding Scheme 4, after hydroxyl substitution in the phenol molecule, aromatic ring breaking is followed due to the cycloaddition of another ozone molecule and, finally, other ozone addition reactions to unsaturated carboxylic acids formed lead to low molecular weight saturated carboxylic acids. These acids, aldehydes and, in some cases, ketones are usually the end products of ozone reactions which are not precursors of halogenated compounds with the exception of some ketones. Then, previous utilization of ozone to chlorination allows significant reduction of trihalomethane formation potential (THMFP) or halogenated compounds formation potential (TOXFP). In case of high alkalinity, hydroxyl radical oxidation takes place to also yield similar byproducts that direct ozone reactions. Another advantage of ozone is its high capacity for being combined with other agents (oxidants, catalysts, and/or radiation) to yield more hydroxyl radicals, what are called ozone AOPs. This has implications even on THMs or TOX removal since ozone alone is not reactive with many halogenated compounds. On the contrary, hydroxyl radicals generated in ozone AOPs can react with THMs or TOX. However, some ozone DBPs can also be harmful, for instance, when water contains bromide ion. In this case, bromoform and hypobromous acid are formed and, eventually, depending on the conditions, bromate ion, an important priority pollutant. Then, the levels of bromide in surface water needs surveillance if ozone is used for THMFP and TOXFP control. Some considerations about bromate control have been specifically reviewed in Section 9. Also, the ozone dose has to be controlled because if added very low, it could increase the precursors concentration due to partial oxidation of first TOX precursors. For instance, water samples containing 1 mg L^{-1} 1,3-cyclohexanedione, a DBP precursor, treated with an ozone dose of 30 mg L^{-1} during 15 and 30 min and then diluted 100 times and chlorinated (1 mg L^{-1} Cl_2 dose) led to $CHCl_3$ concentrations of 77 and 15 μg L^{-1}, respectively, while without preozonation, $CHCl_3$ formation was 50 μg L^{-1} [31]. Ozone added at very high dose could form bromoform and other brominated organics such as bromohydrines [32]. In spite of its faster kinetics through two possible routes and high disinfectant and oxidizing power application of ozone also present another drawback: It cannot be used as residual disinfectant and chlorine or another residual disinfectant has to be used at the end of a DWTP. In any case, the residual disinfectant dose needed in a DWTP with a pre-ozonation step is much lower than in a conventional process without pre-ozonation, especially when a biological activated carbon step is placed after ozonation. For example, Langlais et al. [23] reported that chlorine demand was reduced from 4.5 mg L^{-1} to 3.5 and 2.7 mg L^{-1} when water from St. Rose treatment plant in Laval (Canada) was treated with rapid sand filtration, rapid sand filtration and ozonation, and rapid sand filtration plus ozonation and biological activated carbon, respectively. The savings in chlorine dose were in some case comparable to the cost of ozonation [23].

3.2. Chlorine Dioxide

Chlorine dioxide started to be used in DWTP in 1944, that is, much later than chlorine or ozone. The first application of chlorine dioxide in DWTP was for taste and odor control in Niagara Falls, State of New York. Then, it was most commonly used for bleaching in textile industries [21]. Depending on the way of synthesis, concentration and presence or not of chlorine, chlorine dioxide may lead to THMs or TOX formation while reacting with humic substances. Chlorine dioxide when used alone no THMs or TOX is formed but accompanied by chlorine, which could be formed in its preparation method, halogenated compounds can appear in the treated water. In a detailed studied, Rav-Acha [33] already described the main reactions and mechanisms of chlorine dioxide with many organics including humic substances. He concluded that since the main way of chlorine dioxide reaction with these substances is as one electron acceptor, its reactions a more selective and mainly yield quinones, hydroquinones and low molecular weight aldehydes and carboxylic acids. For instance, Scheme 5 shows a proposed mechanism of reaction of chlorine dioxide

and phenolate, also a precursor molecule of TOX [33].
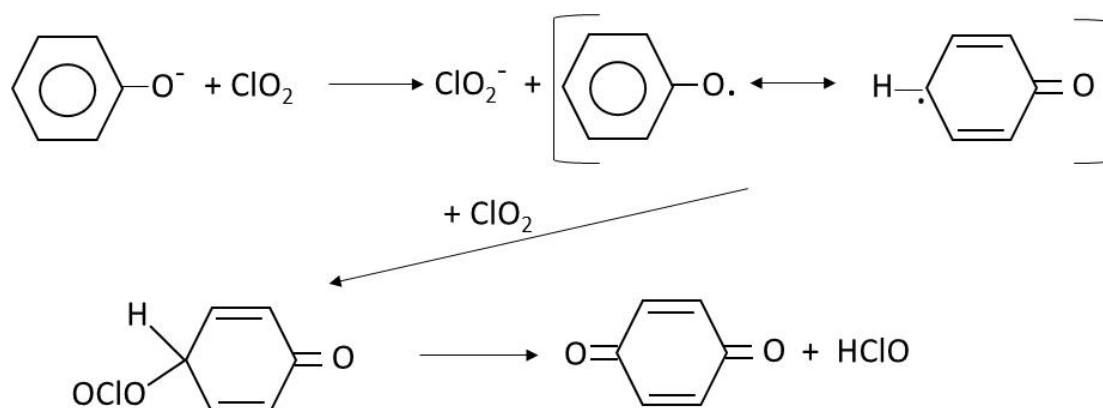
Scheme 5. Reaction of chlorine dioxide and phenol, from [23].

It is shown that the final products are p-benzoquinone and hypochlorous acid but some amount of chlorite is also formed. The presence of hypochlorous acid is likely responsible of TOX formation when precursor molecules are in excess [34]. More information about chlorine dioxide DBPs and toxicity is given in Sections 4 and 5.

3.3. Chloramines

Chloramines are formed in the reaction of chlorine with amine in a three consecutive steps where mono, di and trichloramine are formed:

$$HClO + NH_3 \rightarrow NH_2Cl + H_2O \tag{3}$$

$$HClO + NH_2Cl \rightarrow NHCl_2 + H_2O \tag{4}$$

$$HClO + NHCl_2 \rightarrow NCl_3 + H_2O \tag{5}$$
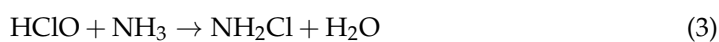
For practical cases, it is monochloramine the species used as disinfectant. The way of chloramine formation, from addition of chlorine to amine or vice versa, already present in water or by adding a previously prepared monochloramine solution to the water, highly affects the appearing of chlorinated byproducts because of the free chlorine remaining in the first two cases [35]. However, even in the case of monochloramine solution application to water, hypochlorite (at alkaline pH) or hypochlorous acid (at acid pH) eventually will appear in water due to monochloramine hydrolysis. Then, using monochloramine as disinfectant always leads to chlorinated organics. Monochloramine is the less effective disinfectant and oxidant species among the four reviewed in this work but its capability of forming chlorinated organics is also the lowest. As a consequence, chloramines, depending on the TOXFP of the water, can be recommended as secondary disinfectant for the control of DBPs because their residual disinfectant property. A different question arises when talking about nitrogen containing disinfection byproducts (NDBPs) such as haloacetamides (HAcAm). In this case, chloramination may result in a higher formation potential of these compounds than chlorination.

3.4. UV Disinfection

Although chemical disinfectants are used in DWTPs because of the need of a residual disinfectant and DBPs control, the use of UV disinfection of water is highly extended due to some advantages over chemical oxidants as reported by Song et al. [36]. These advantages are the absence of DBPs, low health risk, easy operation and maintenance, minimum reaction time, and high disinfection power. However, problems associated to UV disinfection arise when treating natural waters containing humic substances. Efficiency of disinfection highly depends on the transparency of water and the presence of colored water

due to humics reduces the UV absorption and lower pathogen removal rates. This negative effect could be reduced by increasing the energy dose and lowering the wavelength of emitted radiation but at a higher cost.

3.5. Other Disinfection Processes

Literature also gives examples of water disinfection processes different from the use of chemical oxidants or radiation though some of them are intimately related with them. This happens, for example, with the simultaneous use of radiation and a semiconductor catalyst, that is, photocatalytic oxidation [37]. This process has the attractive possibility of using solar light to excite the catalyst [38,39]. In photocatalytic oxidation, an AOP process, hydroxyl radicals generated can inactivate microorganisms, including viruses, bacteria, spores, and protozoa. However, since hydroxyl radicals are strong oxidants, DBPs similar to those found in ozone processes can be produced and cytotoxicity of catalyst particles requires further studies. Other examples of disinfection processes are based on membranes [40], hydrodynamic cavitation [41], nanoparticles such as in photocatalysis or in membranes [42], or with magnetic materials [43]. However, more work is needed so that these processes can be put into practice.

4. Nature of DBPs from Classical Oxidant-Disinfectants Agents Used in DWTPs

Soon after the uncover of THMs in chlorinated drinking water many works were carried out to ascertain the nature of generated products not only from chlorine but also from the application of the other alternative oxidants commented before. One of the first studies on this matter was carried out by Coleman et al. in 1980 [44] who identified 400 compounds from a chlorinated fulvic acid extract. Among these compounds, polynuclear chlorinated aromatic hydrocarbons and polychlorinated biphenyls represented an important fraction. Also, regarding DBPs of alternative oxidants, Glaze in 1986 [45] published a review on ozonation DBPs, highlighting the formation of hydroperoxidic byproducts, unsaturated aldehydes and hypobromous acid or even permanganate ions, the two later from the oxidation of bromide and manganous ions, respectively. Regarding chlorine dioxide DBPs, at that time, Werdehoff and Singer in 1987 [46] reported some TOX and THMs formation from chlorine dioxide oxidation of humics. They also checked that these chlorinated organic compounds were mainly due to residual chlorine formed accompanying the synthesis of chlorine dioxide. They also reported the formation of chlorite ion as main inorganic byproduct. Throughout these last three decades, a lot of work has been done on DBPs identification [32] and some reviews on this matter have been published [47]. Also, published studies report works not only on DBPs identified from chlorination [48], but also from chloramination [49,50], ozonation [32], and chlorine dioxide NOM oxidation [51,52]. Most of identified DBPs come from water chlorination and mainly involve organochlorine compounds but some treat the presence of brominated (Br-DBPs) and iodinated (I-DBPs) DBPs formed from chlorine, ozone or chlorine dioxide when natural waters contain bromide or iodide, respectively [32,53]. In these works, oxidation of bromide and iodide yields hypobromous and hypoiodous acids, respectively, which in turn oxidize NOM to form Br-DBPs and I-DBPs. Also, from the oxidation of chlorine, ozone or chlorine dioxide, bromite, and iodite are formed that in a fast step are oxidized to bromate and iodate, respectively.

DBPs are classified as regulated (R-DBPs) and non-regulated (NR-DBPs) whether or not some maximum contaminant level (MCL) has been imposed from official government environmental organizations such as USEPA or the European Chemical Agency (ECA), (called standard values in this case). Regulated DBPs are among the most halogen organics identified. These are four out of ten THMs: Those containing chlorine and bromine and five out of nine haloacetic acids (HAAs) (only with chlorine and bromine atoms): Mono, di and trichloroacetic acids and mono and dibromoacetic acids. For total THM, USEPA, and ECA have imposed MCL (or standard values) of 80 and 100 µg L^{-1}, respectively, while for total HAAs, MCL are 60 µg L^{-1} imposed for both official organisms. Regarding inorganic DBPs, bromate has 10 µg L^{-1} and chlorite 1000 and 250 µg L^{-1}, also from these organizations,

USEPA and ECA, respectively. The rest of the identified DBPs are non-regulated and main family groups are listed in Table 3 with some representative example compound. Many of these DBPs are formed from chlorination but also from chloramination, ozonation and chlorine dioxide application. Richardson et al. [54] in an extensive and detailed review gives numerous examples of DBPs from the oxidation with the four mentioned disinfectants and from sequential oxidations such as ozonation or chlorine dioxide treatment followed by chlorination or chloramination. New DBPs are continuously being identified as Pan et al. [55] did in 2017. These authors reported 13 new polar phenolic chlorinated and brominated DBPs or How et al., also in 2017 [56], about organic chloramines. Literature shows detailed explanations about the formation mechanisms of these DBPs which are out of the scope of this work.

Table 3. Family groups of unregulated DBPs identified in water during disinfection processes, representative compounds and average detection concentration levels (ADC) [1].

NR-DBP Family Group	Representative Compound	ADC, μg L^{-1}
Halogenated compounds		
THMs [4]	Iodoform	0.2 [2]
HAAs [4]	Bromochloracetic acid	<1 [1]
Halonitromethanes	chloropicrin (trichloronitromethane)	0.5 [2]
Haloacetonitriles	dichloroacetontrile	3.08 [2]
Haloacetamides	dichloroacetamide	1.62 [2]
Haloamines	N-chloroaminoacetic acid [3]	-
Haloaldehydes	trichloroacetaldehyde	3.67 [2]
Haloketones	trichloropropanone	3.55 [2]
Halofuranones	MX: 3-chloro-4-(dichloromethyl)-5-hydroxy-2(5H)-furanone	<1.0 [1]
Haloquinones	2,6-Dichloro-1,4-benzoquinone	<1.0 [1]
Iodinated DBP (other than THM and HAACs)	Iodoacetaldehyde	<1.0 [1]
Halogencyanide	Cyanogen chloride	1.54 [2]
Non halogenated compounds		
Aldehydes	Formaldehyde	3.46 [2]
Ketones	Dimethylglyoxal	<1.0 [1]
N-Nitrosamines	N-nitrosodimethylamine	0.01 [2]

[1] Richardson et al. [54] also shows other less important family groups. [2] From [57]. [3] From [58]. [4] Regulated DBPs.

5. Issues Related to DBPs Toxicity

As it was reported in the 1970s the reason for applying alternative disinfectants to chlorine was the potential toxic character of THMs and other halogenated organics found in finished chlorinated drinking water [59]. Specifically, the US National Cancer Institute in 1976 published that chloroform was carcinogenic in rodents [60]. Soon after, epidemiological studies suggested some relation between chlorinated drinking water and the occurrence of bladder, colon, and rectal cancer [61,62]. Since then, many studies on the evaluation of safety and hazard of DBPs have been reported [63]. According to DeMarini [64], at present, 20 out of 22 DBPs are rodent carcinogens, more than 100 genotoxic and 1000 water samples have been found to be mutagenic. It has been shown that brominated DBP are more carcinogenic than the chlorinated ones [54] and genotoxicity and cytotoxicity decrease in the following order for halogenated DBPs: Iodinated > brominated > chlorinated [65]. Generally, every DBP evaluated is genotoxic [64]. Comparing chlorinated and ozonated DBPs, the former are more genotoxic than the latter, at least, with *Salmonella* [66]. Regarding the way of DBPs exposure, some works [67] have reported higher cancer risk with the inhalation/dermal way than with oral intake. From inhalation or dermal way, volatile DBPs go directly to the blood stream, bypassing the liver, and once in the bladder they can be activated by some mutagen. From oral intake, DBPs go first to the liver where they

could be detoxified. This is particularly important in swimming pool water and bath spa water where, in addition, many nitrogen containing DBPs (N-DBPs) have been found likely due to urine present in these waters. N-DBPs like nitrosamines have been found even more cytotoxic and genotoxic than their corresponding halogenated organics [68].

6. The Role of AOPs in the Removal of Precursors and DBPs

Different AOPs have been applied to eliminate NOM or formed DBPs in a refinement stage focused on drinking water production. AOPs are capable to completely mineralize organic contaminants at mild operating conditions of pressure and temperature though the balance between cost and mineralization requirements is a key issue. At moderate conditions, partial oxidation of NOM components into more reactive compounds to form DBPs can occur. In contrast, a very high mineralization is usually expensive and may not be economically feasible. This section reviews some of the main issues concerning the application of different AOPs for NOM and DBPs removal.

6.1. Elimination of Precursors or DBPs Formation Potential

Advanced oxidation processes have been studied for DBPs precursor removal due to their oxidation ability through hydroxyl radical (HO$^\bullet$) fast and non-selective reactions with organic compounds [69,70]. However, research efforts are needed in terms of improved efficiency, development of less expensive installation and operating conditions [70].

DBP formation potential (DBPFP) represents the level of the formation of different DBPs (or total TOX) in the worst scenario using high excess of disinfectant. This a useful tool to assess the effectiveness of a specific treatment to remove the DBPs precursors, mainly NOM. Since 1980 the number of publications related to AOPs applied to NOM or surrogate removal to reduce DBPFP has progressively increased. The search presented in Figure 2 shows the number of publications in JCR (source WOS) between 1980–2020 and includes different combinations of the keywords: Advanced oxidation, natural organic matter, disinfection by-products, trihalomethanes, haloacetic acids, halonitromethanes, haloketones, haloacetamides, ozone; and their abbreviations, for drinking water treatment.
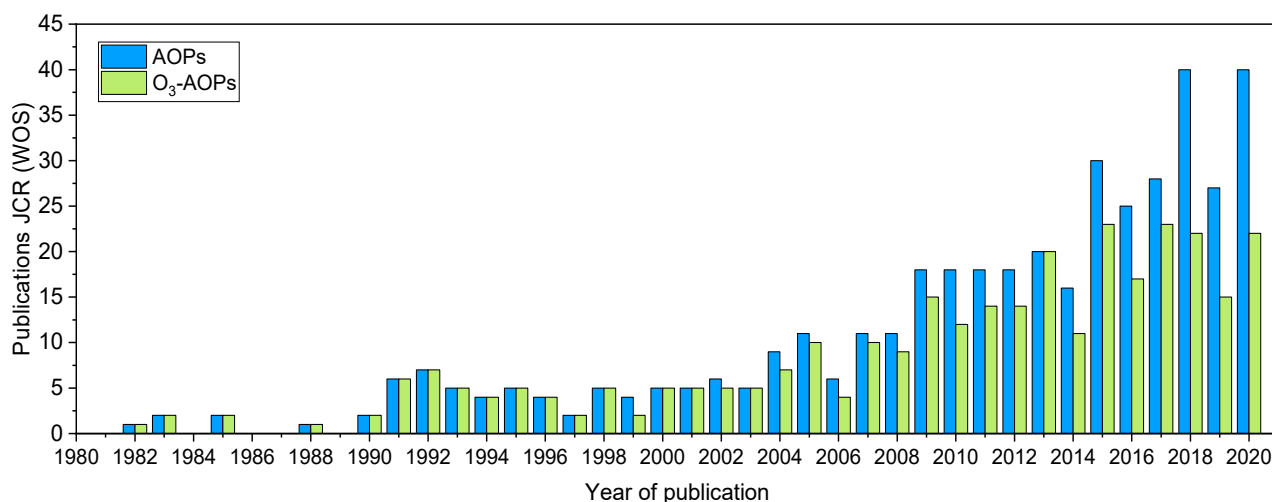
Figure 2. Reports in AOPs and ozone-AOPs for DBPFP or NOM removal for drinking water in the last 40 years.

Matilainen and Sillanpää [71] and Sillanpää et al. [70] comprehensively reviewed the application of AOPs for the removal of NOM in the periods between 2006–2009 and 2010–2016, respectively. This section is focused on the abatement DBPs precursors, mainly NOM, highlighting the formation of DBPs and some key factors in the application of AOPs for DBPFP removal without the aim of compiling all the research found. The application of these processes to the elimination of other microcontaminants in surface water such

as pharmaceuticals or personal care products without subsequent DBPs analyses are not reviewed here.

6.1.1. Classic Ozonation Processes

The first study published by Glaze et al. [72] was focused on the degradation of natural trihalomethane precursors by O_3 and O_3/UVC processes in raw waters with high DOC levels. They found that secondary precursors of greater refractivity were produced by ozonation but they could be simultaneously destroyed by UVC combined with ozone. This was due to the formation of high concentration of hydroxyl radicals in the combined process, less selective than ozone, favoring indirect reactions to some extent. Since then, the works in the last two decades of the 20th century have been mainly related to classical ozone based-AOPs, with the main aim of increasing the production of hydroxyl radicals compared to O_3 alone, O_3/H_2O_2, O_3/UVC, O_3/H_2O_2/UVC and also the process H_2O_2/UVC [73]. These processes are well established and have been deeply investigated at lab scale, pilot scale and even at full-scale [74]. In general, the oxidation changes the nature of NOM structures into more hydrophilic compounds, being hydrophobic fractions (humic and fulvic structures) the main responsible for THMs and trihaloacetic acid formation, whereas the more hydrophilic ones are related to dichloroacetic acid generation and the formation of higher concentration of brominated DBPs [75–77]. In this line, even with the highest THMs and HAAs formation potential removal by combined O_3/UV treatment, bromine-containing DBPs present increased toxicity being the conditions between oxidant and UV dose crucial to minimize the risks [78]. Also, the particular characteristics of the NOM play a key role in the suitability of a specific treatment [70,79].

In addition to the classical ozonation and ozone-AOPs, homogeneous and heterogeneous catalytic treatments such as Fenton-related, photocatalytic oxidation or persulfate processes, have been studied for NOM or surrogates elimination in drinking water [69–71].

6.1.2. Fenton Related Processes

Fenton reaction involves the combination of hydrogen peroxide and a metal salt or oxide catalyst, commonly iron, to produce hydroxyl radicals responsible for NOM oxidation and mineralization through the following main reactions:

$$Fe^{2+} + H_2O_2 \rightarrow Fe^{3+} + OH^- + HO^\bullet \tag{6}$$

$$Fe^{3+} + H_2O_2 \rightarrow Fe^{2+} + H^+ + HO_2^\bullet \tag{7}$$

The presence of radiation in photo-Fenton process accelerates the reduction of Fe^{3+} improving the yield of $HO^\bullet$ generation:

$$Fe^{3+} + H_2O \xrightarrow{h\nu} Fe^{2+} + H^+ + HO^\bullet \tag{8}$$

Murray and Parsons [80] studied the elimination of NOM through Fenton and photo-Fenton using UVC as radiation source. They found that the three treatments at optimum conditions reached 90% removal of DOC (DOC_0 = 7.5 mg L^{-1}), dropping THMFP from 140 to below 10 µg L^{-1}. The economic assessment disfavored these processes compared to conventional treatments but neither the use of a different radiation source nor the possibility of a more restrictive regulation (not only THMs), were considered. In this line, Moncayo-Lasso et al. [81] treated surface water by solar photo-Fenton in a CPC reactor (compound parabolic collector) using natural sunlight. They demonstrated the performance of the process to mineralize up to 80% of NOM (TOC_0 = 7.44–7.81 and 4.12–5.02 mg L^{-1}) from surface water containing dissolved iron or with Fe^{2+} supplement at pH = 5. They found a beneficial effect of photoactive natural components present in the natural water on the process leading to a more efficient mineralization than using dihydroxy-benzene as a model compound. Unfortunately, the DBPFP before and after chlorine disinfection was not analyzed in this work either the formation of other oxidation by-products. Moncayo-Lasso

et al. [82] also studied the photo-Fenton process using simulated solar radiation to eliminate NOM at pH = 6.5, which introduces an advantage with respect to Fenton related treatments usually carried out at pH near 3. They used Fe^{3+} at low concentration for the treatment of surface water with TOC_0 = 7.1 mg L^{-1}, demonstrating the effectiveness of the system for the transformation and partial mineralization of NOM previously treated with a sand filter system. The THMFP dropped from 160 to 20 μg L^{-1} at the optimum conditions. However, the transformation of NOM can lead to different DBPs precursors that have not been considered in these works.

6.1.3. Photocatalytic Oxidation

Heterogeneous photocatalysis based in the interaction of a semiconductor, mainly *TiO₂*, with radiation to produce reactive oxidizing species (ROS) is a complex mechanism that can be generally described by the following reactions:

$$TiO_2 \xrightarrow{h\nu} h^+ + e^- \tag{9}$$

$$h^+ + (H_2O, OH^-, Ti - OH) \to HO^\bullet \tag{10}$$

$$e^- + O_2 \xrightarrow{[...]} HO^\bullet \tag{11}$$
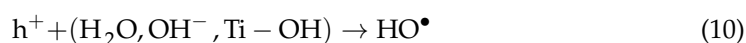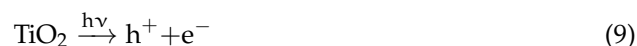
where organic molecules can react both in the catalyst surface with photogenerated holes (h^+) or in the liquid phase with hydroxyl radicals or other ROS.

Photocatalytic oxidation using suspended TiO_2 for NOM removal has been studied by different authors. Lee and Ohgaki [83] observed an initial increase in THMFP at short treatment times with the system TiO_2/UVC and different surface waters with DOC_0 = 1.1–3.5 mg L^{-1}. This effect has been subsequently observed by different authors with different surface waters using TiO_2/UVA [84,85]), TiO_2/UVC [86] and even TiO_2/solar radiation [87]; concluding, in general, that sufficient radiation doses are needed to achieve the desired elimination, depending on raw water characteristics, and an initial negative impact of photocatalysis on DBPFP is expected at low UV doses.

Apart from suspended TiO_2, Murray and Parsons [88] studied different supported TiO_2 demonstrating that can be effective combined with UVC for NOM removal. Later, Murray et al. [89] studied pelletized TiO_2 to adsorb NOM from different surface waters (DOC_0 = 17.0–5.4 mg L^{-1}) at bench scale and then used UVC to regenerate the TiO_2 pellets by oxidation. They observed a reduction of DOC concentration of source water by 70% with the subsequent THMFP reduction in a multistage process. Also Kent et al. [90] compared the efficiency of suspended and fixed TiO_2 using nanostructured thin films and UVC with river water (DOC_0 = 5.34 mg L^{-1}). No complete DOC elimination was reached but they obtained removals of total trihalomethane formation potential (TTHMFP) and total haloacetic acid formation potential (THAAFP) of approximately 20% and 90%, respectively, being fixed TiO_2 configuration less effective than suspended TiO_2.

6.1.4. Sulfate-Radical Processes

Sulfate radical-based AOPs are based on the generation of $SO_4^{\bullet-}$ radicals from persulfate (PS) or peroxymonosulfate (PMS) activation by temperature, metal ions, solid catalysts, radiation, ultrasound, etc. For NOM removal and DBPFP reduction, mainly homogeneous metal ions or UV activation have been used:

$$S_2O_8^{2-} + M^{n+} \to M^{(n+1)} + SO_4^{\bullet-} + SO_4^{2-} \text{ (M = metal ion)} \tag{12}$$

$$HSO_5^- + M^{n+} \to M^{(n+1)} + SO_4^{\bullet-} + HO^- \text{ (M = metal ion)} \tag{13}$$

$$S_2O_8^{2-} + h\nu \to 2SO_4^{\bullet-} \tag{14}$$

$$HSO_5^- + h\nu \to SO_4^{\bullet-} + HO^\bullet \tag{15}$$

$$SO_4^{\bullet-} + H_2O \to SO_4^{2-} + HO^\bullet + H^+ \tag{16}$$
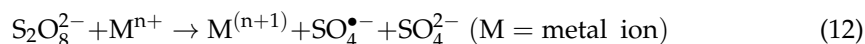
Lu et al. [91] studied the system Co^{2+}-PMS and reported the NOM reconfiguration upon exposure to sulfate radicals with a great increase in the DBPFP, concretely chloroform, trichloroacetic acid, and dichloroacetic acid. Also, the formation of reactive bromine species through $SO_4^{\bullet-}$ and Br^- reaction was demonstrated.

Hua et al. [92] studied the DBP alteration from NOM and model compounds after UV/PS treatment and subsequent chlorination. They found that the yields of THMs and dichloroacetonitrile (DCAN) from NOM decreased by 50% and 54%, respectively, after UV/PS followed with chlorination, whereas those of chloral hydrate (CH), 1,1,1-trichloropropanone and trichloronitromethane (TCNM) increased by 217%, 136%, and 153%, respectively. They demonstrated the impact of different structures of the precursors on DBP formation through different surrogates (benzoic acid, resorcinol or methylamines). Wang et al. [93] also studied Br-DBPs during UV/PS oxidation demonstrating the potential negative effects of Br^- on sulfate radical-AOPs, which need to be considered if this technology is applied in practice. In the same line, Wang et al. [94] studied the formation of iodinated DBPs during heat activated PS using phenol as model compound in the presence of iodide. They concluded that I^- was transformed into free iodine leading to iodinated DBPs that can further be degraded by additional $SO_4^{\bullet-}$ and transformed to iodate. All these works highlight the crucial impact of sulfate radicals in the presence of bromide, iodide or chloride.

6.1.5. Chlorine/UV Process

The combination of chlorine/UV has been recently studied for NOM degradation. With radiation of sufficient energy, the photolysis of hypochlorous acid and hypochlorite can lead to hydroxyl and chlorine radicals as follows:

$$HOCl \rightleftarrows H^+ + ClO^- \quad pKa = 7.58 \tag{17}$$

$$HOCl + h\nu \rightarrow HO^\bullet + Cl^\bullet \tag{18}$$

$$ClO^- + h\nu \rightarrow O^{\bullet-} + Cl^\bullet \tag{19}$$

$$O^{\bullet-} + H_2O \rightarrow HO^\bullet + OH^- \tag{20}$$
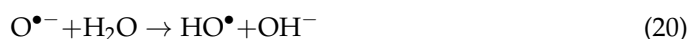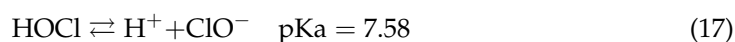
Pisarenko et al. [95] investigated the generation of DBPs during NOM degradation by combination of chlorine (electrochemically generated or from hypochlorite solution) with UVC and UVA radiation. They found that $Cl^\bullet$ and $HO^\bullet$ radicals generated oxidized NOM from river water ($DOC_0 = 2.6$ mg L^{-1}) and different surrogates (o-methoxybenzoic acid and 4,6-dioxoheptanoic acid) increasing HAA formation but with no negative impact on THM formation. UVC resulted in lower overall DBP formation than UVA. Also, Wang et al. [96] studied the process at pilot scale with river water ($DOC_0 = 1.5$–3.5 mg L^{-1}). They concluded that the treatment was effective and the DBPs formed were comparable to that from H_2O_2/UV also tested. The main drawback was the formation of chlorate during the treatment up to 17% of the total chlorine used. Liu et al. [97] reported the formation of DBPs in the system chlorine-chloramine/UVC. They found that the mass ratio of HOCl to NH_2Cl played a key role in the control of DBPs formation and that the presence of Br^- increased DBPFP but it can be reduced with higher radiation doses (Br^- transformed to bromate).

6.1.6. Electrochemical AOPs

Electrochemical AOPs (EAOPs) have been mainly applied for wastewater more than for drinking water treatment due to technical and economic aspects [98]. Trellu et al. [99] studied the removal of humic acids from drinking water by anodic oxidation and electro-Fenton processes. They concluded that EAOPs are promising processes for the production of high quality organic-free water, particularly when BDD anode is used but no disinfection by-products were analyzed. Mao et al. [100] compared conventional ozonation with electro-peroxone (E-peroxone, E-H_2O_2/O_3) in the removal of NOM ($DOC_0 = 3.2$ mg L^{-1}).

They found that E-peroxone was less efficient at reducing chlorination DBPs. However, the formation of bromate was significantly reduced in the combined treatment. More research is needed in these processes and their combinations to boost the application in real conditions.

6.1.7. Some Considerations on AOPs for DBPFP Removal

Many studies have determined that the application of AOPs operating with limited energy or chemical inputs can lead to an increase in the DBPFP as compiled Mayer et al. [101]. Therefore, intensified treatments with high enough oxidant concentration or exposure time are required. In this scenario, the effectiveness of ozone-based AOPs for DBPFP depletion for drinking water treatment has led to the investigation of other catalytic and photocatalytic ozone treatments with the aim of improving the use of ozone. These processes are deeply reviewed in Sections 7 and 8.

6.2. DBPs Removal

Although DBPs can be controlled through removing NOM in the drinking water treatment process, it is not only difficult to remove NOM completely, but DBPs are inevitably produced when the remaining chlorine is released to rivers and reacts with NOM. Because of variability in DBPs characteristics, complete elimination from drinking water by single technique is impossible. A quick search in database Scopus with key words "disinfection by-products removal AND oxidation processes" give more than two hundred entries.

6.2.1. Ozone Based Processes

Ozone-based processes, other than catalytic/photocatytic ozonation, have been used for removing DBPs from water supplies. As it can be inferred from Table 4, N-nitrosamines and chloroacetic acids (CAAs) are the main disinfection by-products investigated. N-nitrosamines are highly toxic disinfection by-products formed in drinking water treatment process. More than 80% of N-nitrosamines are carcinogenic, teratogenic and mutagenic. USEPA has classified N-nitrosodimethylamine (NDMA) as a probable human carcinogen [102]. N-nitrosamines cannot be sufficiently removed during conventional water and wastewater treatment processes and could permeate through reverse osmosis (RO) membrane filtration in water reclamation systems. In this sense, NDMA degradation by ozone-based AOPs has been investigated. However, these works indicated that conventional ozonation had very limited effect on NDMA oxidation [102]. Zhang et al. [102] found that, compared with UV irradiation, ozone was less effective for the abatement of N-nitrosamines. Less than 20% of N-nitrosamines were oxidized after ozonation. However, when 2 mg L^{-1} of H_2O_2 was added into ozonation system, the degradation efficiencies of N-nitrosamines were significantly improved. Xu et al. [103] investigated the removal efficiency of NDMA using UV/O_3 and evaluated the ability of UV/O_3 to diminish the regeneration of NDMA after degradation. It was showed that 99% NDMA removal was achieved both in UV and UV/O_3 system, while the oxidized fraction of NDMA was only 10% at pH = 6 by ozone alone ($[O_3]_0$ = 6.6 mg L^{-1} (0.14 mM), $[NDMA]_0$ = 0.1 mM). The introduction of ozone during the UV process had little influence on NDMA removal, but had a large impact on NDMA degradation products. Lee et al. [104] compared the efficiency of conventional ozonation and the AOP (O_3/H_2O_2) for NDMA oxidation. The degradation effectiveness of NDMA was only 13% ($[NDMA]_0$ = 1 mM) at pH = 7 and 12 min contact time, by 40 mM ozone alone. In contrast, 85% of NDMA was removed by the AOP (O_3/H_2O_2, $[O_3]_0$ = 40 mM, $[O_3]_0/[H_2O_2]_0$ = 2) under the same reaction conditions. It appeared that the reaction with $HO^\bullet$ radicals dominated NDMA ozonation, and methylamine (MA) was the primary amino product of this NDMA oxidation. In this sense, Lv et al. [105] investigated the degradation of NDMA by ozonation. The effects of initial NDMA concentration (50–800 ng L^{-1}), ozone dosage (0.02–0.2 mM), and pH (5–8) were studied in detail in the context of NDMA degradation. The amount of removed NDMA increased as the initial NDMA concentration rose ($[O_3]_0$ = 4.8 mg L^{-1}, pH = 7.6). Higher ozone dosage

([NDMA]$_0$ = 400 ng L^{-1}, pH = 7.6) and pH enhanced removal efficiency. Increasing pH was favorable for NDMA oxidation ([O$_3$]$_0$ = 0.1 mM, [NDMA]$_0$ = 400 ng L^{-1}). Inhibition of NDMA degradation was observed when a hydroxyl radical scavenger, t-butanol, was added during the ozonation process. Hydroxyl radicals generated from ozone played a critical role in the degradation of NDMA.

Table 4. Works on DBPs removal by ozone-based processes.

Target DBPs	Processes Applied	Reactor and Experimental Conditions	Main Results	Ref.
9 N-nitrosamines	O$_3$ O$_3$/H$_2$O$_2$	1 L glass beaker with magnetic stirring. 30 min degradation experiments; room temperature (21 °C); [N-nitrosamines] = 100 ng L^{-1}; [H$_2$O$_2$] = 2 mg L^{-1}; [O$_3$] = 1.5 mg L^{-1}	O$_3$/H$_2$O$_2$ process got the highest removal efficiency of 36.6% (NDMA)—91.4% (NDBA) among all the investigated methods. In comparison, ozonation merely removed less than 20% of N-nitrosamines (except NDphA for 29.3%).	[102]
Chloroacetic acids MCA DCA	O$_3$/H$_2$O$_2$ O$_3$ (pH = 11)	Planar falling film reactor. Seven UVA lamps (15W, 360 nm) fixed inside the reactor. Intensity UV light: 1 mW cm^{-2}; water flow rate: 1 L min^{-1}, volume 0.5 L; [CAA] = 1 mM; pH 3, pure gaseous oxygen rate of 10 L h^{-1}, ozone gas with 130 ± 5 mg L^{-1} ozone at a power of 30 W.	Chloroacetic acids are highly resistant towards direct ozonation in the darkness as only about 2% degradation was observed after 90 min treatment (pH 3). However, increasing the pH of the solution to 11 shows a dramatic improvement in the degradation efficiency and by the combination of O$_3$ with H$_2$O$_2$.	[106]
NDMA in ultrapure water and natural water (River Sanhaowu)	O$_3$ (pH = 7.6)	Batch and continuous experiments. A sealed cylindrical reactor with a volume of 5 L. The reactor was stirred mildly and set in the dark at room temperature (24 ± 1 °C). Buffer solution (5 mM phosphate and 1 mM carbonate, prepared with ultrapure water) and pH 7.6). [O3]$_0$ = 0.1 mM (4.8 mg L^{-1}), [NDMA]$_0$ = 400 ng L^{-1}.	Ozonation was an efficient process for NDMA degradation. The removal efficiency was affected by initial NDMA concentration; higher NDMA dosing required higher ozone utilization. NDMA oxidation was favored at high ozone dosage and high pH. NDMA ozonation under various pH as well as hydroxyl radical (HO$^\bullet$) inhibition experiments verified that HO$^\bullet$ generated from ozone dominated NDMA oxidation.	[105]
DCA in aqueous media.	O$_3$ O$_3$/UVC	The photo-reactor was a cylinder made of Teflon™ closed at both ends with two demountable, flat, circular windows made of quartz. Reactor length 5.2 cm, and the inner diameter 5.2 cm (V$_{Rirra}$ = 110.4 cm^3). Dissolved ozone concentrations of 1.46 to 2.1 × 10^{-7} mol cm^{-3}. 15 and 40 W lamps. [DCA]$_o$ = 20, 40 and 50 ppm; pH 3.5 ± 0.1.	O$_3$ or UVC by themselves did not result in appreciable decomposition of DCA. Conversely, the O$_3$/UV combination can be considered a suitable process for degrading DCA in water. The combination of ozone and UVC radiation produces a significant amount of hydrogen peroxide as an important reaction by-product.	[107]

<div align="center">

Table 4. *Cont.*

</div>

Target DBPs	Processes Applied	Reactor and Experimental Conditions	Main Results	Ref.
NDMA in distilled water.	O_3/UVC	A cylindrical glass reactor with 700 mL valid sample bulk. Low-pressure Hg lamp (8W, emission at 253.7 nm). $[NDMA]_0$ = 0.1 mmol L^{-1}, pH 6.0, irradiation 1000 W cm^{-2}, $[O_3]_0$ = 6.6 mg L^{-1}.	UV irradiation and the UV/O_3 combination are effective methods for NDMA removal from drinking water. The introduction of ozone into the UV process had little influence on the effectiveness of NDMA removal. However, it had a great influence on the formation of degradation products from NDMA. As the main products, DMA and NO^{2-} decreased markedly in the UV/O_3 process compared with UV irradiation.	[103]
DCA TCA	O_3 O_3/UVC O_3/H_2O_2 O_3/H_2O_2/UVC	A cylindrical stainless steel column (2 L vol.). Its diameter and height are 100 and 300 mm, respectively. Inside the reaction column is a quartz well containing a UV lamp with a diameter of 30 mm and a height of 300 mm—a 15-W low pressure mercury vapor lamp (254 nm). Ozone adding (mg min^{-1}): 0.3 $\pm$ 0.06; $[H_2O_2]_o$ = 2.5 mg L^{-1}; wavelength of UV lamp (nm): 254; power input of UV lamp (W): 15; reaction volume (L): 2; Initial DCA and TCA concentration (mg L^{-1}): 2.0.	O_3/UV showed to be more suitable for the decomposition of DCA and TCA in water among the six methods of oxidation. Decomposition of DCA was easier than TCA by AOPs.	[108]
NDMA in buffered deionized water and natural waters.	O_3 O_3/H_2O_2	500 mL glass bottle equipped with a dispenser. ($[NDMA]_0$ = 1 µM, $[O_3]_0$ = 40 µM, ratio of $[O_3]_0$/$[H_2O_2]_0$ = 2. 10 mM phosphate buffer.	In experiments with natural waters, NDMA could not be significantly oxidized during conventional ozonation. In the AOP O_3/H_2O_2, ozone doses of 160–320 mM ($[O_3]_0$/$[H_2O_2]_0$ = 2:1) were necessary for > 50% NDMA oxidation depending on the HO$^\bullet$ scavenging rates of the natural waters. Bromate formation may be the limiting factor for NDMA oxidation during ozonation and ozone-based AOPs in bromide containing waters.	[104]

On the other hand, it is well known that CAAs are widely present in water treated by chlorination processes and are resistant against ozonation in the darkness. The results obtained by Hama Aziz [106] showed that single ozonation was an inefficient method for the destruction of the CAAs as only about 2% degradation was observed after 90 min treatment (pH = 3). However, increasing the pH of the solution to 11 showed a dramatic improvement in the degradation efficiency. The fast decomposition of ozone molecule in alkaline solution (pH > 9) to generate powerful and non-selective hydroxyl radicals resulted in efficient degradation of organic pollutants. The addition of hydrogen peroxide to ozonation process, also improved monochloroacetic acid (MCA) and dichloroacetic

acid (DCA) degradation. Lovato et al. [107] studied DCA decomposition in aqueous media employing ozone and UVC radiation. The influence of various parameters, such as pollutant initial concentration (20–50 mg L^{-1}), radiation photon fluency rate at the reactor window and ozone dissolved concentration (1.46 to 2.1 × 10^{-7} mol cm^{-3}) was studied. Oozne or UVC by themselves did not result in appreciable decomposition of DCA within the studied reaction time (180 min). Conversely, the O$_3$/UV combination can be considered a suitable process for degrading DCA in water. Also, the combination of ozone and UVC radiation produces a significant amount of hydrogen peroxide as an important reaction by-product. Finally, Wang et al. [108] studied the decomposition of DCA and trichloroacetic acid (TCA) from water by means of single oxidants: Ozone, UV radiation; and by the AOPs constituted by combinations of O$_3$/UV radiation, O$_3$/H$_2$O$_2$, O$_3$/H$_2$O$_2$/UV radiation. Single O$_3$ or UV did not result in perceptible decomposition of HAAs within the applied reaction time (30 min). O$_3$/UV showed to be more suitable for the decomposition of DCA and TCA in water among the methods of oxidation tested.

6.2.2. Ozone Free Processes

Regarding other than classic ozonation treatments [109], Table 5 shows the most illustrative works dealing with advanced oxidation systems used for removal of DBPs in water supplies in the last 25 years.

Table 5. Works on DBPs removal by ozone free processes.

Target DBPs	Processes Applied	Reactor Configuration	Experimental Conditions	Ref.
THMs HAAs HANs HKs	Heterogeneous Fenton-like reaction + GAC filtration.	Pilot plant that includes mixing tank, mechanical flocculation tank, tube settler, sand filter column, intermediate water tank, heterogeneous Fenton column, active carbon column, water-producing water tank and automatic control device.	The design flow of single-set process is 2 m^3 h^{-1}. Poly aluminum chloride (PACL): 30 mg L^{-1}; dosage of H$_2$O$_2$ is 0.15 mM (5 mg L^{-1}).	[110]
MCA DCA TCA	UVA/TiO$_2$; UVA/BiOCl.	50 mL quartz reactor with a recycling water glass jacket. Light source a 500 W xenon lamp (simulated sunlight, containing 4% UV light).	T = 298 K, 40 mg BiOCl/TiO$_2$ (P25) (1g L^{-1}) dispersed in 40 mL model pollutant (20 mg L^{-1}). Reaction time: 60 min.	[111]
TCA	Advanced oxidation/reduction processes (AORPs): the vacuum UV (VUV; 185 nm + 254 nm).	A tubular glass photoreactor. Internal diameter of 25 mm and a height of 400 mm. Working vol of 100 mL. 5.7 W dichromatic low-pressure mercury UV lamp emitting UV at two distinct wavelengths (185 and 254 nm).	50 mg L^{-1} TCA, pH = 7; reaction time = 20 min.	[112]
THMs	Photo-Fenton process: UV/Fe/H$_2$O$_2$	Photochemical reactor equipped with a 254 nm low-pressure mercury UV-C lamp. Stirred with magnetic bar.	The average fluence rate was 0.93 mW cm^{-2}. T (25–31 °C). Reaction time: 60 min. CFe(II) = 2 mg L^{-1}. C$_{H2O2}$ = 20 mg L^{-1}. pH = 7.2–7.4; CHCl$_3$=163.6 µg L^{-1}, CH$_2$BrCl = 145.3 µg L^{-1}, CHBr$_2$Cl = 131.8 µg L^{-1}, CHBr3 = 124.6 µg L^{-1}.	[113]

Table 5. *Cont.*

Target DBPs	Processes Applied	Reactor Configuration	Experimental Conditions	Ref.
DCA TCA	A combination of Ferrate [Fe(VI)] and UV irradiation.	Self-made photoreactor (effective volume 0.5 L) equipped with a cooling system and placed on a magnetic stirrer. A 75-W low-pressure mercury UV lamp (λmax = 365, 310, and 254 nm, respectively) with 0.225 mWcm^{-2} intensity placed in the center of the reactor.	Experimental design: HAAs 100–1000 µg L^{-1}; pH: 3–9; Fe (VI) 10–40 mg L^{-1}; time 5–60 min.	[114]
4HANs 9THMs 4 HAcA 4 HAcAm Chloropicrin 500 nmol each	Reductive electrolysis.	Norit GAC (0.4 g) placed in a 1.5 cm × 4 cm cylinder constructed from sheet graphite to serve as the working cathode. It was then transferred to the cathodic chamber of an electrolysis cell.	A constant potential of -1000 mV vs. SHE was applied to the cathode, while cathodic chamber was continuously stirred with a Teflon-lined magnetic stir bar.	[115]
TCA	TiO$_2$ photocatalytic process combined with Fenton reagent.	Self-made cylindrical reactor with cool water recycling cloth and a UV light tube. The UV light (kmax = 254 nm) 50 W low pressure mercury lamp placed in the center of the reactor and equipped with a protective quartz tube.	Irradiation intensity was about 35 Mw cm^{-2}; TCAA aqueous solution (150 mL) containing TiO$_2$. Flow rate of 40 mL min^{-1} of O$_2$. [TCA] = 0.01 mmol L^{-1}, UV irradiation intensity= 35 mW cm^{-2}, [TiO$_2$] = 1.0 g L^{-1}, [Fe^{2+}] = 0.1 mmol L^{-1}, [H$_2$O$_2$] = 1.8 mmol L^{-1}, natural pH = 6.	[116]
TCA	Ferrate(VI) a multipurpose chemical, is used as coagulant and oxidant.	Self-made photoreactor (effective volume 0.5 L) equipped with a cooling system and placed on a magnetic stirrer.	Initial pH of solution (3–9), ferrate (VI) dosage (1–10 mg L^{-1}), contact time (5–60 min), trichloroacetic acid (100–1000 µg L^{-1}), and initial turbidity (1–10 NTU).	[117]
TCA	Fenton with TiO$_2$ photocatalytic oxidation.	Self-made photoreactor equipped with cool water recycling and a UV light tube. 50 W low-pressure mercury lamp placed in the center of the reactor and equipped with a protective quartz tube.	Irradiation intensity was about 35 mW cm^{-2}. TCA aqueous solution (150 mL, 2 mg L^{-1}). [TiO$_2$] = 1.0 g L^{-1}, [Fe^{2+}]$_0$ = 5.6 mg L^{-1}, m(Fe^{2+}):m(H$_2$O$_2$) = 1:10, intensity (UV) = 35 mW cm^{-2}, flow rate (O$_2$) = 40 mL min^{-1}. pH = 5.8 (without adjustment).	[118]
THMs EPA method 551/1	UV/ZnO/H$_2$O$_2$	A photoreactor equipped with 4 UV lamps in the reactor corners.	5 mL of concentrated solution (30%) H$_2$O$_2$; 0.5 g of ZnO in 100 mL of drinking water samples with constant reaction time (1hr) and UV irradiation.	[119]
4THMs	Sonophotolytic degradation.	Rectangular shape of stainless-steel reactor (L100, W100, H250) and ultraviolet lamps (4). Transducer was located in a bottom of the reactor.	The applied ultrasonic frequency was 500 kHz and the electrical powers were 0–52.55 W. Electrical power of each lamp was 10.5 W. 10 mg L^{-1} of THMs mixture (1.5 L).	[120]

Table 5. *Cont.*

Target DBPs	Processes Applied	Reactor Configuration	Experimental Conditions	Ref.
TCA	A sequential Fe^0 (zero valent iron) and BAC column system.	Fe^0 column and a BAC column made of glass, 30 cm in length and 3 cm in id.	1.2 µM TCA; pH of the feed water was approximately 6.0. The feed was initially treated by the Fe^0 column (BET was 1.3 m^2 g^{-1}) and then the BAC column.	[121]
17 DBPs (i.e., halomethanes, haloacetonitriles, halopropanones, chloral hydrate, and trichloroni-tromethane) at low concentration (μg L^{-1})	Electrochemical reduction using a resin impregnated graphite cathode.	Flow-through electrochemical reactor consisting of two polycarbonate frames (internal dimensions of $20 \times 5 \times 1.2$ cm).	The cathode potential from -700 to -900 mV vs. SHE.	[122]
TCA	High-frequency sonoelectrochemical methods.	A sonoreactor (0.5 L of volume) consisting of a cylindrical flask equipped with a cooling jacket where the electrodes (18 cm^2 on each side) were placed.	0.5 mM TCAA aqueous solution; 850 kHz ultrasonic irradiation, titanium cathode, and a platinized titanium anode.	[123]
MCA DCA TCA	Iron-based bimetallic particles: Two kinds of dry Pd/Fe nanoparticles (Pd/Fe^{-1} and Pd/Fe^{-2}).	A series of glass vials (60 mL). The vials were sealed with Teflon-lined rubber septa and aluminium cap.	Pd content = 0.1 wt%, Pd/Fe loading = 3 g L^{-1}, initial concentration of chloroacetic acid = 20 mg L^{-1}, and reaction time = 180 min.	[124]
4THMs	Photocatalysis with TiO^2 (slurry).	Photo-Cat Lab consists of an air compressor for oxygenation of the system; eight 75-watt, low-pressure, mercury arc bulbs in series; and a submicron-pore-size ceramic membrane filter that produces TiO2-free effluent.	Batch configuration. Process flow rate of 25 L min^{-1}; initial system volume of approximately 16 L. the average intensity of the UV bulbs was approximately 7.0 Mw cm^{-2}. 400 mg L^{-1} TiO_2.	[86]
MCA DCA TCA	Photocatalytic degradation over various bare and silver-deposited Degussa P25 TiO^2 particles.	A medium scale (V = 2.5 dm^3) photochemical reactor.	Irradiation performed under anaerobic and aerobic conditions. Flow rate of gases (air and Ar) was 40 dm^3 h^{-1}; light source (40 W, λmax = 350 nm), initial concentration of TiO_2 (rutile, anatase, P25) was 1 g dm^{-3}. initial concentration of MCA, DCA, and TCA was adjusted to be 1 mM.	[125]
DCA TCA	Electrochemical treatment (dehalogenation).	Packed-bed flow reactor. The reactor was composed of two glass compartments separated by a cationic exchange membrane.	Initial concentration of HAAs 10.5 mM. Flow rate: 1 mL min^{-1}; electrolysis potential: $-0.200-$$-0.400$ V (vs. SCE).	[126]

Table 5. *Cont.*

Target DBPs	Processes Applied	Reactor Configuration	Experimental Conditions	Ref.
4THMs	Ultrasonic (US) irradiation, hydrogen peroxide (H_2O_2), Fenton's oxidation, US/H_2O_2 and $US/H_2O_2/Fe^2$	200 mL conical closed glass reactor kept in a temperature-controlled bath	THMs solute mixture, at 10 mg L^{-1} for each compound, in deionized water. Initial pH adjusted to 3.5 by 1N H_2SO_4. 250–500 mg L^{-1} H_2O_2 and 20–40 mg L^{-1} $Fe^{(2+)}$.90 min reaction.	[127]
4THMs Iodoform (CHI_3)	Sonodegradation	200 mL conical closed glass reactor kept in a temperature-controlled bath	100 mL aqueous solution at 25 °C. frequency of 20 kHz; acoustic intensity 3.75 W cm^{-2}; initial pH 5.4–5.8.	[128]
4 THMs CHI_3	Sonodegradation	200 mL conical closed glass reactor kept in a temperature-controlled bath.	Ultrasonic frequency of 20 kHz. presence of inorganic components. increase the ultrasonic intensity, from 0.9 to 7.0 W cm^{-2}. the power density, from 0.123 to 0.368 W mL^{-1}.	[129]
4THMs CHI_3	Ultrasonic irradiation	200-mL conical closed glass reactor kept in a temperature-controlled bath.	Ultrasonic irradiation 20 kHz. Acoustic intensity 3.75 W cm^{-2}, and the power density 0.184 W mL^{-1}. initial pH 5.4–5.8 without buffer addition. Initial conc. of THMs 10 mg L^{-1}.	[130]
MCA DCA TCA	Photodegradation in the presence of titanium dioxide suspensions.	Reaction vessel 350-mm long quick fit condenser tube. Connections to a thermostatic water bath. Two mercury vapor greenhouse lamps were used to mimic sunlight radiation ($\lambda >$ 400 nm).	250 cm^3 of approximately 0.1 mol dm^{-3} solutions of the HAAs. 0.1 g of finely powdered titanium dioxide was added as a photocatalyst.	[131]
MCA DCA TCA MBA (bromoacetic acid)	Iron Fe (0) particles.	Batch experiments. 125 mL serum bottles.	Aqueous HAA solution buffered at pH 7.5 with 50 mM deoxygenated MOPS. 0.3 g of iron and rotated at 45 rpm. Different Initial HAA Concentrations: 15–405 μM.	[132]
TCA	Ultraviolet (UV) photolysis, ultrasound (US) sonolysis and their combination.	Quarz reactor immersed in a thermostathic bath. Two UV lamps located on either side of the sample reactor.	TCA (2.89×10^{-4} M). Vreacción 36 mL. pH 3.5; T = 30 °C.	[133]
HAAs: TCA TBA (tribromoacetic acid) CDBA (chlorodibromoacetic acid) BDCA (bromodichloroacetic acid)	Reduction with zerovalent iron (Fe^0).	Batch experiments (glass serum bottle).	0.5 g of Fe(0) in 36 mL of DI water. Desired conc. (100–200 μM). RT up to 94 h. No pH buffer employed. Initial pH values ranged 3.62 to 4.14 and final rose to 5.60 to 6.23.	[134]

Table 5. *Cont.*

Target DBPs	Processes Applied	Reactor Configuration	Experimental Conditions	Ref.
4THMs	Fentons Reagent.	The reactors consisted of 54 mL Pyrex test tubes filled to capacity with stock THM solution, plus Fenton's reagent, and sealed with septum-fitted screw caps.	pH = 3.5 [THM]$_o$ = 37.2 µg L^{-1} each [H$_2$0$_2$] = 3.7 Mm; [Fe^{2+}] = 0.19 mM.	[135]
TCA	Photocatalysis with TiO$_2$ and thermal decomposition.	Photocatalysis: The reactor equipped with a suprasil-glass adapter for the UV-lamp. Reaction vessel has inlet and outlet ports of Teflon tubes for bubbling air and N$_2$. The apparatus was closed. Thermal: A double-walled thermostated jar of glass was used.	0.5 g TiO$_2$ were suspended in 500 mL aqueous solution containing 10 mmol (20 mM) of trichloroacetic acid. 20 W-Hg low pressure lamp.	[136]

As it can be seen from Table 5 among the various harmful DBPs removed from water supplies, HAAs are the most investigated. As it is known, they are the second most important DBPs after THMs and are highly stable and non-volatile compounds. Trichloroacetic acid (TCA) and dichloroacetic acid (DCA), the two main fractions of HAAs, are important because of their potential risks to human, aquatic, and plant life. Thus, realizing the danger of chloroacetic acids, different advanced oxidation techniques or electrochemical methods are proposed to eliminate them from water. A great deal of effort has been devoted to HAAs removal by biological activated carbon (BAC) processes. However, it has generally been found that while mono- and di-HAAs are relatively easily biodegradable, tri-HAAs are recalcitrant to biodegradation [121].

The breaking of C-Cl bond can result in the degradation of chloroacetic acids. TCA and degradation by-products can be reductively removed by zero valent iron (ZVI) or bimetallic particles. Reduction of HAAs through dehalogenation by using zero valent iron (Fe^0) or other element-doped Fe^0 (such as the bimetallic Pd/Fe, Cu/Fe and Si/Fe) have been reported [134]. In contrast to the order of HAAs biodegradability, the susceptibility of HAAs to Fe^0 reduction normally follows the order of tri-HAAs, di-HAAs, and lastly mono-HAAs. Di- and mono-HAAs were usually observed as the dehalogenation intermediates or end-products [121]. However, the potential release of metal ions affects water quality, leading to secondary pollution in long term. Electrochemical reductive dechlorination is efficient for TCA, and the stepwise dechlorination from TCA and DCA to MCA is achieved [126]. Because the degradation of TCA, DCA, or MCA strictly depends on current density, electrodes are easily corroded by high current in this electrochemical process. To increase the degradation efficiency of TCA and simultaneously protect the electrodes, Esclapez et al. [123] have developed a hybrid sonoelectrochemical process at a low current density and obtained satisfying dechlorination efficiency. Summarily, the break of C-Cl bond is an efficient degradation channel for TCA in ultrasonic (and sono-photolytic degradation [133]) or electrochemical or special reductive reagents reaction, and Cl$^-$, DCA, MCA and CO$_2$ are the major by-products in aqueous solution [116].

In addition, the breakage of C-C bond can also produce the removal of chloroacetic acids. In this sense, decomposition of mono-, di-, and trichloroacetic acid in aqueous titania suspensions was studied by several researchers [111]. It has been concluded that two types of reactions may be responsible for the TiO$_2$-mediated photodegradation of chloroacetic acids: (1) Direct reactions between the photogenerated charge carriers and the organic molecules and (2) reactions of hydroxyl radicals or other oxygen containing radicals with the organic molecules [125]. MCA and DCA are readily decomposed over UV-irradiated TiO$_2$ catalyst in aqueous media to form CO$_2$ and HCl. On the other hand,

using bare TiO_2, TCA is degraded with a very low efficiency [111]. TCA has no C–H bond, and such a molecule has been found to be hardly reactive in TiO_2-based photocatalytic systems. For that reason, an efficient Fenton assisted TiO_2 photocatalytic hybrid process have developed [116,118]. These works report that exists a noticeable synergetic effect dominantly caused by the oxidation– reduction recycling reaction of $Fe^{3+} \leftrightarrow Fe^{2+}$ between Fenton and TiO_2 photocatalytic oxidation. Also, an AOP based on combination of Ferrate with UV illumination was investigated in terms of kinetics, by-products analysis and application of surface methodology for degradation of CAAs [114].

On the other hand, the most significant group of DBPs formed during chlorination is THMs. Compounds of this group: Chloroform, bromodichloromethane, chlorodibro-momethane, and bromoform, were recognized as potential human or animal carcino-gens [119], as detailed before. AOPs are promising techniques to efficiently and effec-tively convert these compounds into better biodegradable or less harmful substances. Several types of AOPs have been developed using Fenton Reagent [129], photo-Fenton pro-cess [113], UV/ZnO nanocatalyst/H_2O_2 [119], photocatalysis with titanium dioxide [86], ultrasonic degradation [127–130], and sonophotolytic process [120].

Finally, from Table 5, it can be concluded that major ozone-free processes tested for DBPs removal have been photocatalysis and sonodegradation/sonophotolytic degrada-tion. From an applied point of view, Gerrity et al. [86] studied different scenarios using a pilot-scale TiO_2 photocatalysis reactor. DBPs may form in clear wells prior to distribution that could also be destroyed before the water is released into the distribution system. Since photocatalysis will destroy a chlorine residual, the water would have to be rechlorinated prior to discharge. The authors concluded that when focusing on photocatalytic destruction of DBPs rather than precursors and formation potential, several problems still exist. Opti-mization of this process should be considered in future studies to address some relatively high energy requirements and the need of rechlorination. In general, this technology has a number of promising aspects but should be considered on a case-by-case basis. Regarding to the high-frequency sonoelectrochemical methods for DPBs mitigation have been applied in a laboratory scale, Esclapez et al. [123] claim that the use of the electricity as unique reactant and the mineralization of the trichloroacetic acids and its by-products make the sonoelectrochemical technology a serious alternative to current technologies.

7. Elimination of DBP Precursors by Catalytic Ozonation Processes

In this section after description of some features about proposed mechanisms of catalytic ozonation, literature about removal of DBP precursors or what is called DPBFP is reviewed.

7.1. Catalytic Ozonation

Several strategies have been proposed to efficiently increase the generation of hy-droxyl radicals during ozonation favoring indirect reactions. Many groups have started to investigate a new ozone advanced oxidation process named catalytic ozonation, that is, the simultaneous use of ozone and substances (catalysts) that activate its decomposition to increase the formation of hydroxyl radicals and also to increase not only the removal of pollutants from water but also the mineralization of the total organic carbon content [137]. Catalytic ozonation was starting, in fact, in the middle of 20th century, in 1949, with the use of soluble catalysts, that is, with metal cations such as Co^{2+} [138]. However, this kind of process was not feasible from health and environmental aspects since these catalysts, as heavy metals, are contaminants. Hence, studies were oriented to the use of solid ma-terials of different nature, what it is called heterogeneous catalytic ozonation. It has to be highlighted; however, that also what is called homogeneous catalytic ozonation is a heterogeneous process since gaseous ozone is transferred to the water to react. Then, the catalytic ozonation process where the catalyst is a solid was named the heterogeneous catalytic ozonation process. According to WOS database in the last 10 years about 400 pub-lications have been reported in literature about heterogeneous catalytic ozonation. Three

main families of catalyst types have mainly been used since then: Metal oxide catalysts, carbonaceous materials and ceramic materials [139]. More recently, however, a new type of potential catalyst has appeared: Metal based organic frameworks (MOFs) of high specific surface area and tunable pore structure [140,141]. In addition to this number of publications some review works [142–145] have also appeared highlighting the main aspects concerning this process.

As a summary, it can be said that works already published deal with synthesis and characterization of catalysts, application of the new catalyst to remove some given organics taken as model compounds, mechanism of the process, a few of them study the kinetics and some also give data on toxicity, activity, and stability of the catalysts. In addition to the diversity of results obtained which is the consequence of the different methodologies, equipment, analytical procedures, etc., applied, the most relevant fact is the high variation in the reaction mechanism proposed which is also due to the variability of methods of catalyst preparation, analytical techniques, etc., and the lack of knowledge about catalyst stability, by-products formed and ecotoxicity. In fact, the mechanism of catalytic ozonation can be due to direct reactions of ozone or to reactions of hydroxyl radicals coming from the decomposition of ozone on the catalyst surface. Usually, it is expected that the mechanisms of catalytic ozonation fulfilled some of the following requirements:

- Ozone adsorbed on the surface of the catalysts is decomposed into reactive species.
- Organic molecules are adsorbed on the surface of the catalysts with subsequent ozone attacks.
- Both ozone and organic molecules are adsorbed on the catalyst surface and surface reactions take place.

Steps of these mechanisms follow the well-known LHHW or ER mechanisms [146]. These mechanisms, as indicated above, may imply both the formation of hydroxyl radicals or direct reactions between adsorbed ozone and target compounds. For instance, Liu et al. [147] proposed the following simple mechanism for the catalytic ozonation of nitrobenzene with a Zn/SiO_2 catalyst:

$$ZnO/SiO_2 + O_3 \rightleftarrows S\text{--}HO \tag{21}$$

$$S\text{--}HO \rightarrow Fe_3O_4/CoO/Al_2O_3 + HO^\bullet \tag{22}$$

$$HO^\bullet + pCNB \rightleftarrows Products \tag{23}$$

where it is seen that hydroxyl radicals are formed as adsorbed species, then they are release to water bulk to oxidize the organic compound. On the contrary, Andreozzi et al. [148] for the catalytic ozonation of oxalic acid with a manganese oxide catalyst reported the adsorption of the target compound (oxalic acid) to form a manganese oxalate complex that then reacts with dissolved ozone, that is, as a surface direct reaction:

$$Mn(III)OH_2^+ + C_2O_4^{2-} \rightleftarrows MnC_2O_4^- + H_2O \tag{24}$$

$$MnC_2O_4^- \rightleftarrows Mn^{2+} + CO_2^{\bullet-} + CO_2 \tag{25}$$

$$MnC_2O_4^- + O_3 + 2H^+ \rightarrow 2CO_2 + O_2 + MnOH_2^+ \tag{26}$$

Other examples of catalytic ozonation mechanisms have been reported with hydroxyl radicals or ozone (adsorbed or in solution) as main oxidants. Martins and Quinta-Ferreira [149] proposed the following LHHW mechanism for the Mn-Ce-O catalytic ozonation of phenolic acids:

$$Mn\text{--}Ce\text{--}O + Phenolic\ acids(P) \rightleftarrows P\text{--}S \tag{27}$$

$$O_3 + S \rightleftharpoons O_3 - S \tag{28}$$

$$P-S + O_3 - S \rightarrow \text{Products} + Mn-Ce-O. \tag{29}$$

Mechanism proposals are not limited to metal oxide catalysts. For example, Ikhlaq et al. [150] studied the catalytic ozonation of some pharmaceuticals, volatile organic compounds and carboxylic acids with a ZSM-5 zeolite constituted by $xSiO_2/yAl_2O_3$. They proposed a LHHW mechanism as shown in Scheme 6 where ozonation also goes through a direct surface reaction between ozone and organic adsorbed species.

Scheme 6. Mechanism of catalytic ozonation over zeolite ZSM-5 [150] (Reprinted with permission of Appl. Catal. B: Environ, 154-155, Ikhlaq, A.; Brown, D.R.; Kasprzyk-Hordern, B., Catalytic ozonation for the removal of organic contaminants in water on ZSM-5 zeolites, pg110-122. Copyright (2014), with permission from Elsevier).

On the opposite side, Zao et al. [151] reported a hydroxyl radical formation and reaction when using a cordierite material ($2MgO-2Al_2O_3-5SiO_2$) to catalyze the ozonation of nitrobenzene:

$$\text{Catalyst}-OH + O_3 \rightarrow HO^\bullet \tag{30}$$

$$HO^\bullet + NB \rightarrow \text{Products} \tag{31}$$
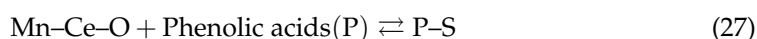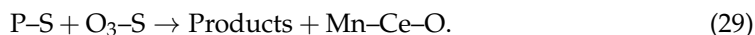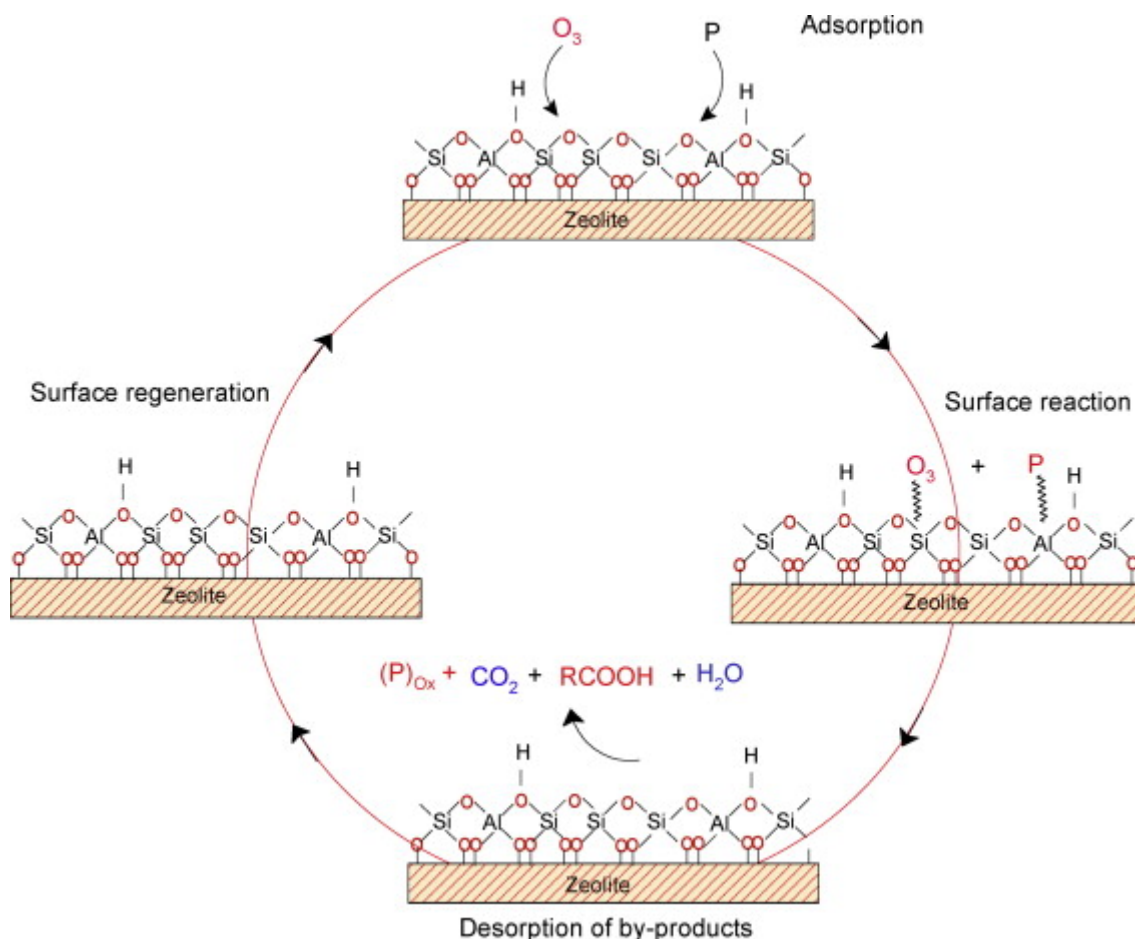
The authors confirmed the presence of hydroxyl radicals with the Spin trapping/ EPR technique.

Many examples are also given in literature on the use of carbonaceous materials such as activated carbon, multi-walled carbon nanotubes, xerogels, and graphene oxide [152–156] where these materials were used as main catalyst or as support of metal oxides. Again, discrepancies are observed in the mechanism proposed. Thus, some au-

thors have reported that some functional groups of the catalyst surface can be modified by ozone, by enhancing the specific surface area, and decreasing the total volume of the catalyst [157]. However, some others showed that, once the modified carbon was ozonated, its specific surface area was slightly diminished, and the total volume of the pores remained unchanged [158]. Another important issue is the in situ regeneration of the catalyst, or the predominance of catalytic properties and adsorption–oxidation processes in the catalytic ozonation process [157]. Other works have indicated that ozonation reduces the catalytic properties of activated carbon due to a decrease of basic groups and an increase in the number of oxygenated surface functional groups such as hydroxyl and carboxylic acid groups and nitro aromatic compounds [159].

Most of the research works have been carried out with the objective of wastewater treatment and with different organic pollutants such as dyes, pharmaceuticals, personal care products or model molecules such as oxalic and phenol. Regarding to DBP precursors or NOM removal, Table 6 summarizes the main results of reports on catalytic ozonation for drinking water highlighting those in which DBPs are analyzed.

7.1.1. Catalysts

The main catalytic materials used for NOM or humic/fulvic acids removal were metal oxides, ceramic materials, and carbonaceous materials and the properties more frequently analyzed were composition (by XRD, XRF, or ICP), textural properties by N_2 adsorption-desorption, pHpzc, and crystallinity by XRD. Some studies have also reported surface composition by XPS or FTIR.

Among metal oxides, titanium dioxide, TiO_2 has been used both in slurry reactors in the form of suspended nanoparticles (mainly the commercial TiO_2 P25) or supported in different materials. The characterization of powder TiO_2 P25 has been widely studied and the main features were 50 $m^2\,g^{-1}$ BET surface area, anatase/rutile ratio 80/20, crystallite size 21 nm and pHpzc = 6.7 [167]. These studies [175] probed that at the conditions used, no improvement was observed in THMFP removal from surface water compared to ozonation, but less brominated species were formed in catalytic ozonation. On the contrary, in another work [173], with higher catalyst loading but synthetic humic acid solution, a positive effect in the THMFP removal of water treated by catalytic ozonation was observed. The catalyst loading and the composition of NOM may play a key role in the process (more information in Sections 7.1.3 and 7.1.4).

TiO_2 has also been used supported onto different materials, mainly Al_2O_3, clays, and zeolites. Many of these supports have also catalytic activity for ozone decomposition [143]. For the first time, Allemane et al. [187] studied TiO_2/Al_2O_3 combined with ozone for the degradation of fulvic acid and, at high O_3 doses, the catalytic activity was demonstrated but no DBPs were analyzed. In the same line, Volk et al. [186] observed higher mineralization of fulvic acid using TiO_2/Al_2O_3 than ozone alone with a decrease in the chlorine demand of the treated water though no DBPs were detected. No characterization studies were reported here. On the contrary, Gracia et al. [184,185] compared the catalytic activity of TiO_2 supported on Al_2O_3, attapulgyte (a clay) and silica gel for the degradation of NOM. The best results in terms of mineralization of precursors were obtained with the TiO_2/Al_2O_3 catalyst whose main characteristics can be observed in Table 6, highlighting again the importance of adsorption mainly related with the role of Al_2O_3, BET surface area, pH_{pzc} of the solid, characteristics of NOM and pH of the solution. Only the works reported by Chen et al. [177] and Chen and Wang [170], using the same experimental set up, checked the efficiency of TiO_2/Al_2O_3 in the DBPs formation potential elimination from surface water, obtaining a significant reduction up to 50% of THMFP and HAAFP in the water treated by catalytic ozonation at the conditions tested (see Table 6).

Table 6. Works on catalytic ozonation of DBPs precursors.

Target Water	Catalyst and Main Properties	Reactor and Experimental Conditions	Main Results	Ref.
Humic acid	α-Al_2O_3 SBET = 45.8 m^2 g^{-1} Pore volume 0.162 cm^3 g^{-1} pHpzc = 4.2 Crystallite size 41.7 nm Mn_2O_3 SBET = 15.6 m^2 g^{-1} Pore volume 0.008 cm^3 g^{-1} pHpzc = 5.9 Crystallite size 15.9 nm XPS before and after ozonation indicates the change in the oxidation state of Mn and Al in both materials and the hydroxylation of the surface.	Semi-batch column reactor H = 68 cm, d = 8 cm V = 1 L Ozone flow rate = 0.063 m^3 h^{-1} C_{O3l} = 4–8 mg L^{-1} Catalyst loading 0.1–0.5 g L^{-1} C_{HA} = 50 mg L^{-1} T = 25 °C pH = 5.5	Al_2O_3 nanocatalysts showed better performance than Mn_2O_3 in HA removal using lower ozone dosage due to favorable surface charge. Mn_2O_3 decomposes O_3 faster tan Al_2O_3. Adsorption of HA contributes to its catalytic ozonation. Higher adsorption capacity of Al_2O_3. Some deactivation observed in 4 consecutive runs. No post-chlorination. No DBPs were analyzed.	[160]
Humic acid	Fe coated pumice Prepared from natural pumice with $FeCl_3$ impregnation. BET, TEM, XRD, DLS, FTIR and pHpzc XRD: α-FeOOH Particle size 200–250 nm. SBET = 10.56 m^2 g^{-1} pHpzc = 7.13	Semi-batch column reactor V = 1 L Ozone dose 0.333 g min^{-1} C_{O3ge} = 6–12 mg L^{-1} Catalyst loading 25–100 mg L^{-1} C_{HA} = 10 mg L^{-1} T = 22 °C pH = 3–10, 6.72	Improved efficiency of catalytic ozonation (80% DOC removal vs. 20% ozonation). Contributions: *Surface adsorption 21.3% *$HO^\bullet$ radicals 66.2% *Sole ozonation 12.5% Scavenger experiments with t-BuOH and phosphate confirmed the role of hydroxyl radicals in solution. Iron leaching < 13 µg L^{-1} No post-chlorination. No DBPs were analyzed.	[161]
Humic acid	Ce-Ti composites Sol-gel synthesis Ce/Ti = 0.2–1.0 Calcination at 600 °C XRD showed cubic fluorite CeO_2 structure. Crystallite size decreased with Ce content, increasing SBET (not reported).	Semi-batch column reactor (h = 500 mm; D = 60 mm) V = 1 L Q = 0.5 L min^{-1} 30 min reaction time C_{O3ge} = 16.91 mg L^{-1} Catalyst loading 0.3 g L^{-1} C_{HA} = 30 mg L^{-1} COD = 260 mg L^{-1} pH = 6.91	The highest efficiency was found for Ti-Ce (1/0.8) composition due to its high surface area and low pHpzc. Increased the ozone efficiency by 62%. Apparent first order rate constants for homogeneous (0.054 g L^{-1} min^{-1}) vs. heterogeneous (0.067 g L^{-1} min^{-1}). Less of 50% heterogeneous contribution. The distribution of molecular weights tends to lower values in catalytic ozonation. No post-chlorination. No DBPs were analyzed.	[162]

Table 6. *Cont.*

Target Water	Catalyst and Main Properties	Reactor and Experimental Conditions	Main Results	Ref.
Humic acid	Fe coated Zeolite (ICZ) Zeolite clinoptilolite Synthesis by impregnation and precipitation at basic pH, dried at 105 °C. SEM and XRD analyses showed 2.132% Fe and the ICZ morphology. Granular activated carbon (GAC, from Merck) Dp = 1.5 mm SBET = 971.7 m^2 g^{-1}	Semi-batch stirred reactor V = 2 L 1 h reaction time C_{O3l} = 10 mg L^{-1} (monitored) Q = 2 L min^{-1} Catalyst loading 0.75 g L^{-1} C_{HA} = 30 mg L^{-1} DOC = 8.52 mg L^{-1} pH = 6.50–11	DOC removal by ozone alone was 21.4% and increased up to 62% for ICZ-O_3 and 48.1% for GAC-O_3. The efficiency of the process was also tested with different humic acid fractions (<100 and <50 kDa). Fe leaching was analyzed near 60 µg L^{-1} at the beginning of the reaction. Kinetics was studied and showed the efficiency of both catalysts. Better results with ICZ in general. No post-chlorination. No DBPs were analyzed.	[163]
Humic acid	ZnO (Sigma Aldrich) 99.9% Density 5,61 g cm^{-3} Particle size < 5 µm	Semi-batch stirred reactor V = 2 L Inner diameter 12 cm Ozone dose 0.190 mg min^{-1} 2 h reaction time Catalyst loading = 0.25 g L^{-1} DOC_0 = 5.86 mg L^{-1} pH = 5.33 Ambient temperature	The degradation of HA by catalytic ozonation was much more effective (60% mineralization) than ozonation alone (30%). DFT modelling showed O_3 disproportionation on the ZnO surface to form reactive oxygen species. No post-chlorination. No DBPs were analyzed.	[164]
NOM River water (Harbin Mo Panshan, Harbin, China)	FeOOH-goethite pHpzc = 6.8 SBET = 97 m^2 g^{-1} Average pore size 23.2 nm CeO_2 pHpzc = 6.7 SBET = 116 m^2 g^{-1} Average pore size 12.6 nm MgO pHpzc = 11.1 SBET = 105 m^2 g^{-1} Average pore size 16.7 nm SEM and XRD analyses to confirm structure and morphology.	Ozonation in semi-continuous mode T = 20 °C V = 1 L Catalyst loading 100 mg L^{-1} Qg = 150 mL min^{-1} DOC_0 = 2.68 mg L^{-1} pH = 7.53 tert-BuOH as $HO^\bullet$ scavenger	UV254 removal was mainly from direct ozonation. CeO_2 was the best system in UV254 removal (69%). FeOOH (27.24%) and MgO (18.66%) better in mineralization than O_3 alone (10.7%) and O_3/CeO_2 (2.24%). Adsorption plays a negative effect in mineralization. Fractionation of DOC. Catalytic stability was high, with very low ions leaching (up to 11 µg L^{-1}) and SEM, XRD of used catalysts similar than for fresh samples. No post-chlorination. No DBPs analysis.	[165]

Table 6. *Cont.*

Target Water	Catalyst and Main Properties	Reactor and Experimental Conditions	Main Results	Ref.
Oxalic acid (OA) Dimethyl phthalate (DMP) and NOM surface water (Jingmi Cannel, Beijing, China)	RuO_2/ZrO_2-CeO_2 pHpzc = 6.0 Powder (less than 4 um) and pelletized (2 mm) 0.5 wt.% Ru SBET = 170 m^2 g^{-1} By XRD: Cubic CeO_2, RuO_2 detected. $RuO_2/Al2O_3$ 0.5–5 mm 0.1 wt.% Ru SBET = 113–183 m^2 g^{-1} RuO_2/AC Particle size 6–10 mesh 1–1.5 mm 0.5 wt.% Ru AC ash content 7.8 wt.% (mainly SiO_2, Al_2O_3 and Fe_2O_3) SBET = 945.2 m^2 g^{-1}	Cylinder reactor, bubble column D = 5 cm L = 120 cm V = 1 L Semi-batch for catalytic activity: Cat. Dosage = 2 g L^{-1} Ozone dosage 116 mg h^{-1} Qg = 400 mL min^{-1} Continuous operation for stability tests: Qw = 20 mL min^{-1} Hydraulic time 60 min Experiment time 48 h Cat. Dosage = 40 g TOC_0 = 2.25–3.20 mg L^{-1} pH = 7.2–8.5 T = 15 °C Chlorination: pH = 7 Excess of chlorine T = 25 °C, 7 days	High efficiency in catalytic ozonation for OA and DMP, adsorption of intermediates. NOM mineralization but high adsorption capacity is observed. RuO_2/ZrO_2-CeO_2 had higher stability than Ru/AC and Ru/Al_2O_3. Post-chlorination and DBPs. HAAFPs removal improved from 38–57%. THMFPs from 50–64% but O_3 alone reacts fast with THMs precursors.	[166]
Humic acid and NOM Porsuk River (Turkey)	Degussa P-25 TiO_2 80/20 anatase/rutile SBET 50 m^2 g^{-1} Crystal size 21 nm.	Semi-batch stirred reactor V = 2 L Inner diameter 12 cm 2 h reaction time DOC (HA) = 5.8 mg L^{-1} DOC (NOM) = 3.76 mg L^{-1} pH = 5.5–6.0 Catalyst dose 0.25–1 g L^{-1} Ambient temperature O_3 dose 0.190 mg min^{-1}	DOC removal of humic acid was highly improved by catalytic ozonation (from 30% to 70%). The process was less effective with NOM. Adsorption plays an important role. By DFT modelling, $HO^\bullet$ are supposed to be formed from adsorbed O_3 and its decomposition onto TiO_2 surface in the presence of H_2O. No post-chlorination. No DBPs were analyzed.	[167]

Table 6. *Cont.*

Target Water	Catalyst and Main Properties	Reactor and Experimental Conditions	Main Results	Ref.
Humic acid	CuO (nanopowder, Sigma-Aldrich) $SBET = 0.64 \text{ m}^2 \text{ g}^{-1}$ Pore volume = $0.002 \text{ cm}^3 \text{ g}^{-1}$ Monoclinic structure.	Semi-batch stirred reactor V = 2 L Inner diameter 12 cm Ozone dose $0.190 \text{ mg min}^{-1}$ 60 min reaction time DOC = 5.86 mg L^{-1} pH = 5.5–6 T = 23 °C Catalyst dose 0.25 g L^{-1}	CuO presented catalytic activity in the ozonation of humic acid, with 80% of DOC removal in a short time. It was fond that adsorption, desorption, oxidation and chelating reactions took place in solution. The DFT approach proposed that $HO^{\bullet}$ radicals formed in the catalyst surface initiate the heterogeneous catalytic ozonation reaction. No post-chlorination. No DBPs were analyzed.	[168]
Bromide in UP water Humic acid	TiO_2 P25 Anatase/rutile 80/20 Nano-SnO_2 Tetragonal pase Dcrystal) 9.7 nm	Cylindrical bubble column (d = 8 cm, h = 40 cm) V = 2 L Vr = 1.5 L Br- = 0.40 mg L^{-1} C_{O3} liquid = 3.38 mg L^{-1} pH = 6 Ccat = 100 mg L^{-1} T = 26 °C CHumic acid = $0–3.0 \text{ mg L}^{-1}$	Analysis of the BrO_3^- formed by O_3 and catalytic O_3 The presence of both catalysts reduces the formation of BrO_3^- during ozonation. Inhibition of BrO_3^- formation with increasing humic acid concentration. No other DBPs analyzed.	[169]
NOM surface water (Wu-Lo River) pCBA	Fe-Mn oxide 23.0 % Fe 8.17% Mn 68.77% O $SBET = 262.0 \text{ m}^2 \text{ g}^{-1}$ pHpzc = 5.9 Acidic groups = 181 ueq g^{-1} Basic groups = 636 TiO_2-$\alpha Al_2 O_3$ 7.69% Ti 29.29% Al 63.02% O $SBET = 14.5 \text{ m}^2 \text{ g}^{-1}$ pHpzc = 8.3 Acidic groups = 2074 ueq g^{-1} Basic groups = 0.71 ueq g^{-1}	Fluidized bed reactor Semi-continuous operation D = 6 cm L = 38 cm Gas flow rate 100 mL min^{-1} Vr = 1.04 L Reaction time 60 min O_3 concentration 2.5 mg L^{-1} Catalyst loading 1.25 g L^{-1} $DOC_0 = 8.22–11.26 \text{ mg L}^{-1}$ pH = 8.15–8.57 THMFP = $216–266 \text{ µg L}^{-1}$ HAAFP = $509–553 \text{ µg L}^{-1}$ T = 20 °C Chlorination: According to SM 2350 Residual chlorine $0.2–1 \text{ mg L}^{-1}$, pH 7, 48 h contact time.	Kinetics of O_3 decomposition, Rct Fe-Mn catalyst presented high hydroxyl radical exposure. Fe-Mn catalyst showed a best performance in O_3 decomposition, DOC (30%) and UV254 (85%) removal. Post-chlorination and DBPs analyses demonstrated that catalytic ozonation reduced THMs (70%) and HAA9 (75%) formation.	[170]

Table 6. *Cont.*

Target Water	Catalyst and Main Properties	Reactor and Experimental Conditions	Main Results	Ref.
NOM-surface water polluted with DOC from domestic and agricultural effluents (Wu-Lo River, Pintung, Taiwan)	α-FeOOH goethite Precipitation synthesis SBET = 61.9 m^2 g^{-1} SEM morphology micro needles.	Fluidized bed reactor Semi-continuous operation D = 6 cm L = 38 cm Gas flow rate 50 mL min^{-1} Vr = 1.04 L Reaction time 60 min O$_3$ concentration 2.5 mg L^{-1} Catalyst loading 0.5–1.5 g L^{-1} DOC$_0$ = 9.21 mg L-1 pH = 7.6 T = 20 °C Chlorination: According to SM 2350 Residual chlorine 0.2–1 mg L^{-1}, pH 7, 48 h contact time.	Higher efficiency in DOC removal by catalytic ozonation. Post-chlorination and DBPs No BrO$_3^-$ detected, THMs and 9HAAs highly reduced by catalytic ozonation + biofiltration. The bromine incorporation factor of THMs and HAAs increases with catalyst dosage.	[171]
Humic acid Bromide	Ferrate (VI)	Homogeneous ozonation Flasks, Vr = 0.5 L Ferrate dose 0.1–5 mg L^{-1} C$_{Br-}$ = 100–1500 µg L^{-1} DOC$_0$ = 0.1–10 mg L^{-1} C$_{O3}$ = 1.5–4 mg L^{-1} T = 5–40 °C pH = 3–11	Ferrate (VI) reduced BrO$_3^-$ during catalytic ozonation. Humic acid content decreased bromate formation. No post-chlorination. No other DBPs were analyzed.	[172]
Humic substances in phosphate buffer.	Degussa P-25 TiO$_2$ 80/20 anatase/rutile SBET 50 m^2 g^{-1}	Catalytic ozonation/Ultrafiltration Reactor membrane module and mixing tank. Injection of O$_3$ in a Y-type mixer. Gas flow rate 50–150 mL min-1 CO$_3$ gas = 2.5–10 mg L^{-1} TiO$_2$ loading 0–5 g L^{-1} DOC$_0$ = 8 mg L^{-1} pH = 2 (O$_3$ decomposition) Chlorination: SM 2350 (residual chlorine 0.5–2 mg L^{-1} after 48 h, pH 7).	Reduction of THMs formed during post-chlorination after catalytic ozonation. Positive effect of the TiO$_2$ loading. Membrane permeate recovered 93% by catalytic ozonation vs. 78% in ozonation alone.	[173]

Table 6. *Cont.*

Target Water	Catalyst and Main Properties	Reactor and Experimental Conditions	Main Results	Ref.
Bromide	Ferrate (VI)	Homogeneous ozonation Flasks, Vr = 0.5 L Ferrate dose 1–5 mg L^{-1} C_{Br^-} = 100–1500 µg L^{-1} C_{O3} = 0–5 mg L^{-1} T = 5–40 °C pH = 3–11	Ferrate (VI) reduced BrO_3^- during catalytic ozonation No post-chlorination No other DBPs were analyzed.	[174]
NOM from groundwater (Banat, Serbia)	Aeroxide P25 TiO$_2$ 80/20 anatase/rutile SBET = 50 m^2 g^{-1}	Ozonation: Reactor bubble glass column D = 85 mm V = 2 L Vr = 1.5 L Gas flow rate 8 L h^{-1} Contact time 3–25 min O$_3$ dosage 0.4–3.0 mg O$_3$/mg DOC Catalyst dose 1 mg L^{-1} DOC$_0$ = 9.85 mg L^{-1} pH = 7.46 Chlorination: SM 2350 (residual chlorine 0.5–2 mg L^{-1} after 48 h, pH 7).	Removal THMFP 48% (no improvement observed compared to ozonation) Removal HAAFP 44% Less brominated species and haloacetonitrile after catalytic ozonation.	[175]
Humic substances	Bone charcoal (BC) Prepared at 600 °C for 4 h (bone from cattle and sheep). XRD revealed calcium phosphate (hydroxyapatite form) and amorphous carbon. XRF: CaO 92.9%; P2O5 3%; MgO 0.6%; SiO2 0.095%; MnO 0.008%. Boehm titration: Surface acidic groups 0.71 meq g^{-1} Surface basic groups 0.33 meq g^{-1} SBET = 121 m^2 g^{-1} pHpzc = 8.5	Semi-batch operation V = 1 L Catalyst 2 g C_{HS} = 15–100 mg L^{-1} Ozone 0.5 mg L^{-1} min^{-1} T = 15–40 °C pH = 2–12	The catalyst improves the reaction rate of HS degradation by 1.43- and 1.56- fold compared to ozonation. Kinetics and mechanism analysis. Kinetic studies showed that the rate greatly increased in the presence of BC. The reaction rate is related to BC dosage, HS concentration, pH, temperature. The presence of t-BuOH confirmed the main degradation route by hydroxyl radicals. Ea = 10 kJ mol^{-1} Diffusion controlled reaction. No chlorination. No DBPs were analyzed.	[176]

Table 6. *Cont.*

Target Water	Catalyst and Main Properties	Reactor and Experimental Conditions	Main Results	Ref.
NOM from surface water (Dong-Gang River, Pingtung, Taiwan)	$TiO_2/\alpha Al_2O_3$ No characterization studies reported	Fluidized bed reactor Continuous operation Gas flow rate 100 mL min^{-1} Water flow rate 50 mL min^{-1} O_3 concentration 2.5 mg L^{-1} Catalyst loading 0–25 g DOC_0 = 2.8–4.7 mg L^{-1} pH = 7.82–8.15 T = 20 °C Chlorination: According to SM 2350 Residual chlorine 0.2–1 mg L^{-1}, pH 7, 48 h contact time.	The combined catalytic ozonation significant reduced DOC up to 51.4% and DBPFP up to c.a. 50% (THMs and HAA6 analyses). The amount of catalyst had a positive effect in the process.	[177]
Dimethyl phthalate (DMP) and NOM in surface water (Jingmi Cannel, China)	Ru/AC Particle size 6–10 mesh 1–1.5 mm 0.5 wt.% Ru AC ash content 7.8 wt.% (mainly SiO_2, Al_2O_3 and Fe_2O_3) SBET = 945.2 m^2 g^{-1}	Cylinder reactor, bubble column D = 5 cm L = 120 cm V = 1 L Semi-batch for catalytic activity: Cat. Dosage = 2 g L^{-1} Ozone dosage 118 mg h^{-1} Q 300 mL min^{-1} Continuous operation for stability tests: Qw = 20 mL min^{-1} Cat. Dosage = 40 g COD_0 = 2.25–3.29 mg L^{-1} pH = 7.2–8.5 T = 25 °C Chlorination: pH = 7 Excess of chlorine T = 25 °C, 7 days	Ru/AC active in catalytic ozonation improved DMP mineralization. Stable for 42 h with no Ru leaching and 75% DOC removal. In natural water, Ru/AC-O_3 was better than O_3 alone for DOC removal (40% vs. 10%) and DBPFP reduction (60% vs. 40%); THMFP and HAAFP analyzed.	[178]

Table 6. *Cont.*

Target Water	Catalyst and Main Properties	Reactor and Experimental Conditions	Main Results	Ref.
NOM (Songhua River, Harbin, China)	FeOOH-goethite pHpzc = 7.0 SBET = 68.4 m^2 g^{-1} Average pore size 24 nm Surface OH density = 0.5 mmol g^{-1} CeO$_2$ pHpzc = 6.6 SBET = 117 m^2 g^{-1} Average pore size 7.9 nm Surface OH density = 0.4 mmol g^{-1} D = 0.075–0.3 mm	Ozonized water (20 mL; 10 mg O$_3$ L^{-1}) VT = 40 mL DOC = 10 mg L^{-1} O$_3$/DOC = 1 10 min reaction time pH = 7 T = 18 °C Fractionation of NOM with XAD-8 and XAD-4 amberlite resins: HOA: Hydrophobic acid HON: Hydrophobic neutral HIA: Hydrophilic acid HIB: Hydrophilic base Fluorescence analyses.	Ozonation decrease the aromaticity of humic-like structures and increases the generation of carboxylic groups. Catalytic ozonation improve the destruction of humic-like structures. Ozonation of HOA and HIA yields by-products with low aromaticity and low molecular weight. Catalytic ozonation enhances the formation of these by-products from HIA and improves the destruction of highly polycyclic aromatic structures. No post-chlorination. No DBPs were analyzed.	[179]
Humic and fulvic acid in distilled water	MnO$_2$ No characterization studies reported.	Cylinder reactor (bubble column, semi-batch operation, total recirculation of water) D = 7 cm L = 1.5 m V = 5 L O$_3$ dose = 47 mg L^{-1} in 30 min TOC$_0$ = 28–38 mg L^{-1} pH = 8.9 T = 19 °C	TOC removal 79% in catalytic ozonation vs. 67% in single ozonation. No post-chlorination. No DBPs were analyzed.	[180]
NOM-surface water (Lake Lansing, Michigan USA)	Fe$_2$O$_3$ over ceramic membrane (Al$_2$O$_3$/ZrO$_2$/TiO$_2$) Average Fe$_2$O$_3$ particles 4–6 nm (TEM)	Conditions of ozone-membrane system: Water recirculation rate = 2.75 L min^{-1} T = 20 °C O$_3$ flow rate: 100 mL min^{-1} Transmembrane pressure = 0.5 bar O$_3$ gas concentration = 2.5 mg L^{-1} Ozone injection before membrane module DOC$_0$ = 8.6–11.6 mg L^{-1} pH = 7.7–8.6 Chlorination SM 2350 (residual chlorine 0.5 mg L^{-1} after 48 h, pH 7).	Decomposition of O$_3$ in the membrane surface. DOC reduced > 85% Decrease of THMFP (90%), HAAFP (85%) and also the concentration of aldehydes, ketones and ketoacids.	[181] [182]

Table 6. *Cont.*

Target Water	Catalyst and Main Properties	Reactor and Experimental Conditions	Main Results	Ref.
DOC in river water (Japan)	Powdered AC (membrane as separator)	Ozonation: Reactor characteristics not specified. Column before membrane module O_3 dose = 1–2 mg L^{-1} AC dose 10 mg L^{-1} DOC_0 = 2.4 mg L^{-1} Q water = 5.5 m^3 day^{-1} Chlorination conditions not specified.	Combination of PAC and O_3 improved the performance of the subsequent membrane system. DOC reduced 59% T-THMFP reduced 75%	[183]
Humic acid solution NOM from Ebro River (Zaragoza, Spain)	TiO_2 (anatase Probus, SBET = 8.5 m^2 g^{-1}) 2.5 wt.% supported by adsorption on: Attapulgyte (clay, SBET = 104 m^2 g^{-1}) α-Al_2O_3 (SBET = 164 m^2 g^{-1}) Silica gel (SBET = 362 m^2 g^{-1}) Calcination T = 350–600 °C Granular form, d = 2–4 and 4–6 mm. TiO_2/Al_2O_3 catalyst characterization: SBET = 132 m^2 g^{-1} Pore volume = 0.33 cm^2 g^{-1} Pore size = 4.4 nm (12%); 20.56 um (88%). Anatase phase by XRD	Glass fixed bed reactor Semi-batch mode Humic acid experiments: V = 650 mL O_3 = 405 mg O_3 h^{-1} 30 min contact time C HA = 5.34 mg TOC L^{-1} pH = 7.2 Catalyst loading: 2.5–10 g L^{-1} NOM experiments: V = 2 L O_3 = 396.4 mg O_3 h^{-1} Contact time 2–4 min. Catalyst loading: 2.5 g L^{-1} TOC_0 = 4.46 mg L^{-1} pH = 7.94 Stability tests (4 consecutive runs): C Humic acid = 6.65 mg L^{-1} TOC pH = 7.62 Catalyst loading = 2.5 g L^{-1} V = 650 mL O_3 405 mg O_3 h^{-1} 30 min contact time	TOC and UV254 removal were slightly greater in the presence of a catalyst (60% vs. 32% in O_3 for TOC). The best results were obtained with TiO_2/Al_2O_3 calcined at 500 °C with a concentration of 2.5 g L^{-1} of catalyst and particle diameter 2–4 mm. The importance of adsorption is highlighted. Higher doses of O_3 have a positive effect in catalytic ozonation. Stability tests with the best catalyst showed a good stability with similar TOC, UV254 and pH results after the 4 experiments. No post-chlorination. No DBPs were analyzed.	[184] [185]

Table 6. *Cont.*

Target Water	Catalyst and Main Properties	Reactor and Experimental Conditions	Main Results	Ref.
Fulvic acid extracted from surface water (Cebron, France)	Commercial TiO_2 over Al_2O_3 beads Dbeads = 1.5–2.5 mm No characterization provided	Ozonation: Reactor: Conical glass flask 1.3 L V reaction = 1 L Contact time = 10 min O_3 dose = 2–6.5 mg L^{-1} (homogeneous experiments) C_{CAT} = 10 g L^{-1} DOC_0 = 2.84 mg L^{-1} H_2O_2/O_3 ratio = 0.35 mg H_2O_2/mg O_3 pH = 7 Chlorination: Cl_2 dose = 2 mg L^{-1} Contact time 1 h pH = 7	Catalytic ozonation increased ozone consumption. Higher mineralization (24%) compared with O_3 and H_2O_2/O_3 systems. Chlorine demand was minimized in catalytic ozonation. No DBPs were analyzed.	[186]
Model compounds: Fulvic acid Protein disaccharide	Granular catalyst TiO_2/Al_2O_3 GAT 925 SI D = 4 mm For comparison: BST: TiO_2 stick compacted APF: Granular TiO_2/Clay	Tested TiO_2/O_3 and $TiO_2/O_3/H_2O_2$ Bubble column Semi-continuous reactor with recirculation of the aqueous solution Total height 2 m D = 40 mm Porous glass to support the catalyst in the middle Q = 2.4–2.8 L h^{-1} C_{O3g} = 60–90 mg L^{-1} pH = 8 TOC_0 = 12 mg L^{-1} H_2O_2/O_3 = 0.4 g/g Catalyst loading 30 g L^{-1} Room temperature	Cumulative effect of adsorption and ozonation. At high ozone dosage TOC abatement by catalytic ozonation is observed (80% vs. 50% in O_3). APF was not stable under the conditions tested due to mechanic friction. No chlorination. No DBPs were analyzed.	[187]

Different iron oxides/hydroxides have been studied for catalytic ozonation mainly bare FeOOH, Fe_2O_3 and Fe_3O_4 or supported in different materials [143]. α-FeOOH-goethite has been used in other studies that reported SBET 60–97 m^2 g^{-1} and pH_{pzc} near 7. The properties of this material for catalytic ozonation have also been deeply discussed in Bai et al. [188]. In general, a higher efficiency in NOM mineralization was observed by catalytic ozonation compared to ozone alone. Only Wang et al. [171] analyzed post-chlorination DBPs in treated surface water and observed that THMs and HAAs were highly reduced by catalytic ozonation (combined with biofiltration).

Regarding the supported Fe-catalysts, Karnik et al. [181,182] used Fe_2O_3 over a ceramic membrane composed by $Al_2O_3/ZrO_2/TiO_2$ (no characterization reported) in the hybrid catalytic ozonation/ultrafiltration system and studied the decomposition of ozone in the membrane surface, obtaining a high removal of THMFP and HAAFP (higher than 85%) from surface water at the conditions shown in Table 6. Other authors supported FeOOH or Fe_2O_3 species over zeolite [163] or natural pumice [161] and observed an important catalytic effect of these materials in the degradation of synthetic humic acid solutions but no DBPs were analyzed in their works.

Other metal oxides and composite materials have been tested as catalysts. Turkay et al. [164,168] checked the effectiveness of CuO and ZnO nanoparticles with high crystallinity in the degradation of humic acid and NOM from surface water studying the possible mechanism by DFT modelling but no DBPs analyses. Wang et al. [166,178] studied the performance of RuO_2 supported onto activated carbon, Al_2O_3 and ZrO_2-CeO_2 using oxalic acid, dimethyl phthalate as target compounds and also NOM from surface water. They fully characterized the catalysts (see Table 6) with main differences between S_{BET} in AC supported catalyst. All the systems showed a high catalytic activity and improved ozonation results. THM precursors reacted fast with ozone alone but the THMFP and HAAFP were highly reduced in catalytic ozonation. Some aspects about the activity and stability of these catalytic systems are commented in the next sections.

Different manganese materials also showed catalytic activity for ozonation of NOM or humic and fulvic acids. Alsheyab and Muñoz [180] studied MnO_2 and at the conditions tested TOC removal improved from 67% in single ozonation to 79% in catalytic ozonation (pH = 8.9). No characterization and no DBPs studies were reported. Recently, Salla et al. [160] tested Mn_2O_3 as catalyst for humic acid ozonation that resulted in rapid ozone decomposition, neither DBPs were studied. Only Chen and Wang [170] prepared a mixed Fe-Mn oxide (8.17% Mn) with high surface area (262 m^2 g^{-1}) for NOM removal and reduced THMs and nine HAA up to 70 and 75% respectively.

Cerium oxide have been used as support but also presented catalytic activity for the process. Zhang et al. [179] synthetized CeO_2 with pH_{pzc} = 6.6 and high S_{BET} = 117 m^2 g^{-1}. The elimination of DOC from surface water was between 30–50% of different NOM fractions compared to 3–6% obtained in ozonation alone. On the contrary, a similar CeO_2 material was tested by Wang et al. [165] that found that their adsorption capacity exerted a negative effect in mineralization (lower than ozonation alone). Later, Zhang and Wang [162] synthetized different CeO_2-TiO_2 composites and studied the Ce/Ti ratio effect. They found that CeO_2 main phase was cubic fluorite and the positive effect of Ce content by increasing BET surface area because of lower crystallite sizes. An optimum Ce/Ti ratio of 0.8 was found due to the high surface area (expected) and low pH_{pzc} that improved adsorption properties and lead to lower molecular weight organics from humic acid degradation. Unfortunately, no post-chlorination DBPs were analyzed.

Regarding the use of carbonaceous materials as catalysts, though they have been widely used in catalytic ozonation of different organic pollutants, a few studies have been found for humic acid and NOM removal with post-chlorination and DBPs analyses. Shioyama et al. [183] combined powder activated carbon with membrane filtration for surface water treatment, which improved the performance of the subsequent membrane system reducing DOC up to 59% and T-THMFP up to 75%. Gümüs and Akbal [163]

also studied the degradation of humic acid with granular activated carbon reaching 48% compared to 21% in ozonation alone though no DBPs were analyzed.

7.1.2. Catalytic Activity, Stability, and Reusability

No straightforward conclusions can be reached about the catalytic activity of the different catalysts checked at different operating conditions. However, some of the previous reported studies in Table 6 compare different materials that can differ in the active phase or the support.

Allemane et al. [187] and Gracia et al. [184,185] compared different TiO_2 catalytic systems. In their work, the relevance of the support was pointed out, being Al_2O_3 the best option that increased adsorption of NOM. The latter works also studied the stability of the TiO_2/Al_2O_3 catalysts in four reaction cycles of NOM catalytic ozonation at the operating conditions in Table 6. A good stability was maintained with similar TOC, UV254, and pH results after the four experiments.

Chen and Wang [170] compared the behavior of TiO_2/Al_2O_3 and a Fe-Mn oxide in the degradation of NOM and DBPFP of surface water. Fe-Mn presented the best performance in O_3 decomposition, DOC, UV254, and DBPFP removals. This was attributed to the catalytic activity of Fe and Mn species and to the highest specific surface area of this catalyst which improved the adsorption of NOM.

Also, the series of Wang et al. [166] demonstrated the importance of the support in RuO_2 supported catalysts. RuO_2/ZrO_2-CeO_2 resulted highly efficient compared to Al_2O_3 or AC as support, although a high adsorption capacity can also mask mineralization results. HAAFPs improved from 38–57% and THMFPs from 50–64% when comparing catalytic ozonation and ozonation, but O_3 alone reacts fast with THMs precursors. The best performance is ascribed to the efficiency of the redox Ce^{4+}/Ce^{3+} couple in the material which enhances the catalytic activity of very well dispersed Ru species. This catalyst was also more stable in continuous operation (only 48 h were checked with no Ru leaching).

The three works by Turkay et al. [164,167] have been performed using the same experimental set up and with quasi-similar operating conditions but with different catalysts. They studied the catalytic behavior of CuO, TiO_2 and ZnO nanopowders, respectively. All the materials presented an improved DOC removal (from humic acid with the same concentration and pH) which increased from 30% for ozone alone to 80% for CuO, 70% TiO2 and 60% ZnO. Thus, CuO seems the most active catalytic system but, in terms of stability, although not studied, probably TiO_2 is a better candidate for future works since Zn and Cu ions are easily leachable.

On the other hand, Wang et al. [165] compared the catalytic activity of FeOOH, CeO_2, and MgO. Whereas CeO_2 presented a better UV254 removal, FeOOH and MgO showed the best DOC mineralization results. In this work, adsorption onto CeO_2 seems to play a negative effect in its catalytic performance. The stability of all the materials was checked by ion leaching and SEM and XRD of the used catalysts with no significant changes in morphology or structural properties.

Recently, Salla et al. [160] compared classical Al_2O_3 with Mn_2O_3 catalysts in humic acid degradation. The favorable surface charge of Al_2O_3 led to a better performance in humic acid removal, but Mn_2O_3 promoted a faster decomposition of O_3. This last catalyst led to higher ozone consumption. Catalytic stability was studied in four consecutive runs. Some catalyst deactivation is observed with changes in the oxidation state of Mn and Al and the surface hydroxylation of both catalysts was observed by XPS.

Therefore, some controversial effects are still unknown such as the role of the adsorption of some NOM species (NOM fractionation) onto the catalysts surface or the true catalytic activity of the active species in comparable conditions. In terms of stability, long term and deep characterization would be desirable to check the real applicability of these materials.

7.1.3. Reactors and Variables Studied

Bubble columns or vessels were used in semi-batch mode operation, batch for liquid phase, continuous for gas phase have been usually selected for catalytic ozonation processes. The catalyst, depending on the particle size, has been suspended in slurry or fluidized bed reactors, or packed in fixed bed reactors. In any case, they are three-phase reactors with gas–liquid–solid phases in which matter transfer will play a key role. Figure 3 shows a scheme of the typical ozonation experimental set up.
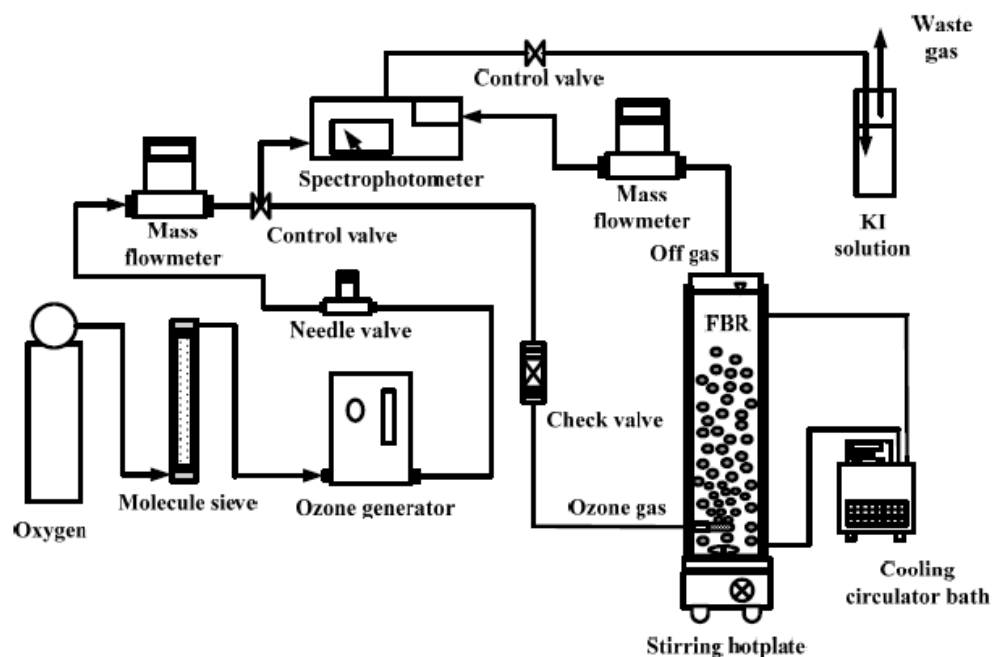
Figure 3. Experimental set up for catalytic ozonation experiments at lab scale [171] (From Wang, Y.H.; Chen, K.C. Removal of disinfection by-products from contaminated water using a synthetic goethite catalyst via catalytic ozonation and a biofiltration system. *Int. J. Environ. Res. Public Health* **2014**, *11*, 9325–9344. doi.org/10.3390/ijerph110909325).

In general, the installation is composed by an air or oxygen cylinder, an ozone generator which sends the ozone gas into the reactor, in line ozone analyzers (at gas inlet and/or gas outlet), mass flow controllers, and ozone destruction systems (KI solution, AC filter or UV analyzers with catalytic destruction). The reactor usually comprises a glass or acrylic column or vessel with variable volume (mainly 1–2 L) provided with a bottom diffuser for ozone inlet which favors mass transfer, magnetic or mechanical stirring, gas inlet, and gas outlet and sampling port. Some reactors are provided with thermostatic baths for temperature control, and temperature or analytic probes (ozone, pH) can be included in the reactor. Usually, the reactor is filled with the water to treat having some head space for gas outlet. The catalyst is usually added, and a pre-adsorption or homogenization time is spent before ozonation. Then the containing ozone stream is bubbled into the reactor and the catalytic ozonation experiment begins.

Among the typical operating conditions studied are DOC concentration, pH, catalyst loading, and ozone dose (Table 6). Ambient temperature was used in most of the works. Regardless of natural surface water or synthetic humic or fulvic acid solutions, DOC values are usually in the range 2–10 mg L^{-1}. Mortazavi et al. [176] detected a positive effect of DOC increasing the apparent reaction rate of catalytic ozonation as DOC increased.

It is well-known the role of pH on ozone reactions that has been usually described and commented in the introduction section. The application of the process for drinking water makes sense at the pH of natural waters (pH 6.0–8.5) and most of the studies are performed at natural pH. However, the relevance of pH in the NOM and catalyst charge has been

evaluated. In this line, Salla et al. [160] assigned the best catalytic performance of Al_2O_3 with higher humic acid adsorption and lower ozone dosage due to favorable negative surface charge at the conditions studied (pH = 5.5 > pH_{pzc} = 4.2). This also affects the adsorption capacity of the catalysts for different NOM fractions (acidic, neutral, hydrophilic or hydrophobic). On the other hand, Mortazavi et al. [176] in their study evaluated the influence of pH on the catalytic ozonation performance of bone charcoal to remove humic substances in the range of pH 2–12. They found that heterogeneous catalytic ozonation contribution was much higher at low pH and ozonation alone contribution increases with alkalinity due to the relative importance of indirect ozone reactions. In addition, at pH = 8 < pH_{pzc} = 8.5 of the catalysts, a positive catalytic effect is still observed due to hydroxyl groups in the catalyst surface that act as Lewis acid sites for ozone decomposition. Therefore, depending on the catalyst nature, the catalytic effect could be improved also in alkaline solutions.

Catalyst loading is also an important parameter to optimize. The optimum dose is highly dependent on the catalyst nature and on the particle size used. The range used in the works reported in Table 6 for semi-batch experiments are as wide as 1 mg L^{-1} for TiO_2 in slurry, 10 mg L^{-1} for activated carbon or 30 g L^{-1} of TiO_2/Al_2O_3. In continuous operation, the space time (mass of catalyst/flow of water) ranged from 500–2000 g min L^{-1} [177]. In general, at sufficient ozone dose, the catalyst loading exerted a positive effect on the degradation rate of NOM. However, experimental check is needed in any different case.

In the same line, the optimization of ozone dose will mark the economic feasibility of the process in terms of ozone consumption/power energy required for ozone production. In general, research works reported in Table 6 applied high ozone dose and high ozone concentration in the gas phase with common values ca 10 mg L^{-1}. However, ozone concentrations used were as varied as 2–90 mg L^{-1}. Molnar et al. [175] observed that DOC removal did not improve at high ozone doses (0.1–3 mg O_3/mg DOC) using TiO_2/O_3 catalytic ozonation compared to ozonation alone, but attributed this effect to the pH of the natural water and the scavenging effect of carbonate/bicarbonate. On the contrary, Wang et al. [173], found a positive effect in the ozone dosage in the permeated flux of their hybrid system. However, no relevant changes were observed in TOC or UV254 removal or THMFP.

7.1.4. Mechanisms and Kinetics for the Removal of DBPs Precursors

General mechanisms such as presented in reactions (21) to (31) have been accepted for NOM or humic/fulvic acids degradation by catalytic ozonation depending on the catalyst used.

In general, humic/fulvic substances are easily degraded by ozone direct reactions due to the presence of unsaturated bonds and aromatic rings to produce other compounds less reactive towards ozone but also with different reactivity towards subsequent chlorine treatment. These other compounds, carboxylic acids, or aliphatic molecules, can be degraded by reactive oxygen species formed by catalytic decomposition of ozone (hydroxyl radical, ozonide radical, etc.) both in the liquid phase or near the catalyst surface/adsorbed. They may react with organic molecules with low selectivity, thus leading to a high mineralization of NOM.

Considering the transformation of NOM in different species prior to mineralization, it is important to know the chlorine reactivity of the different fractions formed during catalytic ozonation. Thus, Zhang et al. [179] observed that ozonation alone decreases the aromaticity of humic-like structures and increases the generation of carboxylic groups. Catalytic ozonation with FeOOH and CeO_2 catalysts also improved the destruction of humic-like structures and enhanced the destruction of the hydrophilic acid fraction destroying polycyclic aromatic structures. Unfortunately, no DBPFP was studied in this work.

Allemane et al. [187] proposed the adsorption of O_3 and NOM onto TiO_2/Al_2O_3 surface and the generation of oxidizing species in the surface. This trend has been observed in many of the studies dealing with TiO_2/Al_2O_3 [184,185]. With respect to the contribution

of adsorption, direct reactions, indirect reactions during catalytic ozonation, Alver and Kilic [161] studied the mechanism of humic acid removal by Fe coated pumice catalytic ozonation in the presence of different scavengers (t-BuOH and phosphate). They observed the high contribution of hydroxyl radicals in solution to the overall process. The studies of Turkay et al. [164,167] for the degradation of humic acid are based in DFT modelling calculations to stablish the interaction of reactants with the catalyst surface. They concluded that $HO^\bullet$ radicals formed in the catalyst surface initiate the heterogeneous reaction in CuO with important contributions of adsorption-desorption and chelating [168]. For TiO_2, $HO^\bullet$ radicals are supposed to be formed from adsorbed O_3 and its decomposition onto TiO_2 surface in the presence of water molecules [167]. Finally, they proposed the O_3 disproportionation over ZnO surface to form reactive oxygen species [164].

In the same line, Gümüs and Akbal [163] studied the degradation of humic acid using GAC and Fe-coated zeolite as catalysts. For GAC they proposed a general mechanism reported by Beltrán et al. for the degradation of diclofenac [189,190]. In this mechanism adsorbed ozone reacts with adsorbed organic compounds to yield hydrogen peroxide which eventually might react with adsorbed ozone to form hydroxyl radicals:

$$DOC_1 + GAC \rightleftarrows DOC_1 - GAC \tag{32}$$

$$O_3 + GAC \rightleftarrows O_3 - GAC \tag{33}$$

$$DOC_1 - GAC + O_3 - GAC \rightarrow DOC_2 + H_2O_2 + GAC \tag{34}$$

$$H_2O_2 + GAC \rightleftarrows H_2O_2 - GAC \tag{35}$$

$$H_2O_2 - GAC + O_3 - GAC \rightarrow HO^\bullet + GAC \tag{36}$$

$$DOC_1 + HO^\bullet \rightarrow DOC_2 + HO_2^\bullet \tag{37}$$
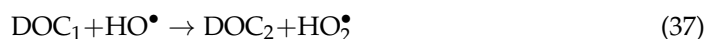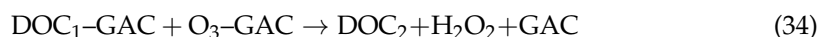
For Fe-coated zeolite (ICZ), they proposed the following mechanism:

$$ICZ - OH + O_3 \rightleftarrows ICZ(O_3)_S \rightleftarrows ICZ - O^\bullet + HO_3^\bullet \tag{38}$$

$$ICZ - O^\bullet + H_2O \rightarrow ICZ - OH + HO^\bullet \tag{39}$$

$$HO_3^\bullet \rightleftarrows H^+ + O_3^{\bullet -} \tag{40}$$

$$HO_3^\bullet \rightarrow HO^\bullet + O_2 \tag{41}$$

In this mechanism ozone is adsorbed in terminal –OH groups of the catalyst and then reactive oxygen species are produced that eventually would react with organic compounds (adsorbed or in the bulk liquid phase).

Then, despite the variety of catalysts and the few studies directly dealing with the determination of the mechanisms involved in the catalytic ozonation of humic acid or NOM, some general steps can be hypothesized:

$$Cat + DOC_1 \rightleftarrows Cat - DOC_1 \tag{42}$$

$$Cat + O_3 \rightleftarrows Cat - O_3 \rightarrow Cat - ROS \rightarrow Cat + HO^\bullet \tag{43}$$

$$Cat + DOC_1 + Cat - O_3 \rightarrow DOC_2 + Cat + [H_2O_2] \tag{44}$$

$$Cat - ROS + Cat - DOC_1 \rightarrow DOC_2 + Cat \tag{45}$$

$$DOC_1 + O_3 \rightarrow DOC_2 + [H_2O_2] \tag{46}$$

$$DOC_1 + HO^\bullet \rightarrow DOC_2 + HO_2^\bullet \tag{47}$$

$$DOC_2 + HO^\bullet \rightarrow CO_2 + H_2O \tag{48}$$
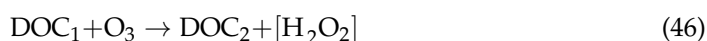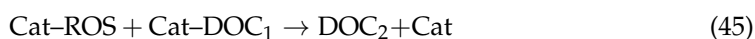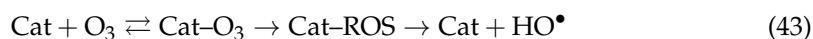
where Equations (42)–(45) represent heterogeneous reactions and Equations (46)–(48) are some of the well-known homogeneous ozone/hydroxyl radical reactions. This sequence

will be completed by the general ozonation and $HO^\bullet$ mechanisms in water [26,191,192]. DOC_1 represents initial humic/fulvic substances that readily react with ozone or hydroxyl radicals to form organic compounds with lower molecular weight (DOC_2 accounting for carboxylic, aldehydes, aliphatic compounds, etc.) usually refractory to direct ozone attack that can be further mineralized by hydroxyl radicals. The reactivity of different DOC fractions towards chlorine and their subsequent DBPFP is crucial to stablish the need of achieving an advanced oxidation degree or a high mineralization. Therefore, the importance of each reaction should be the objective of future works to tailor the catalytic properties and to modify operating conditions for the degradation of NOM of specific characteristics to reduce DBPFP. It is necessary to point out that the analysis of the latter will be mandatory regardless of the mineralization achieved.

Regarding the kinetics of the process, only a few works dealing with kinetics beyond calculating apparent rate constants have been carried out. Mortazavi et al. [176] proposed the following kinetics for the degradation of humic acid using bone charcoal as catalysts. They worked reaching ozone saturation before humic acid injection in the reaction medium and, therefore, the system is considered homogeneous from the point of view of ozone. The contribution of both heterogeneous reactions taking place on the catalyst surface and homogeneous reactions by ozone and radicals in the liquid phase are represented:

$$-\frac{dC_{HA}}{dt} = (k_{homo}^{HA} + k_{hetero}^{HA} C_{S-OH})C_{HA} \tag{49}$$

$$k_{homo}^{HA} = k_1^{HA} C_{O3} + k_2^{HA} C_{HO^\bullet} \tag{50}$$

$$k_{hetero}^{HA} = k_3^{HA} C_{O3} + k_4^{HA} C_{HO^\bullet} \tag{51}$$

$$\ln\frac{C_{HA}}{C_{HA0}} = -(k_{homo}^{HA} + k_{hetero}^{HA} C_{S-OH})t = -kt \tag{52}$$

$$k = k_{homo}^{HA} + k_{hetero}^{HA} C_{S-OH} \tag{53}$$

where k represents the overall reaction rate constant and k_1^{HA}, k_2^{HA}, k_3^{HA}, k_4^{HA}, k_{homo}^{HA}, and k_{hetero}^{HA} represent the HA degradation rate constants corresponding to a homogeneous reaction with ozone, a homogeneous reaction with hydroxyl radical, a heterogeneous reaction with ozone, a heterogeneous reaction with hydroxyl radicals, and global homogeneous and heterogeneous reactions, respectively; C_{HA}, and C_{HA0} are the concentrations of HA at any time and time zero; C_{HO} and C_{S-HO} represent the hydroxyl radical concentration in liquid phase or in the catalyst surface and C_{O3} is de dissolved ozone concentration. This study is based on UV254 nm measurements and no mineralization is considered. As can be deduced from Equation (53), the rate of humic acid degradation resulted in apparent first order kinetics whose apparent rate constant k was determined at different operating conditions. With experiments at different temperature an activation energy value (E_a) of 10 kJ mol^{-1} was calculated.

Chen and Wang [170] studied the catalytic decomposition of ozone over Fe-Mn oxide and TiO_2/Al_2O_3 catalysts through simple first order kinetics approximation:

$$-\frac{dC_{O3}}{dt} = k_d C_{CATALYST} C_{O3} \tag{54}$$

$$\frac{C_{O3,t}}{C_{O3,0}} = \exp(-k_d t) \tag{55}$$

where k_d is the observed pseudo first-order reaction rate constant of O_3 decomposition of the catalytic ozonation system, C_{O3} is the dissolved ozone concentration and t is the reaction time. They found values of 2.8×10^{-3}, 9.0×10^{-3} and 4.1×10^{-3} s^{-1} for ozonation and Fe-Mn oxide, TiO_2/Al_2O_3 catalytic ozonation, respectively. They ascribed the low decomposition rate found for TiO_2/Al_2O_3 to the presence of phosphate that may be adsorbed in the catalyst surface.

To study the ozone exposure, hydroxyl radical exposure and the ratio between $HO^\bullet$ and O_3 concentration, Chen and Wang [170] also applied the R_{ct} concept from Elovitz and von Gunten [193] using data from experiments in the presence of p-chlorobenzoic acid (pCBA) at low concentration through the following equations:

$$\frac{dC_{pCBA}}{dt} = -k_{HO-pCBA}C_{pCBA}C_{HO^\bullet} \tag{56}$$

$$\ln\frac{C_{pCBAt}}{C_{pCBA0}} = -k_{HO-pCBA}\int C_{HO^\bullet}dt \tag{57}$$

$$R_{CT} = \frac{\int C_{HO^\bullet}dt}{\int C_{O3}dt} \tag{58}$$

$$\ln\frac{C_{pCBAt}}{C_{pCBA0}} = -k_{HO-pCBA}R_{CT}\int C_{O3}dt. \tag{59}$$

In this scheme, pCBA is considered to react only with hydroxyl radicals due to the low rate constant of its reaction with ozone. C_{pCBAt} and C_{pCBA0} are the concentrations of pCBA at any time and time zero, respectively, $k_{OH-pCBA}$ is the rate constant of HO-pCBA reaction, $C_{HO^\bullet}$ is the concentration of hydroxyl radical and C_{O3} is the dissolved ozone concentration. They found values for R_{ct} from 3.6×10^{-8} mol $HO^\bullet$/mol O_3 for single ozonation up to 14×10^{-8} and 9.8^{-8} mol $HO^\bullet$/mol O_3 for Fe-Mn oxide and TiO_2/Al_2O_3 catalytic ozonation, respectively. This is indicative of the improved capacity of Fe-Mn oxide catalyst to generate hydroxyl radicals during the process.

Gümüs and Akbal [163] used a second-order kinetic model for humic acid catalytic ozonation (kinetic equations not shown) using Fe coated zeolite (ICZ) and GAC as catalysts. They reported different rate constants for ozonation at different dissolved O_3 concentrations, catalyst doses, pH and molecular weight of initial DOC (<100 and <50 kDa). They observed the high catalytic activity of ICZ vs. GAC and also demonstrated the highest reactivity of the humic acid fraction <100 kDa with ozone, being catalytic processes much more effective for the fraction <50 kDa.

In general, no complex mechanistic kinetics has been developed for catalytic ozonation of NOM, being an important gap for catalytic systems optimization. In addition, taking into account every topic of these section, NOM or humic/fulvic acids degradation has been evaluated but there is a lack of studies covering the formation of different DBPs also with global parameters determination such as AOX that are important to check the real applicability of this process for drinking water treatment.

7.2. Photocatalytic Ozonation

As a difference from catalytic ozonation, so far literature only reports just one work dealing with the combination of ozone, catalyst and light, that is, photocatalytic ozonation (PhCatOz) to remove natural organic matter, NOM, or humics from water [194]. Photocatalytic ozonation is an emerging AOP where hydroxyl radicals may generate from different mechanisms including adsorption and oxidation of water or hydroxyl groups on the valence band of the catalyst, ozone decomposition, reactions of ozone and oxygen with electrons of the conduction band of the catalyst or even reaction of ozone with possible hydrogen peroxide formed from superoxide ion recombination or from direct ozone-organics reactions [27]. The basic mechanism NOM PhCatOz is as follows:

Direct ozone reactions with NOM:

$$O_3 + NOM \rightarrow O_3-DBP + H_2O_2 \tag{60}$$

Direct photolysis of NOM (usually at λ < 300 nm):

$$NOM \xrightarrow{h\gamma} UV-DBP \tag{61}$$

In these photolytic reactions, ozone and UV radiation disinfection byproducts are formed (see Section 3). These DBPs eventually, after subsequent ozone and photolysis reactions, are transformed in biodegradable compounds but some may have certain toxicity (i.e., aldehydes, ketones). Bromate can be formed if bromide was initially present.

In addition to reactions (60) and (61), given the presence of aromatic ring structures with hydroxyl substituents groups in NOM, and, hence, the presence of nucleophilic points, ring breakings give rise to the appearance of hydrogen peroxide as has been reported previously for the ozonation of phenol compounds.

Hydroxyl radical formation reactions via direct ozone decomposition, mainly from:

$$O_3 + HO_2^- \rightarrow O_3^{\bullet-} + HO_2^{\bullet} \rightarrow O_3^{\bullet-} + O_2^{\bullet-} \dots \xrightarrow{O_3} \dots \rightarrow 2HO^{\bullet} \tag{62}$$

Catalyst activation via light incidence:

$$Catalyst \xrightarrow{h\nu} h^+ + e^- \tag{63}$$

Hydroxyl radical formation reactions via hole (h+) reduction from the valence band and/or superoxide and ozonide ion radical formation by capturing electrons from the conduction band:

$$h^+ + H_2O, OH^- (adsorbed) \rightarrow HO^{\bullet} \tag{64}$$

$$O_3 + e^- \rightarrow O_3^{\bullet-} \rightarrow \dots \rightarrow HO^{\bullet} \tag{65}$$

$$O_2 + e^- \rightarrow O_2^{\bullet-} \xrightarrow{O_3} O_3^{\bullet-} + O_2 \rightarrow \dots \rightarrow HO^{\bullet} \tag{66}$$

$$2HO_2^{\bullet} \rightarrow H_2O_2 \tag{67}$$

$$H_2O_2 + e^- \rightarrow HO^{\bullet} + OH^-. \tag{68}$$

Hydroxyl radical formation from ozone and hydrogen peroxide photolysis (at $\lambda < 320$ nm):

$$O_3 \xrightarrow{h\nu, H_2O} H_2O_2 + O_2 \xrightarrow{h\nu} 2HO^{\bullet} \tag{69}$$

and reactions of NOM with hydroxyl radicals:

$$NOM + HO^{\bullet} \rightarrow Intermediates \xrightarrow{+HO^{\bullet}} \dots \rightarrow CO_2 + H_2O + Inorganic\ Anions \tag{70}$$
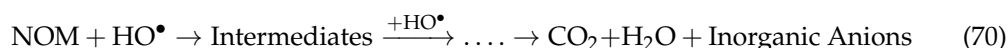
In spite of being an incipient process compared to other AOP such as O_3/H_2O_2, O_3/UVC-UVB, photocatalytic oxidation or Fenton process, PhCatOz has already been the subject of reviews since 2005 [195]. Many works of PhCatOz deal with the removal of model compounds such as pharmaceuticals and pesticides [196] or wastewater [197], with the use of visible or solar light and catalysts such as TiO_2, and others (ZnO, WO_3, C_3N_4, etc.), or TiO_2 composites that allow TiO_2 activation with visible light [198]. For instance, among catalysts checked, MOFs (already quoted in Section 7.1) [199] and graphitic carbon nitride, gC_3N_4 [200] has emerged to improve photocatalytic ozonation rate of pollutants. The use of gC_3N_4 is particularly interesting since this material presents a very high conduction band potential (-1.3 V_{NHE}) that greatly improves the ozone photoelectron capture to diminish electron-hole recombination and improve the formation of hydroxyl radicals [201]. According to WOS data base there are 160 works on photocatalytic ozonation so far published. As said before, however, only the work of Yuan et al. [194] treats photocatalytic ozonation for the removal of humics to reduce THM and TOX formation potential. Nonetheless, treatment of humics or NOM with photocatalysis and ozone as a sequence of processes has some antecedents due to Kerc et al. [202], Bekbolet et al. [203], and Uyguner et al. [204]. In their works, removal of humic acids is accomplished by ozonation, photocatalytic oxidation and the sequential use of the two latter, that is, they used ozonation followed by photocatalytic oxidation in separate processes, and they do not use PhCatOz as the simultaneous application of both processes. Degradation of humics is followed by measuring

the absorbance of remaining water at 254 and 436 nm, corresponding to aromatics and colored compounds, respectively. In some cases, the treated water later undergoes an adsorption or coagulation process to improve organic matter removal. In these works, it is observed the better efficiency of the sequential process to remove the humic matter from water. Nonetheless, only the photocatalytic oxidation is an AOP since ozonation, in most cases, is finished when dissolved ozone was not yet present in water. This means that during the ozonation step humic acids were mainly removed by direct ozone reactions [27]. The work of Bekbolet et al. [203] also gives results of formation potential of THM and some other halogen organic compounds (of chlorine and bromine) such as haloacetic acids, halonitriles and others. The results show the better performance of the sequential oxidation process (ozonation followed by photocatalytic oxidation) to decrease TOXFP. Coming back to the work of Yuan et al. [194], PhCatOz is applied, in this case, to remove a humic acid (its origin is not reported) with ozone, UVC radiation (250–260 nm with 254 nm as main wavelength) and different TiO_2 catalysts in powder or supported form. Supported materials were ceramsite, zeolite, alumina, and activated carbon (AC), while the composite prepared was Fe on TiO_2 nanotubes (Fe-TNT). The catalyst was characterized through XRD, SEM, TEM, EDS, XPS, and N_2 adsorption and UVVis-DRS. With the latter, they observed band gaps of 3.23 and 3.03 eV for their synthesized TNT and Fe-TNT with no influence of the supported material, a logical consequence of its lack of action on optical properties. The authors observed a significant increase of humic acid removal with PhCatOz when using AC as the supported material likely due to the BET surface area, the highest among the synthesized catalysts. They also observed after five consecutive runs with the same catalyst that removal efficiency of humic acid decreased from 94 to 78%. They concluded with the existence of a synergism between AC adsorption and photocatalytic ozonation. However, no data is given about TOXFP or THMFP. However, the results, suggest the importance of PhCatOz to improve the removal of TOX precursors.

8. Elimination of DBPs by Catalytic/Photocatalytic Ozonation Processes

As it can be seen from Table 7, as far as these authors know, there are only six works dealing with catalytic/photocatalytic ozonation processes of DBPs of drinking water. As it occurs with Section 6.2, chloroacetic acids (CAAs) are the most studied.

Table 7. Works on DBPs removal by catalytic/photocatalytic ozonation processes.

Target DBPs	Catalyst and Main Properties	Reactor and Experimental Conditions	Main Results	Ref.
MCA DCA Deionized water	TiO_2 photocatalyst coated on the commercial product "Pilkington ActiveTM glass" (PAGs).	Planar falling film reactor. Seven UVA lamps (15 W, 360 nm) fixed inside the reactor. Intensity UV light: 1 mW cm^{-2}; water flow rate: 1 L min^{-1}, volume 0.5 L; [CAA] = 1 mM; pH 3, pure gaseous oxygen rate of 10 L h^{-1}, ozone gas with 130 ± 5 mg L^{-1} ozone at a power of 30 W.	Single ozonation was ineffective method for the removal of chloroacetic acids. However, a significant enhancement in the degradation and mineralization efficiencies was observed by the combination of ozone with photocatalysis.	[106]
DCA	FMOG: Flower-like nanocomposite (FMOG) consisted of pure β-MnO_2 (PMO) and reduced graphene oxide nanosheets (RGO). Atomic ratio between Mn and O element is ca. 1:2.1.	500 mL glass conical flask. 110 min; flow rate of O_3: 4.47 mmoL min^{-1}, T = 20 °C, concentration of catalyst: 50 mg L^{-1}, and pH = 4.4. [DCAA]$_0$ = 100 mg L^{-1}.	FMOG displayed higher catalytic performance compared with ozonation, and PMO catalytic ozonation.	[205]
DCAcN	Titanium dioxide (Degussa, P-25, anatase/rutile = 75/25%).	Bench and outdoor photocatalytic ozonation systems consisted of the combination of CPC and ozone reactor. Metal halide lamps of different powers (100, 250, and 400 W); UV-solar, 300–800 nm. pH 6.5, 20 ± 1 C, TiO_2 dose 0.4 g L^{-1}, ozone dose 1 g L^{-1} h^{-1}, UV intensity 33.8 W m^{-2}. pH: 3, 6.5, and 10.	Compared to the single process, the UV-solar/TiO_2/O_3 process had the highest DCAN-removal rate. Optimal conditions: pH neutral; 1 g L^{-1} TiO_2 and 1.13 g L^{-1} h^{-1} ozone; T = 20 °C; UV-solar intensity: 4.6–25 W m^{-2}.	[206]
DCA	Immobilized TiO_2 in the form of a well-known commercial product called "Pilkington ActiveTM glass" (PAG) sheet with a contact area of 30×5 cm^2.	A planar reactor: Polymethylmethacrylate box (160 cm^3 vol) covered by an optical window made from the same material. Reactor connected to an ozonation chamber (500 cm^3 vol). 400 mL of dichloroacetic acid solution. 30 W lamp (300–420 nm and a maximum at about 360 nm). T = 25 °C, pH = 3, [DCA]o = 1 Mm. O_3 input concentration: 135 ± 5 mg L^{-1}.	(PAG/O_3/UVA) showed highly modified oxidation properties in the decontamination of DCA in aqueous solutions. Kinetics of first order reactions with respect to dichloroacetic acid were found. Higher initial concentrations of DCA and higher temperatures increased the initial degradation rate. More than 90% of DCA was removed.	[207]

Table 7. *Cont.*

Target DBPs	Catalyst and Main Properties	Reactor and Experimental Conditions	Main Results	Ref.
DCA in simulated water: deionized water with different amounts of humic acid (HA).	Natural bentonite, composed primarily of Ca^{2+}-montmorillonite.	Cylindrical reactors with an inner diameter of 60 mm and a length of 500 mm. Gas flow rate 20 mL min^{-1}; ozone gaseous concentrations of 0.90 mg L^{-1}; 298 K; 2 L simulated water: Deionized water containing 1 mg L^{-1} DCA or different amounts of HA, pH adjusted to 6.0.; Fe^{3+} dosage: 5 mg L^{-1}.	Under the combined effects of adsorption, ozonation and catalytic oxidation, high DCA removal is obtained.	[208]
DCA	Nanometer ZnO powder: Size 90 nm, and surface area (11 m^2 g^{-1}).	Batch experiments. A glass flat-bottomed flask with the inside diameter of 45 cm and the volume of 1.2 L. T = 20 ± 1 °C; initial pH 6.88; [DCA]o = 100 μg L^{-1}; initial ozone concentration 1.96 mg L^{-1}; catalyst dosage 100 mg L^{-1}.	ZnO as catalyst in water significantly improved the ozonation removal of DCA. The degradation efficiency of DCA increased with the increasing pH of solution, catalyst dosage and ozone dosage. The presence of t-BuOH had a negative effect on catalytic ozonation of DCA.	[209]

8.1. Catalytic Ozonation

Due to the selective oxidation property of the ozone molecule, highly structured organic substances cannot be thoroughly mineralized in ozonation alone and low-mass compounds like chloroacetic acids tend to be discharged. In addition, the efficiency of the oxidation can be strongly affected by the presence of natural organic matter which is ubiquitous in drinking or fresh water [208]. Hence, catalytic ozonation, an efficient AOP that introduces homogeneous or heterogeneous catalyst to single ozonation, can increase ozonation efficacy and ozone utilization degree. Especially, heterogeneous catalytic ozonation processes have received increasing attention recently due to the potentially higher effectiveness in the degradation and mineralization of refractory organic pollutants and easier recovery processing [209].

8.1.1. Catalysts

Li et al. [205] studied the potential use of manganese oxide-based nanocomposite in catalytic ozonation of DCA. Manganese oxide (MnOx) is an eco-friendly and inexpensively used catalyst in water treatment. Among various crystal phases of MnOx, β-MnO_2, not only has the highest stability and the lowest water-solubility but can also be easily fabricated in various morphologies such as nanowires, nanorods, nanotubes, and nanoflowers. However, the catalytic performance of single-component β -MnO_2 so far is unsatisfactory. In order to enhance the catalytic property of β -MnO_2, some promising methods such as modifying β -MnO_2 with noble metals or combining β -MnO_2 with other oxides have been developed. In this sense, graphene and its partial oxide counterpart-reduced graphene oxide (RGO) have emerged as promising candidates for fabricating new materials due to their high specific surface area, chemical stability, as well as biocompatibility. It has been proved that composite fabricated by coupling graphene or RGO with semiconductors can achieve a higher catalytic activity. Herein, Li et al. [205] reported a unique three-dimensional (3D) flower-like nanocomposite (FMOG) consisted of pure β -MnO_2 (PMO) and reduced graphene oxide (RGO). Interestingly, FMOG displayed higher catalytic performance compared with ozonation, and PMO catalytic ozonation. Gu and co-workers [208] used bentonite and Fe^{3+} for dichloroacetic acid (DCA) removal from drinking water. Bentonite is a 2:1 type clay mineral. Its unit layer structure consists of one Al^{3+} octahedral sheet placed between two Si^{4+} tetrahedral sheets. It should also be noted that the addition of hydrolysable metal ion species (iron or aluminum) can be rapidly hydrolyzed around the surface of bentonite particles, resulting in a hydroxyl surface. In addition, the hydrozed iron (or iron ion) possesses the ability to catalyze the transformation of O_3 to hydroxyl radicals, and hence further promote the removal of dissolved target organic compounds. Zhai et al. in their study [209] used nanometer ZnO powder as a heterogeneous catalyst for catalytic ozonation of dichloroacetic acid (DCA) in aqueous solution, which is non-toxic, insoluble, and a cheaper transition metal oxide widely used in various processes.

8.1.2. Catalytic Activity, Stability, and Reusability

To demonstrate the catalytic activity of PMO and FMOG, Li et al. [205] compared these catalysts in catalytic ozonation of DCA from drinking water sources. Ozonation alone of DCA achieved 32.7% elimination in 60 min. When the PMO or FMOG were added into the system, the elimination ratio of DCA increased to 39.2% and 46.8% in 60 min, respectively. In this research, DCA was degraded completely in FMOG catalytic reaction after 110 min, while in the same reaction conditions the residual concentration ratio of DCA was 30% and 13.3% for ozonation alone and PMO catalytic reaction. These results indicate an evident catalytic ozonation effect of FMOG for DCA degradation. Also, reusing experiments were carried out to estimate the stability of PMO and FMOG. The used catalyst was separated from the solution by centrifugation. The catalytic activity of FMOG decreases gradually in the first four runs. However, the catalytic activity of PMO decreases more obviously compared with the one of FMOG. In the fifth run, the DCA elimination ratio of PMO dropped to 32.5%, demonstrating a continuous downtrend; while the DCA elimination

ratio of FMOG in the fifth run was 37.7%, which was almost the same as that of the fourth run. SEM of FMOG after fifth catalytic ozonation showed that the flower-like nanostructure was still distinct. These facts indicate that FMOG is a relatively robust catalyst for catalytic ozonation of DCA in practical applications. Gu et al. [208] compared ozonation alone, ozone/bentonite and combined addition of ozone/bentonite/Fe^{3+} (adsorptive ozonation) for removing DCA from water in the presence and absence of HA. In this work, the combination of ozone/bentonite and Fe^{3+}, significantly promotes DCA removal achieving a percentage of about 73% after 40 min reaction time. This improvement was due to the ability of Fe^{+3} in catalyzing ozone decomposition to hydroxyl radical. Hence, in the process of ozonation/bentonite/Fe^{+3}, more $HO^{\bullet}$ radicals are generated. ZnO as catalyst in water significantly improved the ozonation removal of DCA compared with ozonation alone [209]. The addition of ZnO catalyst improved the degradation efficiency of DCA during ozonation, which caused an increase of 22.8% for DCA decomposition compared to the case of ozonation alone after 25 min. Under the same experimental conditions, DCA decomposition was enhanced by increasing catalyst dosage from 100 to 500 mg L^{-1} and ozone dosage from 0.83 to 3.2 mg L^{-1}. The catalytic ozonation process is more pronounced than the ozonation process alone at pH 3.93, 6.88, and 10. With increasing the concentration of t-BuOH from 10 to 200 mg L^{-1}, the degradation of DCA was significantly inhibited in the process of catalytic ozonation, indicating that the degradation of DCA by adding nanometer ZnO powder follows a radical-type mechanism.

8.1.3. Reactors and Variables Studied

In the work of Li et al. [205] catalytic ozonation of DCA was carried out into a 500 mL glass conical flask containing 200 mL of DCA aqueous solution (100 mg L^{-1}) with 10 mg of the as-prepared catalyst at room temperature under magnetic stirring. The effect of pH, the reaction temperature and catalyst dose on the catalytic DCA elimination by using FMOG was studied. Cylindrical reactors were used by Gu et al. [208], with an inner diameter of 60 mm and a length of 500 mm and 2 L working volume. In this work, authors study the efficiency of ozonation alone and catalytic ozonation with bentonite on DCA removal in the presence of different humic acid (HA) concentrations. HA was applied to test the effect of NOM concentrations on catalytic ozonation of DCA. Zhai and co-workers [209] performed the experiments in a laboratory batch reactor, which consisted of a glass flat-bottomed flask with the inside diameter of 45 cm and the volume of 1.2 L. In this study, authors checked the influencing factors on the degradation efficiency of DCA in aqueous solution by ZnO catalytic ozonation, including catalyst dosage, ozone concentration, initial solution pH, and tert-butyl alcohol.

8.1.4. Kinetics and Mechanisms

In all experiments carried out by Li et al. [205], ozone was supplied into the reaction system superfluously and continuously. Therefore, the pseudo first order reaction was employed by authors to investigate kinetics of single and catalytic ozonation, respectively, of DCA. For the DCA ozonation process, the apparent rate constant was 0.0062 min^{-1}. For the catalytic ozonation of DCA process in the presence of PMO, the apparent rate constant augmented to 0.0081 min^{-1}. However, when using FMOG as catalyst, the apparent rate constant increased to 0.0104 min^{-1}. Compared with the PMO catalytic process and the ozonation process, the apparent rate constant of FMOG catalytic process increases 28% and 68% respectively. The remarkable catalytic capacity of FMOG revealed that it can be used as an effective catalyst for the ozonation degradation of DCA. Based on literature, RGO has π electron donating character of the sp^2-bonded carbon structure, which can make FMOG more effective than PMO in transferring electron to ozone, and the polylaminate structure of RGO improved the surface area of the catalyst, which provides more ozonation reaction centers. The synergistic effect of β-MnO_2 and RGO in catalytic ozonation may contribute to the outstanding performance of FMOG. Gu et al. [208] proposed a pseudo first order degradation model. Results showed that the rate of DCA removal with ozonation is close

to that of the ozone/bentonite, and the rate of the adsorptive ozonation is much higher than that of the other two processes. The presence of HA in aqueous solution lowers the rate of the DCA degradation. In ozonation alone, when 4 mg L^{-1} HA was added, the rate is lowered to about 0.006 min^{-1}, which is only 28.6% of the rate when HA is absent. However, in the process of adsorptive ozonation, the negative effect of HA on DCA removal is weakened. When 4 mg L^{-1} HA was added, the rate constant is lowered to 0.052 min^{-1}, about 53% of that in the absence of HA. Zhai et al. [209] supposed that hydroxyl radicals in solution promote the oxidation degradation of DCA. Here, fundamental study was performed using DFT to explore the mechanism of generating hydroxyl radical on the ZnO surface. The DFT calculation results further verified the decomposition of the adsorbed ozone on the catalyst surface and the enhancement of generation of OH responsible for high ZnO catalytic activity, leading to the increase of degradation efficiency of the model pollutant DCA.

8.2. Photocatalytic Ozonation

So far only three works on photocatalytic ozonation of DBPs already formed have been published (see Table 7). As happens in catalytic ozonation works, chloroacetic acids are the chlorine disinfection by-products most studied.

8.2.1. Catalysts and Radiation Use

Degradation of DCA in aqueous solutions using photocatalytic ozonation has been investigated by Hama Aziz [106] and Mehrjouei et al. [207] (see Table 7). The photocatalyst used in both works was titanium dioxide immobilized in the commercial product "Pilkington ActiveTM glass" (PAGs). The great superhydrophilicity of TiO$_2$ photocatalyst provided a homogeneous and stable falling liquid film along the glass sheets. In both works, the application of irradiation with wavelengths in the region of UVA instead of shorter wavelengths promotes the idea of moving towards the use of natural solar light. Hence, radiation use for the photocatalytic experiments was in a range of wavelengths between 300 nm and 420 nm and a maximum at about 360 nm. On the other hand, Shin et al. [206] studied the removal of dichloroacetonitrile (DCAcN) with solar PhCatOz and P25 TiO$_2$ as catalyst (slurry mode). The authors use both UVA-visible lamps of different intensity and solar light as radiation source as an energy-saving and environmental-friendly process.

8.2.2. Catalytic Activity, Stability, and Reusability

Hama Aziz [106] found that the combination of ozonation with photocatalysis (TiO$_2$ on the surface of PAGs irradiated by the UVA) had shown a significant synergistic effect on DCA degradation due to the production of highly reactive hydroxyl radicals either by the direct photolysis of ozone with UVA or by interaction of ozone with the conduction band electrons on the illuminated TiO$_2$. At the same time, a dramatic increase in the mineralization level was achieved. Thus, comparing the degradation efficiencies of DCA by the photocatalytic ozonation (UVA/TiO$_2$/O$_3$) and photocatalytic decomposition of H$_2$O$_2$ (UVA/TiO$_2$/H$_2$O$_2$) processes in terms of the observed rate constants (the degradation of chloroacetic acids was described by pseudo first-order kinetics) indicates that the photocatalytic ozonation provides remarkably higher degradation efficiency than the photocatalytic-H$_2$O$_2$ [106]. Similar results were found by Mehrjouei et al. [207] where photocatalytic ozonation treatment by means of Pilkington ActiveTM glass as a commercial product irradiated by UVA light and combined with ozone (PAG/O$_3$/UVA) showed highly modified oxidation properties in the decontamination of DCA in aqueous solutions compared to both photocatalytic oxidation and ozonation separately. Also, photocatalytic ozonation exhibited high potential in the mineralization of DCA. It was observed that more than 90% of DCA decomposed during the oxidation period was mineralized to carbon dioxide molecules and chloride anions. In Mehrjouei study [207], the degradation of DCA by photocatalytic ozonation in heterogeneous system showed good agreement with the kinetics of first order reactions. However, at initial concentrations of DCA both higher and

lower than 1 mM, the initial degradation rates were found to be slightly different. In the case of DCAN degradation [206], compared to the single process, the UV-solar/TiO_2/O_3 process had the highest DCAN-removal rate. This was due to additional $HO^\bullet$ production by the reaction of ozone with the electrons of the conduction band in the catalyst. The UV-solar/TiO_2/O_3 system showed an enhanced DCAcN-removal rate, and the synergetic index calculated according to equation (71) for a single process was 3.8:

$$\text{SI} = \frac{\text{k}_{\text{Sun/O3/Cat}}}{\text{k}_{\text{Sun/Cat}} + \text{k}_{\text{O3}}} \tag{71}$$

where k values are the apparent pseudo first order rate constants of PhCatOz, solar photocatalysis and ozone processes, respectively.

Works quoted in Table 7 have also studied the photocatalyst stability and activity by conducting cycles of photocatalytic ozonation runs of fresh compound aqueous solutions with the same photocatalyst.

8.2.3. Reactors, Radiation Source, and Variables Studied

A planar falling film reactor was used by Hama Haziz [106] for the photocatalytic experiments. The reactor consists of two photoactive self-cleaning Pilkington Active™ glass (PAGs) sheets, each with a 68×29 cm surface area, connected by a frame of PVC. The falling liquid film was established on the inner side of the PAGs. Seven UVA lamps (each with 15W energy consumption and the maximum wavelength at 360 nm) were fixed inside the reactor and used for UVA irradiation. The incident light intensity of the UV light was $1\,\text{Mw/cm}^2$, and no significant aging effect was found during the experiments. The optimization of water flow rate to generate a stable and homogeneous falling film along the PAG sheets was tested being $1\,\text{Lmin}^{-1}$. The planar reactor used by Mehrjouei et al. [207] was a polymethylmethacrylate box with an internal volume of $160\,\text{cm}^3$ covered by an optical window made from the same material in order to let the irradiation of UVA light pass through and reach the photocatalytic surface of a Pilkington Active™ glass sheet with a contact area of $30.5\,\text{cm}^2$, which was embedded and fixed inside the reactor. For all runs, a volume of 400 mL of DCAA solution was injected through the bottom inlet of the reactor to form a 3 mm liquid layer over the semiconductor surface, and it left the reactor through the top outlet point. The UVA-light source employed in this study was a 30 W lamp with a range of wavelengths between 300 nm and 420 nm and a maximum at about 360 nm. The incident light intensity of this source, as in the case of Hama Haziz [106] was ca. $1\,\text{MW/cm}^2$. In [207] influence of initial concentration and temperature on the degradation rate of DCAA and the ozone consumption level during the oxidation process were investigated. Higher initial concentrations of DCAA and higher temperatures increased the initial degradation rate and, the level of ozone consumption during the photocatalytic ozonation treatment.

Shin et al. [206] for the photocatalytic experiments (bench and outdoor) used the combination of CPC and ozone reactor. CPC contained three quartz tubes (length: 40 cm, diameter: 3 cm, thickness: 1.5 mm) and three stainless modules with reflectors made of polished aluminum. A cylindrical ozone reactor with a cooling system was made of stainless steel (length: 110 cm, diameter: 10.5 cm, and total volume: 9.5 L). For the bench system, UV radiations were obtained from three metal halide lamps of different powers (100, 250, and 400 W), which were placed 60 cm above the CPC reactor at the top of the chamber as artificial solar light. Figure 4 represents the experimental set up used in this work.
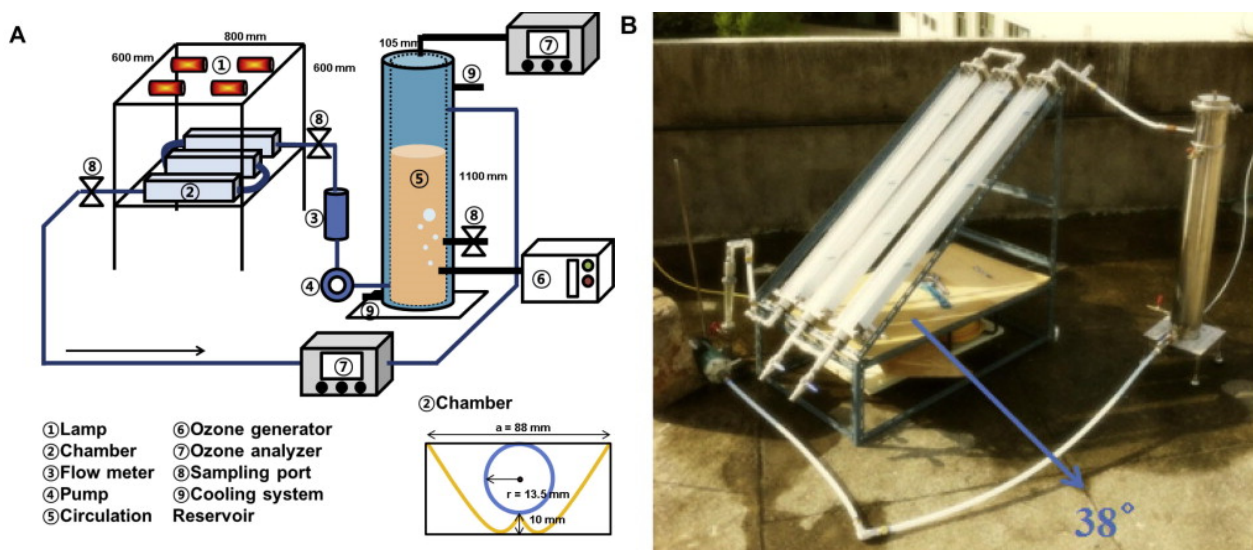
Figure 4. Experimental set up for photocatalytic ozonation experiments at lab and bench scale [206]. (**A**): Flow diagram. (**B**): CPC reactor. (Reprinted with permission from *Chemosphere*, 93, Shin, D.; Jang, M.; Cui, M.; Na, S.; and Khim, J. Enhanced removal of dichloroacetonitrile from drinking water by the combination of solar-photocatalysis and ozonation, 2901–2908. Copyright (2013) With permission from Elsevier).

The UV intensity in the sunlight wavelength range was measured using a spectroradiometer. The irradiation wavelengths of the metal halide lamps (designated as UVsolar, 300–800 nm) and solar light (>300 nm) were similar in terms of the light spectrum. In this research, the major operating parameters such as pH, catalyst (i.e., TiO$_2$) and ozone doses, temperature, and UV intensity were investigated in the removal of DCAN by photocatalytic ozonation. Shin et al. [206] found that the optimal pH for DCAN removal by UV-solar/TiO$_2$/O$_3$ was neutral because of the maximum interaction between TiO$_2$ and DCAN. According to the results of TiO$_2$ and ozone-dose tests, 1 g L^{-1} TiO$_2$ and 1.13 g L^{-1} h^{-1} ozone in photocatalytic ozonation were optimal to afford the highest rate constant. From the temperature variation trials, the highest rate constant (0.033 min^{-1}) was obtained at 20 °C. Temperature simultaneously affected several parameters such as DCAcN adsorption and particle-size change of TiO$_2$, as well as the decomposition and dissolution rates of ozone. Nevertheless, temperatures higher than 20 °C negatively influenced the DCAcN-removal kinetics. In the assays regarding the UV-solar intensity, the kinetic rate constants increased linearly when the UV-solar intensity increased in the range 4.6–25 Wm^{-2}; however, the increasing trend of rate constants were gradually reduced above 25 Wm^{-2}. The test results of the outdoor system indicated that the solar/TiO$_2$/O$_3$ process showed complete removal with rates that are two orders greater than those obtained with solar/TiO$_2$.

To conclude this section, DBPs elimination by catalytic/photocatalytic ozonation has been demonstrated to proceed by indirect or radical ozonation pathways more than direct ozonation. However, the limited studies carried out mainly with DCA, TCA, and DCAN as model DBPs at high concentrations, many of them in ultrapure water opens some questions about the effect of a real water matrix, the optimization of the catalytic systems to improve the degradation, the use of solar radiation or LEDs, long-term behavior of the catalytic systems, etc. that opens the research possibilities in this field. In addition, the economical assessment of these processes to remove DBPs compared to the elimination efficiency of DBPs precursors needs to be balanced to choose a treatment strategy.

9. The Case of Bromate in Ozonation Processes

An additional survey deserves bromate formation/inhibition during ozonation processes when bromide ions are present in surface water. Bromate ion (BrO$_3{}^-$) is a well-known

DBP with a maximum allowed level of 10 μg L^{-1} by many regulations (USEPA, WHO, ECA, etc.) suspected to be a carcinogenic agent. Yang et al. [210] recently reviewed the formation of bromate in chemical oxidation and its control strategies.

Fischbacher et al. [211] reported a multistep mechanism of bromate formation during ozonation in the presence of bromide in which HO• radicals are formed and also contribute to bromate formation according to Scheme 7.
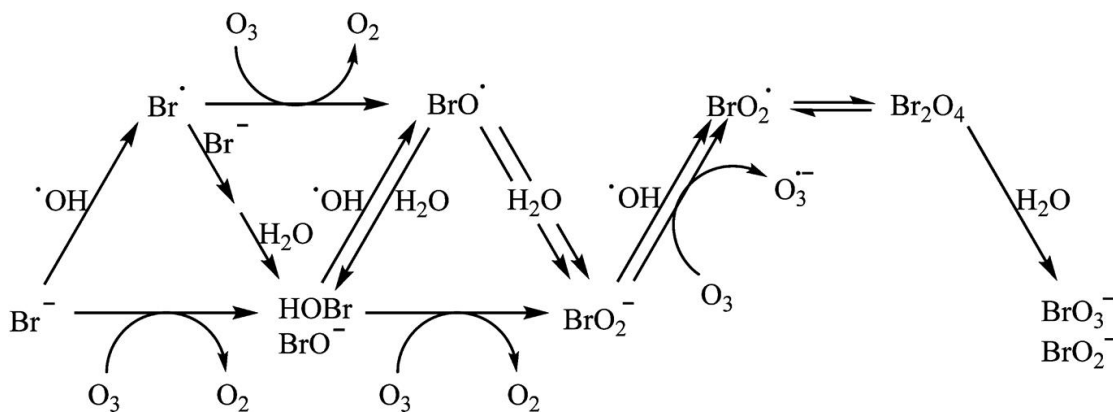
Scheme 7. New reaction pathway of the ozonation of bromide in water [211], (Reprinted with permission from Fischbacher, A.; Löppenberg, K.; von Sonntag, C.; Schmidt, T.C. A new reaction pathway for bromite to bromate in the ozonation of bromide. Environ. Sci. Technol. 2015, 49, 11714–11720, Copyright (2015) American Chemical Society).

Different strategies for the inhibition of bromate formation during ozonation have been extensively studied such as pH depression, ammonia addition, Cl$_2$-ammonia addition, H$_2$O$_2$ addition or optimization of reactor configuration. The main effects of these can be found in Yang et al. [210] and references herein. However, during catalytic/photocatalytic ozonation, the presence of the catalyst can bring new benefits for bromate control. Thus, Han et al. [172,174] in their works of catalytic ozonation using ferrate (VI) as catalyst (see conditions in Table 6) demonstrated that low doses of ferrate up to 5 mg L^{-1} can lead to the reduction or flocculation of BrO$_3$– or HBrO/BrO- by the produced intermediates Fe(III), Fe(II), H$_2$O$_2$, and Fe(III) hydroxydes. Humic acid content decreased bromate formation and also high ambient temperature had a positive effect.

Wu et al. [169] studied the inhibition of nano TiO$_2$ and SnO$_2$ on bromate formation during catalytic ozonation of humic acid and observed that the presence of both catalysts reduced the formation of BrO$_3$– and also a positive effect of increasing humic acid concentration. They hypothesized that the minimization using TiO$_2$ was due to the decomposition of ozone into HO• which rapidly generated H$_2$O$_2$. This hypothesis agrees with the effect of humic acid as HO• and O$_3$ scavenger. This effect has also been observed in other studies with different metal oxides although in ultrapure water or with other organic pollutants.

Regarding photocatalytic ozonation, Parrino et al. [212] studied the formation or reduction of bromate by photocatalysis, ozonation and photocatalytic ozonation using TiO$_2$ as catalyst and UVA radiation. They observed that the sole photocatalysis did not produce bromate ions and in the case of its presence, it was able to reduce bromate to bromide ions. On the contrary, in the combined process, bromate ions were not produced when organics still present. They proposed that photo-generated electrons reduced adsorbed bromate to bromide over the catalyst surface.

Thus, the possibility of controlling bromate by tailoring the catalyst has relevance for real application of catalytic/photocatalytic ozonation in drinking water treatment.

10. Concluding Remarks and Future Challenges

Main conclusions of this work are:

DBPs, specifically THMs, were discovered more than 40 years ago but, still, there is much research on their nature, since many recent papers deal with the founding of new DBPs. Already in 1980 about 400 DBPs were identified in chlorinated fulvic acids. At present, only a few DBPs are regulated with a maximum level concentration (MCL): Total THMs, total HAAs, bromate and chlorite. Nonregulated DBPs form different family groups: Halogenated compounds, ketones, aldehydes, and nitrosamines to quote the most representatives with the first ones as the most abundant formed in DWT. The halogenated compounds, (mainly chlorinated but also brominated and iodinated compounds) constituted by far the main family of DBPs from WTP. Today, many of these compounds have been classified as rodent carcinogens, genotoxic, and mutagenic. This reveals the importance in the development of new analytical methods to quantify also nonregulated DBPs or surrogate parameters to fulfil future regulation in order to produce healthy drinking water.

Both DBPs precursors and DBPs have been treated with different oxidation processes where AOPs are the most representative. Because of the double way of ozone reactions in water, ozone has attracted the interest of many researchers. NOM and bromide ion are the main DBPs precursors treated with AOPs. In the last year, about 40 and 20 works were published on this matter with AOPs and ozone processes, as oxidants, respectively. On the whole, precursors react fast with ozone due to the presence of aromatic rings with hydroxyl substituents groups in humic and fulvic acid macromolecules. However, regarding DPBs removal classical ozone AOPs, such as O_3/UVC or O_3/H_2O_2, have been applied in a few cases to mainly remove a few HAAs (dichloroacetic and trichloracetic acids) and some N-nitrosamines. On the contrary, much more work has been done with ozone free processes such as Fenton, UVC/H_2O_2, and photocatalytic oxidation during the last 25 years. In these works, HAAs are the main DBPs studied. In general, these processes due to the formation of hydroxyl radicals reduce DBP concentrations but high oxidant doses are needed.

Most of the works dealing with catalytic and photocatalytic ozonation are lab-scale studies about catalyst properties, catalytic activity and optimization of operating conditions but much less work has been done to go in deep in the stability and reutilization of the catalysts in long term experiments. These studies are crucial to take a step forward to pilot scale studies with the best catalytic systems mainly for DBPFP removal. In addition, the use of natural radiation or environmentally friendly LEDs should be prioritized in photocatalytic ozonation studies towards sustainable processes. However, comprehensive economic and environmental assessments are also required to balance the benefits of precursors or DBPs removal from drinking water in order to draw the best strategy from economic, environmental and health priorities.

Nomenclature

AC	Activated carbon
AOPs	Advanced oxidation processes
AORPs	Advanced oxidation/reduction processes
AOX	Adsorbable organic halides
BAC	Biological activated carbon

BC	Before Christ
BDCA	Bromodichloroacetic acid
BET	Brunauer, Emmet, and Teller (referred to isotherm and surface area)
Br-DBPs	Brominated disinfection by-products
C_i	Concentration of i
CAAs	Chloroacetic acids
Cat	Catalyst
CDBA	Chlorodibromoacetic acid
CH	Chloral hydrate
CPC	Compound parabolic collector
CT	Parameter used in disinfection with C concentration of chlorine, T contact time
D	Diameter (particle size or reactor diameter)
DBPFP	Disinfection by-products formation potential
DBPs	Disinfection by-products
DCA	Dichloroacetic acid
DCAN	Dichloroacetonitrile
DFT	Density functional theory
DLS	Dynamic light scattering
DMP	Dimethyl phthalate
DOC	Dissolved organic carbon
DWT	Drinking water treatment
DWTP	Drinking water treatment plant
EAOPs	Electrochemical advanced oxidation processes
ECA	European Chemical Agency
EDS	Dispersive X-Ray spectroscopy
EPA	Environmental Protection Agency
E-peroxone	Electro-peroxone
EPR	Electron paramagnetic resonance
ER	Eley-Rideal mechanism
FMOG	Flower-like nanocomposite
FTIR	Fourier transformed infrared spectroscopy
GAC	Granular activated carbon
HA	Humic acid
HAAs	Haloacetic acids
HAcAm	Haloacetamides
HANs	Haloacetonitriles
HIA	Hydrophilic acid
HIB	Hydrophilic base
HKs	Haloketones
HOA	Hydrophobic acid
HON	Hydrophobic neutral
HS	Humic substances
ICP	Inductively coupled plasma
ICZ	Iron coated zeolite
I-DBPs	Iodinated disinfection by-products
JCR	Journal Citation Report
k	Kinetic constant
L	Length
LED	Light emitting diodes
LHHW	Langmuir–Hinshelwood–Hougen–Watson mechanism
MBA	Bromoacetic acid
MCA	Monochloroacetic acid
MCL	Maximum concentration level
MOFs	Metal organic frameworks
NB	Nitrobencene
N-DBPs	Nitrogen containing disinfection by-products
NDBA	N-nitrosodibuthylamine
NDMA	N-nitrosodimethylamine
NOM	Natural organic matter

NR-DBPs	Non-regulated disinfection by-products
NTU	Nephelometric turbidity unit
OA	Oxalic acid
PACL	Poly-aluminium chloride
PAG	Pilkington ActiveTM glass
pCBA	p-Chlorobenzoic acid
PMO	Pure manganese oxide
PMS	Peroxymonosulfate
PS	Persulfate
PZC	Potential of zero charge
Q	Volumetric flow
Rct	Ratio of the hydroxyl radicals to the ozone exposure during ozone processes
R-DBPs	Regulated disinfection by-products
RGO	Reduced graphene oxide
RO	Reverse osmosis
ROS	Reactive oxidizing species
SCE	Saturated calomel electrode
SEM	Scanning electron microscopy
SHE	Standard hydrogen electrode
TBA	Tribromoacetic acid
TCA	Trichloroacetic acid
TCNM	Trichloronitromethane
THAAs	Total haloacetic acids
THAAFP	Total haloacetic acids formation potential
THMs	Trihalomethanes
THMFP	Trihalomethane formation potential
TNT	Titanate nanotubes
TOC	Total organic carbon
TOX	Total organic halogen
TOXFP	Total organic halogen formation potential
TTHMFP	Total trihalomethane formation potential
WHO	World Health Organization
USEPA	United States Environmental Protection Agency
USA	United States of America
UV	Ultraviolet radiation
UVA	Ultraviolet A radiation
UVC	Ultraviolet C radiation
UV-Vis-DRS	Ultraviolet-visible diffuse reflectance spectroscopy
UV254	Referred to absorbance at 254 nm
V	Volume
WOS	Web of Science
X	Halogen
XPS	X-ray photoelectron spectroscopy
XRD	X-ray diffraction
XRF	X-ray fluorescence

References

1. Danil De Namor, A.F. Water purification: From ancient civilization to the XXI Century. *Water Sci. Technol. Water Supply* **2007**, *7*, 33–39. [CrossRef]
2. Merlet, N. Contribution á l'Etude du Mécanisme de Formation des TrihaloméThanes et des Composés Organohalogénés non Volatils Lors de la Chloration de Molecules Modèles. Ph.D. Thesis, Université de Poitiers, Poitiers, France, 1986.
3. White, G.C. Current chlorination and dechlorination practices in the treatment of potable water, wastewater and cooling water. In *Water Chlorination: Environmental Impacts and Health Effects*; Ann Arbor Science Publishers: Ann Arbor, MI, USA, 1978; Volume 1, pp. 1–18.
4. Symons, J.M.; Bellar, T.A.; Carswell, J.K. National organics reconnaissance survey for halogenated organics. *J. Am. Water Work. Assoc.* **1975**, *67*, 634–647. [CrossRef]
5. Rook, J.J. Formation of Haloforms during Chlorination of Natural Waters. *Water Treat. Exam.* **1974**, *23*, 234–243.

6.   Bellar, T.A.; Lichtenberg, J.J.; Kroner, R.C. Occurrence of Organohalides in Chlorinated Drinking Waters. *J. Am. Water Work. Assoc.* **1974**, *66*, 703–706. [CrossRef]

7.   US Environmental Protection Agency. *Lower Mississippi River Facility. New Orleans Area Water Supply Study*; US Environmental Protection Agency: Whasington, DC, USA, 1974.

8.   Chang, S.L. The safety of water disinfection. *Annu. Rev. Public Health* **1982**, *3*, 393–418. [CrossRef]

9.   Glaze, W.H.; Henderson, J.E., IV. Formation of organochlorine compounds from the chlorination of a municipal secondary effluent. *J. Water Pollut. Control Fed.* **1975**, *47*, 2511–2515.

10. Schnitzer, M.; Khan, S.U. *Humic Subtances in the Environment*; Marcel Dekker Inc.: New York, NY, USA, 1972.

11. Steelink, C. Humates and other natural organic substances in the aquatic environment. *J. Chem. Educ.* **1977**, *54*, 599–603. [CrossRef]

12. Croué, J.P. Contribution á l'étude de l'Oxydation par le Chlore et l'Ozone d'Acides Fulviques Naturels Extraits d'Eaux de Surface. Ph.D. Thesis, Université de Poitiers, Poitiers, France, 1987.

13. Corin, N.; Backhand, P.; Kulovaara, M. Degradation products formed during UV-irradiation of humic waters. *Chemosphere* **1996**, *33*, 245–255. [CrossRef]

14. Beckett, R. The Surface Chemistry of Humic Substances in Aquatic Systems. In *Surface and Colloid Chemistry in Natural Waters and Water Treatment*; Beckett, R., Ed.; Plenum: New York, NY, USA, 1990; pp. 3–16.

15. Sirivedhin, T.; Gray, K.A., II. Comparison of the disinfection by-product formation potentials between a wastewater effluent and surface waters. *Water Res.* **2005**, *39*, 1025–1036. [CrossRef]

16. Doré, M.; Goichon, J. Etude d'une methode d'evaluation globale des precurseurs de la reaction haloforme. *Water Res.* **1980**, *14*, 657–663. [CrossRef]

17. Gilca, A.F.; Teodosiu, C.; Fiore, S.; Musteret, C.P. Emerging disinfection byproducts: A review on their occurrence and control in drinking water treatment processes. *Chemosphere* **2020**, *259*, 127476. [CrossRef]

18. Sun, S.; Jiang, T.; Lin, Y.; Song, J.; Zheng, Y.; An, D. Characteristics of organic pollutants in source water and purification evaluations in drinking water treatment plants. *Sci. Total Environ.* **2020**, *733*, 139277. [CrossRef]

19. Gonsioroski, A.; Mourikes, V.E.; Flaws, J.A. Endocrine disruptors in water and their effects on the reproductive system. *Int. J. Mol. Sci.* **2020**, *21*, 1929. [CrossRef] [PubMed]

20. Tak, S.; Vellanki, B.P. Natural organic matter as precursor to disinfection byproducts and its removal using conventional and advanced processes: State of the art review. *J. Water Health* **2018**, *16*, 681–703. [CrossRef]

21. Miller, G.W.; Rice, R.G.; Robson, C.M.; Scullin, R.L.; Kuhn, W.; Wolf, H. *An Assessment of Ozone and Chlorine Dioxide Technologies for Treatment of Municipal Water Supplies*; Environmental Protection Agency, Office of Research and Development, Municipal Environmental Research Laboratory: Cincinnati, OH, USA, 1978; Executive Summary EPA Report; EPA-600/8-78-018 October 1978.

22. Doré, M. Chimie des Oxydants et Traitement des Eaux. *Tech. Doc. Paris* **1989**.

23. Langlais, B.; Reckhow, D.A.; Brink, D.R. *Ozone in Water Treatment: Application and Engineering*; Langlais, B., Reckhow, D.A., Brink, D.R., Eds.; Lewis Publishers: Chelsea, MI, USA, 1991.

24. Glaze, W.H.; Kang, J.W.; Chapin, D.H. The chemistry of water treatment processes involving ozone, hydrogen peroxide and ultraviolet radiation. *Ozone Sci. Eng.* **1987**, *9*, 335–352. [CrossRef]

25. Bailey, P.S. The Reactions Of Ozone With Organic Compounds. *Chem. Rev.* **1958**, *58*, 925–1010. [CrossRef]

26. Staehelin, J.; Hoigne, J. Decomposition of ozone in water in the presence of organic solutes acting as promoters and inhibitors of radical chain reactions. *Environ. Sci. Technol.* **1985**, *19*, 1206–1213. [CrossRef]

27. Beltrán, F.J. *Ozone Reaction Kinetics for Water and Wastewater Systems*; CRC Press: Boca Raton, FL, USA, 2004.

28. Bader, H.; Hoigné, J. Rate Constants of Reactions of Ozone with Organic and Inorganic Compounds in Water -II. Dissociating Organic Compounds. *Water Res.* **1983**, *17*, 185–194.

29. Hoigné, J.; Bader, H. Rate constants of reactions of ozone with organic and inorganic compounds in water-I. Non-dissociating organic compounds. *Water Res.* **1983**, *17*, 173–183. [CrossRef]

30. Kuczkowski, R.L. Ozone and carbonyl oxides. In *1,3, Dipolar Cycloaddition Chemistry*; John Wiley and Sons: New York, NY, USA, 1984; Volume 2A, pp. 197–277.

31. Beltran, F.J.; Gonzalez, M.; GarcÍA-Araya, J.F.; Cabrera, J.L. The use of ozonation to reduce the potential for forming trihalomethane compounds in chlorinating resorcinol, phloroglucinol and 1,3 cyclohexanedione. *Chem. Eng. Commun.* **1990**, *96*, 321–339. [CrossRef]

32. Cavanagh, J.E.; Weinberg, H.S.; Avram, G.; Sangalah, R.; Dean, M.; Glaze, W.H.; Collette, T.W.; Richardson, S.D.; Thruston, A.D. Ozonation Byproducts: Identification of Bromohydrins from the Ozonation of Natural Waters with Enhanced Bromide Levels. *Environ. Sci. Technol.* **1992**, *26*, 1658–1662. [CrossRef]

33. Rav-Acha, C. Review Paper the Reactions of Chlorine Dioxide With Aquatic Organic Materials and. *Water Res.* **1984**, *18*, 1329–1341. [CrossRef]

34. Wajon, J.E.; Rosenblatt, D.H.; Burrows, E.P. Oxidation of Phenol and Hydroquinone by Chlorine Dioxide. *Environ. Sci. Technol.* **1982**, *16*, 396–402. [CrossRef] [PubMed]

35. Rice, R.G.; Gomez-Taylor, M. Occurrence of by-products of strong oxidants reacting with drinking water contaminants—Scope of the problem. *Environ. Health Perspect.* **1986**, *69*, 31–44. [CrossRef]

36. Song, K.; Mohseni, M.; Taghipour, F. Application of ultraviolet light-emitting diodes (UV-LEDs) for water disinfection: A review. *Water Res.* **2016**, *94*, 341–349. [CrossRef]

37. Dalrymple, O.K.; Stefanakos, E.; Trotz, M.A.; Goswami, D.Y. A review of the mechanisms and modeling of photocatalytic disinfection. *Appl. Catal. B Environ.* **2010**, *98*, 27–38. [CrossRef]

38. Fernández, P.; Blanco, J.; Sichel, C.; Malato, S. Water disinfection by solar photocatalysis using compound parabolic collectors. *Catal. Today* **2005**, *101*, 345–352. [CrossRef]

39. Booshehri, A.Y.; Polo-Lopez, M.I.; Castro-Alférez, M.; He, P.; Xu, R.; Rong, W.; Malato, S.; Fernández-Ibáñez, P. Assessment of solar photocatalysis using Ag/BiVO₄ at pilot solar Compound Parabolic Collector for inactivation of pathogens in well water and secondary effluents. *Catal. Today* **2017**, *281*, 124–134. [CrossRef]

40. Madaeni, S.S. The application of membrane technology for water disinfection. *Water Res.* **1999**, *33*, 301–308. [CrossRef]

41. Sun, X.; Liu, J.; Ji, L.; Wang, G.; Zhao, S.; Yoon, J.Y.; Chen, S. A review on hydrodynamic cavitation disinfection: The current state of knowledge. *Sci. Total Environ.* **2020**, *737*. [CrossRef] [PubMed]

42. Li, Q.; Mahendra, S.; Lyon, D.Y.; Brunet, L.; Liga, M.V.; Li, D.; Alvarez, P.J.J. Antimicrobial nanomaterials for water disinfection and microbial control: Potential applications and implications. *Water Res.* **2008**, *42*, 4591–4602. [CrossRef] [PubMed]

43. Pina, A.S.; Batalha, Í.L.; Fernandes, C.S.M.; Aoki, M.A.; Roque, A.C.A. Exploring the potential of magnetic antimicrobial agents for water disinfection. *Water Res.* **2014**, *66*, 160–168. [CrossRef] [PubMed]

44. Emile Coleman, W.; Melton, R.G.; Kopfler, F.C.; Barone, K.A.; Aurand, T.A.; Jellison, M.G. Identification of Organic Compounds in a Mutagenic Extract of a Surface Drinking Water by a Computerized Gas Chromatography/Mass Spectrometry System (GC/MS/COM). *Environ. Sci. Technol.* **1980**, *14*, 576–588. [CrossRef]

45. Glaze, W.H. Brogan & Partners Reaction Products of Ozone: A Review. *Environ. Health Perspect.* **1986**, *69*, 151–157.

46. Werdehoff, K.S.; Singer, P.C. Chlorine Dioxide Effects on Thmfp, Toxfp, and the Formation of Inorganic By-Products. *J. Am. Water Work. Assoc.* **1987**, *79*, 107–113. [CrossRef]

47. Richardson, S.D. Disinfection by-products and other emerging contaminants in drinking water. *TrAC Trends Anal. Chem.* **2003**, *22*, 666–684. [CrossRef]

48. Lavonen, E.E.; Gonsior, M.; Tranvik, L.J.; Schmitt-Kopplin, P.; Köhler, S.J. Selective chlorination of natural organic matter: Identification of previously unknown disinfection byproducts. *Environ. Sci. Technol.* **2013**, *47*, 2264–2271. [CrossRef] [PubMed]

49. Bougeard, C.M.M.; Goslan, E.H.; Jefferson, B.; Parsons, S.A. Comparison of the disinfection by-product formation potential of treated waters exposed to chlorine and monochloramine. *Water Res.* **2010**, *44*, 729–740. [CrossRef]

50. Le Roux, J.; Nihemaiti, M.; Croué, J.P. The role of aromatic precursors in the formation of haloacetamides by chloramination of dissolved organic matter. *Water Res.* **2016**, *88*, 371–379. [CrossRef] [PubMed]

51. Padhi, R.K.; Subramanian, S.; Satpathy, K.K. Formation, distribution, and speciation of DBPs (THMs, HAAs, ClO²⁻, and ClO³⁻) during treatment of different source water with chlorine and chlorine dioxide. *Chemosphere* **2019**, *218*, 540–550. [CrossRef]

52. Gan, W.; Huang, S.; Ge, Y.; Bond, T.; Westerhoff, P.; Zhai, J.; Yang, X. Chlorite formation during ClO₂ oxidation of model compounds having various functional groups and humic substances. *Water Res.* **2019**, *159*, 348–357. [CrossRef]

53. Postigo, C.; Zonja, B. Iodinated disinfection byproducts: Formation and concerns. *Curr. Opin. Environ. Sci. Health* **2019**, *7*, 19–25. [CrossRef]

54. Richardson, S.D.; Plewa, M.J.; Wagner, E.D.; Schoeny, R.; DeMarini, D.M. Occurrence, genotoxicity, and carcinogenicity of regulated and emerging disinfection by-products in drinking water: A review and roadmap for research. *Mutat. Res. Rev. Mutat. Res.* **2007**, *636*, 178–242. [CrossRef] [PubMed]

55. Pan, Y.; Wang, Y.; Li, A.; Xu, B.; Xian, Q.; Shuang, C.; Shi, P.; Zhou, Q. Detection, formation and occurrence of 13 new polar phenolic chlorinated and brominated disinfection byproducts in drinking water. *Water Res.* **2017**, *112*, 129–136. [CrossRef]

56. How, Z.T.; Kristiana, I.; Busetti, F.; Linge, K.L.; Joll, C.A. Organic chloramines in chlorine-based disinfected water systems: A critical review. *J. Environ. Sci.* **2017**, *58*, 2–18. [CrossRef]

57. Mian, H.R.; Hu, G.; Hewage, K.; Rodriguez, M.J.; Sadiq, R. Prioritization of unregulated disinfection by-products in drinking water distribution systems for human health risk mitigation: A critical review. *Water Res.* **2018**, *147*, 112–131. [CrossRef]

58. Kimura, S.Y.; Ortega-Hernandez, A. Formation mechanisms of disinfection byproducts: Recent developments. *Curr. Opin. Environ. Sci. Heal.* **2019**, *7*, 61–68. [CrossRef]

59. Tardiff, R.G.; Garlson, G.P.; Simmon, V. Halogenated organics in tap water: A toxicological evaluation in Water Chlorination. Environmental Impact and Health Effects. *Ann Arbor Sci. Ann Arbor Michigan. USA* **1978**, *1*, 195–209.

60. U.S. National Cancer institute. *Report on the Carcinogenesis Bioassay of Chloroform (CAS No. 67-66-3)*; TR-000. NTIS Rpt No PB264018; U.S. National Cancer institute: Bethesda, MD, USA, 1976.

61. King, W.D.; Marrett, L.D. Case-control study of bladder cancer and chlorination by-products in treated water (Ontario, Canada). *Cancer Causes Control* **1996**, *7*, 596–604. [CrossRef]

62. Hildesheim, M.E.; Cantor, K.P.; Lynch, C.F.; Dosemeci, M.; Lubin, J.; Alavanja, M.; Craun, G. Drinking water source and chlorination byproducts II. Risk of colon and rectal cancers. *Epidemiology* **1998**, *9*, 29–35. [CrossRef]

63. Boorman, G.A.; Dellarco, V.; Dunnick, J.K.; Chapin, R.E.; Hauchman, F.; Gardner, H.; Cox, M.; Sills, R.C.; Boorman, G.A.; Dellarco, V.; et al. Brogan & Partners Drinking Water Disinfection Byproducts: Review and Approach to Toxicity Evaluation Source: Environmental Health Perspectives, Vol. 107, Supplement 1: Reviews in Environmental Health, 1999 (Feb., 1999), pp. 207–217 Published by. *Environ. Health Perspect.* **1999**, *107*, 207–217. [PubMed]

64. DeMarini, D.M. A review on the 40th anniversary of the first regulation of drinking water disinfection by-products. *Environ. Mol. Mutagen.* **2020**, *61*, 588–601. [CrossRef] [PubMed]

65. Wagner, E.D.; Plewa, M.J. CHO cell cytotoxicity and genotoxicity analyses of disinfection by-products: An updated review. *J. Environ. Sci.* **2017**, *58*, 64–76. [CrossRef] [PubMed]

66. Demarini, D.M.; Abu-Shakra, A.; Felton, C.F.; Patterson, K.S.; Shelton, M.L. Mutation spectra in salmonella of chlorinated, chloraminated, or ozonated drinking water extracts: Comparison to MX. *Environ. Mol. Mutagen.* **1995**, *26*, 270–285. [CrossRef]

67. Villanueva, C.M.; Cantor, K.P.; Grimalt, J.O.; Malats, N.; Silverman, D.; Tardon, A.; Garcia-Closas, R.; Serra, C.; Carrato, A.; Castaño-Vinyals, G.; et al. Bladder cancer and exposure to water disinfection by-products through ingestion, bathing, showering, and swimming in pools. *Am. J. Epidemiol.* **2007**, *165*, 148–156. [CrossRef] [PubMed]

68. Le Roux, J.; Plewa, M.J.; Wagner, E.D.; Nihemaiti, M.; Dad, A.; Croué, J.-P. Chloramination of wastewater effluent: Toxicity and formation of disinfection byproducts. *J. Environ. Sci.* **2017**, *58*, 135–145. [CrossRef] [PubMed]

69. Bond, T.; Goslan, E.H.; Parsons, S.A.; Jefferson, B. Treatment of disinfection by-product precursors. *Environ. Technol.* **2011**, *32*, 1–25. [CrossRef]

70. Sillanpää, M.; Ncibi, M.C.; Matilainen, A. Advanced oxidation processes for the removal of natural organic matter from drinking water sources: A comprehensive review. *J. Environ. Manag.* **2018**, *208*, 56–76. [CrossRef]

71. Matilainen, A.; Sillanpää, M. Removal of natural organic matter from drinking water by advanced oxidation processes. *Chemosphere* **2010**, *80*, 351–365. [CrossRef]

72. Glaze, W.H.; Peyton, G.R.; Lin, S.; Huang, R.Y.; Burleson, J.L. Destruction of pollutants in water with ozone in combination with ultraviolet radiation. II. Natural trihalomethane precursors. *Environ. Sci. Technol.* **1982**, *16*, 454–458. [CrossRef]

73. Zhang, Y.; Zhao, X.; Zhang, X.; Peng, S. A review of different drinking water treatments for natural organic matter removal. *Water Sci. Technol. Water Supply* **2015**, *15*, 442–455. [CrossRef]

74. Miklos, D.B.; Remy, C.; Jekel, M.; Linden, K.G.; Drewes, J.E.; Hübner, U. Evaluation of advanced oxidation processes for water and wastewater treatment—A critical review. *Water Res.* **2018**, *139*, 118–131. [CrossRef]

75. Hua, G.; Reckhow, D.A. Characterization of Disinfection Byproduct Precursors Based on Hydrophobicity and Molecular Size. *Environ. Sci. Technol.* **2007**, *41*, 3309–3315. [CrossRef] [PubMed]

76. Lamsal, R.; Walsh, M.E.; Gagnon, G.A. Comparison of advanced oxidation processes for the removal of natural organic matter. *Water Res.* **2011**, *45*, 3263–3269. [CrossRef] [PubMed]

77. De Vera, G.A.; Stalter, D.; Gernjak, W.; Weinberg, H.S.; Keller, J.; Farré, M.J. Towards reducing DBP formation potential of drinking water by favouring direct ozone over hydroxyl radical reactions during ozonation. *Water Res.* **2015**, *87*, 49–58. [CrossRef] [PubMed]

78. Petronijević, M.; Agbaba, J.; Ražić, S.; Molnar Jazić, J.; Tubić, A.; Watson, M.; Dalmacija, B. Fate of bromine-containing disinfection by-products precursors during ozone and ultraviolet-based advanced oxidation processes. *Int. J. Environ. Sci. Technol.* **2019**, *16*, 171–180. [CrossRef]

79. Sakai, H.; Autin, O.; Parsons, S. Change in haloacetic acid formation potential during UV and UV/H$_2$O$_2$ treatment of model organic compounds. *Chemosphere* **2013**, *92*, 647–651. [CrossRef]

80. Murray, C.A.; Parsons, S.A. Comparison of AOPs for the removal of natural organic matter: Performance and economic assessment. *Water Sci. Technol.* **2004**, *49*, 267–272. [CrossRef]

81. Moncayo-Lasso, A.; Pulgarin, C.; Benítez, N. Degradation of DBPs' precursors in river water before and after slow sand filtration by photo-Fenton process at pH 5 in a solar CPC reactor. *Water Res.* **2008**, *42*, 4125–4132. [CrossRef]

82. Moncayo-Lasso, A.; Rincon, A.G.; Pulgarin, C.; Benitez, N. Significant decrease of THMs generated during chlorination of river water by previous photo-Fenton treatment at near neutral pH. *J. Photochem. Photobiol. A Chem.* **2012**, *229*, 46–52. [CrossRef]

83. Lee, S.; Ohgaki, S. Oxidative degradation of toc and thmfp by fluidized bed photocatalysis reactor. *J. Environ. Sci. Heal. Part A* **1999**, *34*, 1933–1944. [CrossRef]

84. Liu, S.; Lim, M.; Fabris, R.; Chow, C.; Drikas, M.; Amal, R. TiO2 Photocatalysis of Natural Organic Matter in Surface Water: Impact on Trihalomethane and Haloacetic Acid Formation Potential. *Environ. Sci. Technol.* **2008**, *42*, 6218–6223. [CrossRef] [PubMed]

85. Liu, S.; Lim, M.; Fabris, R.; Chow, C.; Chiang, K.; Drikas, M.; Amal, R. Removal of humic acid using TiO$_2$ photocatalytic process—Fractionation and molecular weight characterisation studies. *Chemosphere* **2008**, *72*, 263–271. [CrossRef]

86. Gerrity, D.; Mayer, B.; Ryu, H.; Crittenden, J.; Abbaszadegan, M. A comparison of pilot-scale photocatalysis and enhanced coagulation for disinfection byproduct mitigation. *Water Res.* **2009**, *43*, 1597–1610. [CrossRef] [PubMed]

87. Rodríguez, E.M.; Gordillo, M.V.; Rey, A.; Beltrán, F.J. Impact of TiO2/UVA photocatalysis on THM formation potential. *Catal. Today* **2018**, *313*, 167–174. [CrossRef]

88. Murray, C.A.; Parsons, S.A. Preliminary laboratory investigation of disinfection by-product precursor removal using an advanced oxidation process. *Water Environ. J.* **2006**, *20*, 123–129. [CrossRef]

89. Murray, C.A.; Goslan, E.H.; Parsons, S.A. TiO2/UV: Single stage drinking water treatment for NOM removal? *J. Environ. Eng. Sci.* **2007**, *6*, 311–317. [CrossRef]

90. Kent, F.C.; Montreuil, K.R.; Brookman, R.M.; Sanderson, R.; Dahn, J.R.; Gagnon, G.A. Photocatalytic oxidation of DBP precursors using UV with suspended and fixed TiO$_2$. *Water Res.* **2011**, *45*, 6173–6180. [CrossRef]

91. Lu, J.; Dong, W.; Ji, Y.; Kong, D.; Huang, Q. Natural Organic Matter Exposed to Sulfate Radicals Increases Its Potential to Form Halogenated Disinfection Byproducts. *Environ. Sci. Technol.* **2016**, *50*, 5060–5067. [CrossRef] [PubMed]

92. Hua, Z.; Kong, X.; Hou, S.; Zou, S.; Xu, X.; Huang, H.; Fang, J. DBP alteration from NOM and model compounds after UV/persulfate treatment with post chlorination. *Water Res.* **2019**, *158*, 237–245. [CrossRef]

93. Wang, Z.; An, N.; Shao, Y.; Gao, N.; Du, E.; Xu, B. Experimental and simulation investigations of UV/persulfate treatment in presence of bromide: Effects on degradation kinetics, formation of brominated disinfection byproducts and bromate. *Sep. Purif. Technol.* **2020**, *242*. [CrossRef]

94. Wang, L.; Ji, Y.; Lu, J.; Yin, X.; Zhou, Q.; Kong, D. Transformation of iodide and formation of iodinated by-products in heat activated persulfate oxidation process. *Chemosphere* **2017**, *181*, 400–408. [CrossRef]

95. Pisarenko, A.N.; Stanford, B.D.; Snyder, S.A.; Rivera, S.B.; Boal, A.K. Investigation of the use of chlorine based advanced oxidation in surface water: Oxidation of natural organic matter and formation of disinfection byproducts. *J. Adv. Oxid. Technol.* **2013**, *16*, 137–150. [CrossRef]

96. Wang, D.; Bolton, J.R.; Andrews, S.A.; Hofmann, R. Formation of disinfection by-products in the ultraviolet/chlorine advanced oxidation process. *Sci. Total Environ.* **2015**, *518–519*, 49–57. [CrossRef]

97. Liu, Z.; Xu, B.; Zhang, T.Y.; Hu, C.Y.; Tang, Y.L.; Dong, Z.Y.; Cao, T.C.; El-Din, M.G. Formation of disinfection by-products in a UV-activated mixed chlorine/chloramine system. *J. Hazard. Mater.* **2021**, *407*, 124373. [CrossRef] [PubMed]

98. Liao, P.; Al-Ani, Y.; Malik Ismael, Z.; Wu, X. Insights into the role of humic acid on Pd-catalytic electro-fenton transformation of toluene in groundwater. *Sci. Rep.* **2015**, *5*. [CrossRef] [PubMed]

99. Trellu, C.; Péchaud, Y.; Oturan, N.; Mousset, E.; Huguenot, D.; van Hullebusch, E.D.; Esposito, G.; Oturan, M.A. Comparative study on the removal of humic acids from drinking water by anodic oxidation and electro-Fenton processes: Mineralization efficiency and modelling. *Appl. Catal. B Environ.* **2016**, *194*, 32–41. [CrossRef]

100. Mao, Y.; Guo, D.; Yao, W.; Wang, X.; Yang, H.; Xie, Y.F.; Komarneni, S.; Yu, G.; Wang, Y. Effects of conventional ozonation and electro-peroxone pretreatment of surface water on disinfection by-product formation during subsequent chlorination. *Water Res.* **2018**, *130*, 322–332. [CrossRef] [PubMed]

101. Mayer, B.K.; Daugherty, E.; Abbaszadegan, M. Evaluation of the relationship between bulk organic precursors and disinfection byproduct formation for advanced oxidation processes. *Chemosphere* **2015**, *121*, 39–46. [CrossRef]

102. Zhang, Z.; Zhao, Q.; Song, H.; Zhang, J.; Wang, L.; Qi, J.; Liu, Y.; Ma, J. Comparative study about oxidation of trace N-nitrosamines by seven oxidation processes with a sensitivity improved determination method. *Sep. Purif. Technol.* **2020**, *236*, 116009. [CrossRef]

103. Xu, B.; Chen, Z.; Qi, F.; Ma, J.; Wu, F. Inhibiting the regeneration of N-nitrosodimethylamine in drinking water by UV photolysis combined with ozonation. *J. Hazard. Mater.* **2009**, *168*, 108–114. [CrossRef]

104. Lee, C.; Yoon, J.; Von Gunten, U. Oxidative degradation of N-nitrosodimethylamine by conventional ozonation and the advanced oxidation process ozone/hydrogen peroxide. *Water Res.* **2007**, *41*, 581–590. [CrossRef]

105. Lv, J.; Li, Y.; Song, Y. Reinvestigation on the ozonation of N-nitrosodimethylamine: Influencing factors and degradation mechanism. *Water Res.* **2013**, *47*, 4993–5002. [CrossRef]

106. Hama Aziz, K.H. Application of different advanced oxidation processes for the removal of chloroacetic acids using a planar falling film reactor. *Chemosphere* **2019**, *228*, 377–383. [CrossRef]

107. Lovato, M.E.; Martín, C.A.; Cassano, A.E. Degradation of dichloroacetic acid in homogeneous aqueous media employing ozone and UVC radiation. *Photochem. Photobiol. Sci.* **2011**, *10*, 367–380. [CrossRef]

108. Wang, K.; Guo, J.; Yang, M.; Junji, H.; Deng, R. Decomposition of two haloacetic acids in water using UV radiation, ozone and advanced oxidation processes. *J. Hazard. Mater.* **2009**, *162*, 1243–1248. [CrossRef] [PubMed]

109. Zazouli, M.A.; Kalankesh, L.R. Removal of precursors and disinfection by-products (DBPs) by membrane filtration from water; a review. *J. Environ. Heal. Sci. Eng.* **2017**, *15*, 25. [CrossRef] [PubMed]

110. Zhang, Y.; Lu, Z.; Zhang, Z.; Shi, B.; Hu, C.; Lyu, L.; Zuo, P.; Metz, J.; Wang, H. Heterogeneous Fenton-like reaction followed by GAC filtration improved removal efficiency of NOM and DBPs without adjusting pH. *Sep. Purif. Technol.* **2021**, *260*, 118234. [CrossRef]

111. Zhong, J.; Zhao, Y.; Ding, L.; Ji, H.; Ma, W.; Chen, C.; Zhao, J. Opposite photocatalytic oxidation behaviors of BiOCl and TiO$_2$: Direct hole transfer vs. indirect OH oxidation. *Appl. Catal. B Environ.* **2019**, *241*, 514–520. [CrossRef]

112. Moussavi, G.; Rezaei, M. Exploring the advanced oxidation/reduction processes in the VUV photoreactor for dechlorination and mineralization of trichloroacetic acid: Parametric experiments, degradation pathway and bioassessment. *Chem. Eng. J.* **2017**, *328*, 331–342. [CrossRef]

113. Park, J.-A.; Nam, H.-L.; Choi, J.-W.; Ha, J.; Lee, S.-H. Oxidation of geosmin and 2-methylisoborneol by the photo-Fenton process: Kinetics, degradation intermediates, and the removal of microcystin-LR and trihalomethane from Nak-Dong River water, South Korea. *Chem. Eng. J.* **2017**, *313*, 345–354. [CrossRef]

114. Aslani, H.; Nasseri, S.; Nabizadeh, R.; Mesdaghinia, A.; Alimohammadi, M.; Nazmara, S. Haloacetic acids degradation by an efficient Ferrate/UV process: Byproduct analysis, kinetic study, and application of response surface methodology for modeling and optimization. *J. Environ. Manage.* **2017**, *203*, 218–228. [CrossRef]

115. Li, Y.; Kemper, J.M.; Datuin, G.; Akey, A.; Mitch, W.A.; Luthy, R.G. Reductive dehalogenation of disinfection byproducts by an activated carbon-based electrode system. *Water Res.* **2016**, *98*, 354–362. [CrossRef]

116. Zhao, B.; Wang, X.; Shang, H.; Li, X.; Li, W.; Li, J.; Xia, W.; Zhou, L.; Zhao, C. Degradation of trichloroacetic acid with an efficient Fenton assisted TiO$_2$ photocatalytic hybrid process: Reaction kinetics, byproducts and mechanism. *Chem. Eng. J.* **2016**, *289*, 319–329. [CrossRef]

117. Aslani, H.; Nabizadeh, R.; Nasseri, S.; Mesdaghinia, A.; Alimohammadi, M.; Mahvi, A.H.; Rastkari, N.; Nazmara, S. Application of response surface methodology for modeling and optimization of trichloroacetic acid and turbidity removal using potassium ferrate(VI). *Desalin. Water Treat.* **2016**, *57*, 25317–25328. [CrossRef]

118. Zhao, B.; Li, X.; Li, W.; Yang, L.; Li, J.; Xia, W.; Zhou, L.; Wang, F.; Zhao, C. Degradation of trichloroacetic acid by an efficient Fenton/UV/TiO2 hybrid process and investigation of synergetic effect. *Chem. Eng. J.* **2015**, *273*, 527–533. [CrossRef]

119. Alavi, N.; Tahvildarij, K. Removal of trihalomethanes in tehran drinking water by an advanced oxidation process. *Nat. Environ. Pollut. Technol.* **2015**, *14*, 211–216. [CrossRef]

120. Park, B.; Cho, E.; Son, Y.; Khim, J. Distribution of electrical energy consumption for the efficient degradation control of THMs mixture in sonophotolytic process. *Ultrason. Sonochem.* **2014**, *21*, 1982–1987. [CrossRef] [PubMed]

121. Tang, S.; Wang, X.M.; Yang, H.W.; Xie, Y.F. Haloacetic acid removal by sequential zero-valent iron reduction and biologically active carbon degradation. *Chemosphere* **2013**, *90*, 1563–1567. [CrossRef]

122. Radjenović, J.; Farré, M.J.; Mu, Y.; Gernjak, W.; Keller, J. Reductive electrochemical remediation of emerging and regulated disinfection byproducts. *Water Res.* **2012**, *46*, 1705–1714. [CrossRef]

123. Esclapez, M.D.; Tudela, I.; Díez-García, M.I.; Sáez, V.; Rehorek, A.; Bonete, P.; González-García, J. Towards the complete dechlorination of chloroacetic acids in water by sonoelectrochemical methods: Effect of the anodic material on the degradation of trichloroacetic acid and its by-products. *Chem. Eng. J.* **2012**, *197*, 231–241. [CrossRef]

124. Wang, X.; Ning, P.; Liu, H.; Ma, J. Dechlorination of chloroacetic acids by Pd/Fe nanoparticles: Effect of drying method on metallic activity and the parameter optimization. *Appl. Catal. B Environ.* **2010**, *94*, 55–63. [CrossRef]

125. Czili, H.; Horváth, A. Photodegradation of chloroacetic acids over bare and silver-deposited TiO2: Identification of species attacking model compounds, a mechanistic approach. *Appl. Catal. B Environ.* **2009**, *89*, 342–348. [CrossRef]

126. Li, Y.P.; Cao, H.B.; Zhang, Y. Reductive dehalogenation of haloacetic acids by hemoglobin-loaded carbon nanotube electrode. *Water Res.* **2007**, *41*, 197–205. [CrossRef] [PubMed]

127. Shemer, H.; Narkis, N. Trihalomethanes aqueous solutions sono-oxidation. *Water Res.* **2005**, *39*, 2704–2710. [CrossRef] [PubMed]

128. Shemer, H.; Narkis, N. Sonochemical removal of trihalomethanes from aqueous solutions. *Ultrason. Sonochem.* **2005**, *12*, 495–499. [CrossRef] [PubMed]

129. Shemer, H.; Narkis, N. Effects of aqueous solutions composition and acoustic intensity on THM compounds sonolysis. *Environ. Eng. Sci.* **2005**, *22*, 138–144. [CrossRef]

130. Shemer, H.; Narkis, N. Mechanisms and inorganic byproducts of trihalomethane compounds sonodegradation. *Environ. Sci. Technol.* **2004**, *38*, 4856–4859. [CrossRef]

131. Lifongo, L.L.; Bowden, D.J.; Brimblecombe, P. Photodegradation of haloacetic acids in water. *Chemosphere* **2004**, *55*, 467–476. [CrossRef]

132. Zhang, L.; Arnold, W.A.; Hozalski, R.M. Kinetics of haloacetic acid reactions with Fe(O). *Environ. Sci. Technol.* **2004**, *38*, 6881–6889. [CrossRef]

133. Wu, C.; Wei, D.; Fan, J.; Wang, L. Photosonochemical degradation of trichloroacetic acid in aqueous solution. *Chemosphere* **2001**, *44*, 1293–1297. [CrossRef]

134. Hozalski, R.M.; Zhang, L.; Arnold, W.A. Reduction of haloacetic acids by FeO: Implications for treatment and fate. *Environ. Sci. Technol.* **2001**, *35*, 2258–2263. [CrossRef] [PubMed]

135. Tang, W.Z.; Tassos, S. Oxidation kinetics and mechanisms of trihalomethanes by Fenton's reagent. *Water Res.* **1997**, *31*, 1117–1125. [CrossRef]

136. Spangenberg, D.; Mbller, U. Photooxidation and Thermal Decomposition of Trichloroacetic Acid. *Chemosphere* **1996**, *33*, 43–49. [CrossRef]

137. Kasprzyk-Hordern, B.; Ziółek, M.; Nawrocki, J. Catalytic ozonation and methods of enhancing molecular ozone reactions in water treatment. *Appl. Catal. B Environ.* **2003**, *46*, 639–669. [CrossRef]

138. Hill, G.R. The Kinetics of the Oxidation of Cobaltous Ion by Ozone. *J. Am. Chem. Soc.* **1949**, *71*, 2434–2435. [CrossRef]

139. Nawrocki, J.; Kasprzyk-Hordern, B. The efficiency and mechanisms of catalytic ozonation. *Appl. Catal. B Environ.* **2010**, *99*, 27–42. [CrossRef]

140. Yu, D.; Wu, M.; Hu, Q.; Wang, L.; Lv, C.; Zhang, L. Iron-based metal-organic frameworks as novel platforms for catalytic ozonation of organic pollutant: Efficiency and mechanism. *J. Hazard. Mater.* **2019**, *367*, 456–464. [CrossRef]

141. Yu, D.; Wang, L.; Yang, T.; Yang, G.; Wang, D.; Ni, H.; Wu, M. Tuning Lewis acidity of iron-based metal-organic frameworks for enhanced catalytic ozonation. *Chem. Eng. J.* **2021**, *404*, 127075. [CrossRef]

142. Nawrocki, J. Catalytic ozonation in water: Controversies and questions. Discussion paper. *Appl. Catal. B Environ.* **2013**, *142–143*, 465–471. [CrossRef]

143. Wang, J.; Chen, H. Catalytic ozonation for water and wastewater treatment: Recent advances and perspective. *Sci. Total Environ.* **2020**, *704*, 135249. [CrossRef] [PubMed]

144. Rivera-Utrilla, J.; López-Ramón, M.V.; Sánchez-Polo, M.; Álvarez, M.Á.; Velo-Gala, I. Characteristics and behavior of different catalysts used for water decontamination in photooxidation and ozonation processes. *Catalysts* **2020**, *10*, 1485. [CrossRef]

145. Yu, G.; Wang, Y.; Cao, H.; Zhao, H.; Xie, Y. Reactive Oxygen Species and Catalytic Active Sites in Heterogeneous Catalytic Ozonation for Water Purification. *Environ. Sci. Technol.* **2020**, *54*, 5931–5946. [CrossRef]

146. Fogler, H.S. *Elements of Chemical Reaction Engineering*, 3rd ed.; Goodwin, B.M., Ed.; Prentice-Hall: Englewood-Cliffs, NJ, USA, 1999.

147. Liu, Y.; Shen, J.; Chen, Z.; Yang, L.; Liu, Y.; Han, Y. Effects of amorphous-zinc-silicate-catalyzed ozonation on the degradation of p-chloronitrobenzene in drinking water. *Appl. Catal. A Gen.* **2011**, *403*, 112–118. [CrossRef]

148. Andreozzi, R.; Insola, A.; Caprio, V.; Marotta, R.; Tufano, V. The use of manganese dioxide as a heterogeneous catalyst for oxalic acid ozonation in aqueous solution. *Appl. Catal. A Gen.* **1996**, *138*, 75–81. [CrossRef]

149. Martins, R.C.; Quinta-Ferreira, R.M. Catalytic ozonation of phenolic acids over a Mn-Ce-O catalyst. *Appl. Catal. B Environ.* **2009**, *90*, 268–277. [CrossRef]

150. Ikhlaq, A.; Brown, D.R.; Kasprzyk-Hordern, B. Catalytic ozonation for the removal of organic contaminants in water on ZSM-5 zeolites. *Appl. Catal. B Environ.* **2014**, *154–155*, 110–122. [CrossRef]

151. Zhao, L.; Ma, J.; Sun, Z.; Zhai, X. Mechanism of influence of initial pH on the degradation of nitrobenzene in aqueous solution by ceramic honeycomb catalytic ozonation. *Environ. Sci. Technol.* **2008**, *42*, 4002–4007. [CrossRef] [PubMed]

152. Liu, Z.Q.; Ma, J.; Cui, Y.H.; Zhao, L.; Zhang, B.P. Factors affecting the catalytic activity of multi-walled carbon nanotube for ozonation of oxalic acid. *Sep. Purif. Technol.* **2011**, *78*, 147–153. [CrossRef]

153. Restivo, J.; Órfão, J.J.M.; Pereira, M.F.R.; Vanhaecke, E.; Rönning, M.; Iouranova, T.; Kiwi-Minsker, L.; Armenise, S.; Garcia-Bordejé, E. Catalytic ozonation of oxalic acid using carbon nanofibres on macrostructured supports. *Water Sci. Technol.* **2012**, *65*, 1854–1862. [CrossRef] [PubMed]

154. Orge, C.A.; Órfão, J.J.M.; Pereira, M.F.R. Composites of manganese oxide with carbon materials as catalysts for the ozonation of oxalic acid. *J. Hazard. Mater.* **2012**, *213–214*, 133–139. [CrossRef] [PubMed]

155. Orge, C.A.; Órfão, J.J.M.; Pereira, M.F.R. Carbon xerogels and ceria-carbon xerogel materials as catalysts in the ozonation of organic pollutants. *Appl. Catal. B Environ.* **2012**, *126*, 22–28. [CrossRef]

156. Wang, Y.; Duan, X.; Xie, Y.; Sun, H.; Wang, S. Nanocarbon-Based Catalytic Ozonation for Aqueous Oxidation: Engineering Defects for Active Sites and Tunable Reaction Pathways. *ACS Catal.* **2020**, *10*, 13383–13414. [CrossRef]

157. Qu, X.; Zheng, J.; Zhang, Y. Catalytic ozonation of phenolic wastewater with activated carbon fiber in a fluid bed reactor. *J. Colloid Interface Sci.* **2007**, *309*, 429–434. [CrossRef] [PubMed]

158. Sánchez-Polo, M.; Leyva-Ramos, R.; Rivera-Utrilla, J. Kinetics of 1,3,6-naphthalenetrisulphonic acid ozonation in presence of activated carbon. *Carbon N. Y.* **2005**, *43*, 962–969. [CrossRef]

159. Rivera-Utrilla, J.; Sánchez-Polo, M.; Gómez-Serrano, V.; Álvarez, P.M.; Alvim-Ferraz, M.C.M.; Dias, J.M. Activated carbon modifications to enhance its water treatment applications. An overview. *J. Hazard. Mater.* **2011**, *187*, 1–23. [CrossRef] [PubMed]

160. Salla, J.S.; Padoin, N.; Amorim, S.M.; Li Puma, G.; Moreira, R.F.P.M. Humic acids adsorption and decomposition on Mn_2O_3 and α-Al_2O_3 nanoparticles in aqueous suspensions in the presence of ozone. *J. Environ. Chem. Eng.* **2020**, *8*, 102780. [CrossRef]

161. Alver, A.; Kılıç, A. Catalytic ozonation by iron coated pumice for the degradation of natural organic matters. *Catalysts* **2018**, *8*, 219. [CrossRef]

162. Zhang, H.; Wang, J. Catalytic Ozonation of Humic Acids by Ce–Ti Composite Catalysts. *Kinet. Catal.* **2017**, *58*, 734–740. [CrossRef]

163. Gümüş, D.; Akbal, F. A comparative study of ozonation, iron coated zeolite catalyzed ozonation and granular activated carbon catalyzed ozonation of humic acid. *Chemosphere* **2017**, *174*, 218–231. [CrossRef]

164. Turkay, O.; Inan, H.; Dimoglo, A. Experimental and theoretical study on catalytic ozonation of humic acid by ZnO catalyst. *Sep. Sci. Technol.* **2017**, *52*, 778–786. [CrossRef]

165. Wang, Q.; Yang, Z.; Chai, B.; Cheng, S.; Lu, X.; Bai, X. Heterogeneous catalytic ozonation of natural organic matter with goethite, cerium oxide and magnesium oxide. *RSC Adv.* **2016**, *6*, 14730–14740. [CrossRef]

166. Wang, J.; Wang, G.; Yang, C.; Yang, S.; Huang, Q. Catalytic ozonation of organic compounds in water over the catalyst of RuO_2/ZrO_2-CeO_2. *Front. Environ. Sci. Eng.* **2015**, *9*, 615–624. [CrossRef]

167. Turkay, O.; Inan, H.; Dimoglo, A. Experimental study of humic acid degradation and theoretical modelling of catalytic ozonation. *Environ. Sci. Pollut. Res.* **2015**, *22*, 202–210. [CrossRef]

168. Turkay, O.; Inan, H.; Dimoglo, A. Experimental and theoretical investigations of CuO-catalyzed ozonation of humic acid. *Sep. Purif. Technol.* **2014**, *134*, 110–116. [CrossRef]

169. Wu, Y.; Wu, C.; Wang, Y.; Hu, C. Inhibition of Nano-Metal Oxides on Bromate Formation during Ozonation Process. *Ozone Sci. Eng.* **2014**, *36*, 549–559. [CrossRef]

170. Chen, K.C.; Wang, Y.H. The effects of Fe-Mn oxide and TiO_2/α-Al2O3 on the formation of disinfection by-products in catalytic ozonation. *Chem. Eng. J.* **2014**, *253*, 84–92. [CrossRef]

171. Wang, Y.H.; Chen, K.C. Removal of disinfection by-products from contaminated water using a synthetic goethite catalyst via catalytic ozonation and a biofiltration system. *Int. J. Environ. Res. Public Health* **2014**, *11*, 9325–9344. [CrossRef]

172. Han, Q.; Wang, H.; Dong, W.; Liu, T.; Yin, Y. Suppression of bromate formation in ozonation process by using ferrate(VI): Batch study. *Chem. Eng. J.* **2014**, *236*, 110–120. [CrossRef]

173. Wang, Y.H.; Chen, K.C.; Chen, C.R. Combined catalytic ozonation and membrane system for trihalomethane control. *Catal. Today* **2013**, *216*, 261–267. [CrossRef]

174. Han, Q.; Wang, H.; Dong, W.; Liu, T.; Yin, Y. Formation and inhibition of bromate during ferrate(VI)—Ozone oxidation process. *Sep. Purif. Technol.* **2013**, *118*, 653–658. [CrossRef]

175. Molnar, J.; Agbaba, J.; Dalmacija, B.; Klašnja, M.; Watson, M.; Kragulj, M. Effects of Ozonation and Catalytic Ozonation on the Removal of Natural Organic Matter from Groundwater. *J. Environ. Eng.* **2012**, *138*, 804–808. [CrossRef]

176. Mortazavi, S.B.; Asgari, G.; Hashemian, S.J.; Moussavi, G. Degradation of humic acids through heterogeneous catalytic ozonation with bone charcoal. *React. Kinet. Mech. Catal.* **2010**, *100*, 471–485. [CrossRef]

177. Chen, K.C.; Wang, Y.H.; Chang, Y.H. Using catalytic ozonation and biofiltration to decrease the formation of disinfection by-products. *Desalination* **2009**, *249*, 929–935. [CrossRef]

178. Wang, J.; Zhou, Y.; Zhu, W.; He, X. Catalytic ozonation of dimethyl phthalate and chlorination disinfection by-product precursors over Ru/AC. *J. Hazard. Mater.* **2009**, *166*, 502–507. [CrossRef] [PubMed]

179. Zhang, T.; Lu, J.; Ma, J.; Qiang, Z. Fluorescence spectroscopic characterization of DOM fractions isolated from a filtered river water after ozonation and catalytic ozonation. *Chemosphere* **2008**, *71*, 911–921. [CrossRef] [PubMed]

180. Alsheyab, M.A.; Muñoz, A.H. Comparative study of ozone and MnO2/O3 effects on the elimination of TOC and COD of raw water at the Valmayor station. *Desalination* **2007**, *207*, 179–183. [CrossRef]

181. Karnik, B.S.; Davies, S.H.; Baumann, M.J.; Masten, S.J. Fabrication of catalytic membranes for the treatment of drinking water using combined ozonation and ultrafiltration. *Environ. Sci. Technol.* **2005**, *39*, 7656–7661. [CrossRef]

182. Karnik, B.S.; Baumann, M.J.; Masten, S.J.; Davies, S.H. AFM and SEM characterization of iron oxide coated ceramic membranes. *J. Mater. Sci.* **2006**, *41*, 6861–6870. [CrossRef]

183. Shioyama, M.; Kawanishi, T.; Yokoyama, S.; Nuno, M.; Yamamoto, T. Development of advanced ceramic membrane filtration system combined with ozonation and powdered activated carbon treatment. *Water Sci. Technol. Water Supply* **2001**, *1*, 91–96. [CrossRef]

184. Gracia, R.; Cortés, S.; Sarasa, J.; Ormad, P.; Ovelleiro, J.L. Catalytic ozonation with supported titanium dioxide. The stability of catalyst in water. *Ozone Sci. Eng.* **2000**, *22*, 185–193. [CrossRef]

185. Gracia, R.; Cortes, S.; Sarasa, J.; Ormad, P.; Ovelleiro, J.L. Heterogeneous catalytic ozonation with supported titanium dioxide in model and natural waters. *Ozone Sci. Eng.* **2000**, *22*, 461–471. [CrossRef]

186. Volk, C.; Roche, P.; Joret, J.C.; Paillard, H. Comparison of the effect of ozone, ozone-hydrogen peroxide system and catalytic ozone on the biodegradable organic matter of a fulvic acid solution. *Water Res.* **1997**, *31*, 650–656. [CrossRef]

187. Allemane, H.; Delouane, B.; Legube, B. Comparative Efficiency of Three Systems (Os, $O_3/H2O_2$ and O_3/TiO_2) for the Oxidation of Natural Organic Matter in Water. *Ozone Sci. Eng.* **1993**, *15*, 419–432. [CrossRef]

188. Bai, Z.Y.; Wang, J.L.; Yang, Q. Catalytic ozonation of dimethyl phthalate by Ce-substituted goethite. *Int. J. Environ. Sci. Technol.* **2017**, *14*, 2379–2388. [CrossRef]

189. Beltrán, F.J.; Pocostales, J.P.; Alvarez, P.M.; Oropesa, A. Diclofenac removal from water with ozone and activated carbon. *J. Haz. Mater.* **2009**, *163*, 768–776. [CrossRef]

190. Beltrán, F.J.; Pocostales, J.P.; Alvarez, P.M.; Jaramillo, J. Mechanism and kinetic considerations of TOC removal from the powdered activated carbon ozonation of diclofenac aqueous solutions. *J. Hazard. Mater.* **2009**, *169*, 532–538. [CrossRef]

191. Tomiyasu, H.; Fukutomi, H.; Gordon, G. Kinetics and Mechanism of Ozone Decomposition in Basic Aqueous Solution. *Inorg. Chem.* **1985**, *24*, 2962–2966. [CrossRef]

192. Staehelin, J.; Buehler, R.E.; Hoigne, J. Ozone decomposition in water studied by pulse radiolysis. 2. Hydroxyl and hydrogen tetroxide (HO_4) as chain intermediates. *J. Phys. Chem.* **1984**, *88*, 5999–6004. [CrossRef]

193. Elovitz, M.S.; von Gunten, U. Hydroxyl Radical/Ozone Ratios During Ozonation Processes. I. The Rct Concept. *Ozone Sci. Eng.* **1999**, *21*, 239–260. [CrossRef]

194. Yuan, R.; Zhou, B.; Zhang, X.; Guan, H. Photocatalytic degradation of humic acids using substrate-supported Fe3+-doped TiO2 nanotubes under UV/O_3 for water purification. *Environ. Sci. Pollut. Res.* **2015**, *22*, 17955–17964. [CrossRef] [PubMed]

195. Agustina, T.E.; Ang, H.M.; Vareek, V.K. A review of synergistic effect of photocatalysis and ozonation on wastewater treatment. *J. Photochem. Photobiol. C Photochem. Rev.* **2005**, *6*, 264–273. [CrossRef]

196. Mehrjouei, M.; Müller, S.; Möller, D. A review on photocatalytic ozonation used for the treatment of water and wastewater. *Chem. Eng. J.* **2015**, *263*, 209–219. [CrossRef]

197. Mecha, A.C.; Chollom, M.N. Photocatalytic ozonation of wastewater: A review. *Environ. Chem. Lett.* **2020**, *18*, 1491–1507. [CrossRef]

198. Beltrán, F.J.; Rey, A. Solar or UVA-Visible Photocatalytic Ozonation of Water Contaminants. *Molecules* **2017**, *22*, 177. [CrossRef]

199. Yu, D.; Li, L.; Wu, M.; Crittenden, J.C. Enhanced photocatalytic ozonation of organic pollutants using an iron-based metal-organic framework. *Appl. Catal. B Environ.* **2019**, *251*, 66–75. [CrossRef]

200. Cao, S.; Low, J.; Yu, J.; Jaroniec, M. Polymeric Photocatalysts Based on Graphitic Carbon Nitride. *Adv. Mater.* **2015**, *27*, 2150–2176. [CrossRef]

201. Xiao, J.; Xie, Y.; Rabeah, J.; Brückner, A.; Cao, H. Visible-Light Photocatalytic Ozonation Using Graphitic C3N4 Catalysts: A Hydroxyl Radical Manufacturer for Wastewater Treatment. *Acc. Chem. Res.* **2020**, *53*, 1024–1033. [CrossRef]

202. Kerc, A.; Bekbolet, M.; Saatci, A.M. Sequential Oxidation of Humic Acids by Ozonation and Photocatalysis. *Ozone Sci. Eng.* **2003**, *25*, 497–504. [CrossRef]

203. Bekbolet, M.; Uyguner, C.S.; Selcuk, H.; Rizzo, L.; Nikolaou, A.D.; Meriç, S.; Belgiorno, V. Application of oxidative removal of NOM to drinking water and formation of disinfection by-products. *Desalination* **2005**, *176*, 155–166. [CrossRef]

204. Uyguner, C.S.; Suphandag, S.A.; Kerc, A.; Bekbolet, M. Evaluation of adsorption and coagulation characteristics of humic acids preceded by alternative advanced oxidation techniques. *Desalination* **2007**, *210*, 183–193. [CrossRef]

205. Li, G.; Li, K.; Liu, A.; Yang, P.; Du, Y.; Zhu, M. 3D Flower-like β-MnO2/Reduced Graphene Oxide Nanocomposites for Catalytic Ozonation of Dichloroacetic Acid. *Sci. Rep.* **2017**, *7*, 1–7. [CrossRef]

206. Shin, D.; Jang, M.; Cui, M.; Na, S.; Khim, J. Enhanced removal of dichloroacetonitrile from drinking water by the combination of solar-photocatalysis and ozonation. *Chemosphere* **2013**, *93*, 2901–2908. [CrossRef]

207. Mehrjouei, M.; Müller, S.; Möller, D. Synergistic effect of the combination of immobilized TiO₂, UVA and ozone on the decomposition of dichloroacetic acid. *J. Environ. Sci. Health Part A Toxic/Hazardous Subst. Environ. Eng.* **2012**, *47*, 1073–1081. [CrossRef]

208. Gu, L.; Yu, X.; Xu, J.; Lv, L.; Wang, Q. Removal of dichloroacetic acid from drinking water by using adsorptive ozonation. *Ecotoxicology* **2011**, *20*, 1160–1166. [CrossRef] [PubMed]

209. Zhai, X.; Chen, Z.; Zhao, S.; Wang, H.; Yang, L. Enhanced ozonation of dichloroacetic acid in aqueous solution using nanometer ZnO powders. *J. Environ. Sci.* **2010**, *22*, 1527–1533. [CrossRef]

210. Yang, J.; Dong, Z.; Jiang, C.; Wang, C.; Liu, H. An overview of bromate formation in chemical oxidation processes: Occurrence, mechanism, influencing factors, risk assessment, and control strategies. *Chemosphere* **2019**, *237*, 124521. [CrossRef]

211. Fischbacher, A.; Löppenberg, K.; von Sonntag, C.; Schmidt, T.C. A New Reaction Pathway for Bromite to Bromate in the Ozonation of Bromide. *Environ. Sci. Technol.* **2015**, *49*, 11714–11720. [CrossRef]

212. Parrino, F.; Camera-Roda, G.; Loddo, V.; Palmisano, G.; Augugliaro, V. Combination of ozonation and photocatalysis for purification of aqueous effluents containing formic acid as probe pollutant and bromide ion. *Water Res.* **2014**, *50*, 189–199. [CrossRef]